Earth-Science Reviews 215 (2021) 103496

Contents lists available at ScienceDirect

Earth-Science Reviews

journal homepage: www.elsevier.com/locate/earscirev

Review article

Loess landscapes of Europe – Mapping, geomorphology, and zonal differentiation

F. Lehmkuhl [a,*], J.J. Nett [a], S. Pötter [a], P. Schulte [a], T. Sprafke [b], Z. Jary [c], P. Antoine [d], L. Wacha [e], D. Wolf [f], A. Zerboni [g], J. Hošek [h,i], S.B. Marković [j], I. Obreht [a,k], P. Sümegi [l], D. Veres [m], C. Zeeden [a,n], B. Boemke [a], V. Schaubert [a], J. Viehweger [a], U. Hambach [o]

[a] Department of Geography, RWTH Aachen University, Germany
[b] Institute of Geography, University of Bern, Switzerland
[c] University of Wroclaw, Institute of Geography and Regional Development, Wrocław, Poland
[d] CNRS-Université Paris I UPEC, Laboratoire de Géographie Physique, Environnements quaternaires et actuels, Meudon, France
[e] Croatian Geological Survey, Zagreb, Croatia
[f] Department of Geography, TU, Dresden, Germany
[g] Dipartimento di Scienze della Terra "A. Desio", Università degli Studi di Milano, Milano, Italy
[h] Czech Geological Survey, Prague, Czech Republic
[i] Center for Theoretical Study, Charles University and the Academy of Sciences, Jilská 1, 110 00 Praha 1, Czech Republic
[j] Department of Physical Geography, Faculty of Sciences, University of Novi Sad, Trg Dositeja Obradovića 3, 21000 Novi Sad, Serbia
[k] Organic Geochemistry Group, MARUM-Center for Marine Environmental Sciences and Department of Geosciences, University of Bremen, Bremen, Germany
[l] Department of Geology and Paleontology, University of Szeged, Hungary & Institute of Geography and Earth Sciences, University of Szeged, Hungary
[m] Institute of Speleology, Romanian Academy, Cluj-Napoca, Romania
[n] Leibniz Institute for Applied Geophysics, Stilleweg 2, 30655 Hannover, Germany
[o] BayCEER & Chair of Geomorphology, University of Bayreuth, Germany

ARTICLE INFO

Keywords:
Aeolian deposits
Quaternary sediments
Loess map
Loess facies
Dust deposition
Conceptual loess formation model

ABSTRACT

Paleoenvironmental reconstructions on a (supra-)regional scale have gained attention in Quaternary sciences during the last decades. In terrestrial realms, loess deposits and especially intercalations of loess and buried soils, so called loess-paleosol sequences (LPS) are important archives to unravel the terrestrial response to e.g. climatic fluctuations and reconstruct paleoenvironments during the Pleistocene. The analysis of LPS requires the knowledge of several key factors, such as the distribution of the aeolian sediments, their location relative to (potential) source areas, the climate conditions that led to their emplacement and the topography of the sink area. These factors strongly influence the sedimentological and paleoenvironmental characteristics of LPS and show broad variations throughout Europe, leading to a distinct distribution pattern throughout the continent.

We present a new map of the distribution of aeolian sediments (mainly loess) and major potential source areas for Europe. The map was compiled combining geodata of different mapping approaches. Most of the used geodata stems from accurate national maps of 27 different countries. Problematic aspects such as different nomenclatures across administrative borders were carefully investigated and revised. The result is a seamless map, which comprises pedological, geological, and geomorphological data and can be used for paleoenvironmental and archeological studies and other applications.

We use the resulting map and data from key geomorphological cross-sections to discuss the various influences of geomorphology and paleoenvironment on the deposition and preservation of Late Pleistocene loess throughout Europe. We divided the loess areas into 6 main loess domains and 17 subdomains to understand and explain the factors controlling their distribution and characteristics. For the subdivision we used the following criteria: (1) influence of silt production areas, (2) affiliation to subcatchments, as rivers are very important regional silt transport agents, (3) occurrence of past periglacial activity with characteristic overprinting of the deposits. Additionally, the sediment distribution is combined with elevation data, to investigate the loess distribution statistically as well as visually.

* Corresponding author.
E-mail address: flehmkuhl@geo.rwth-aachen.de (F. Lehmkuhl).

https://doi.org/10.1016/j.earscirev.2020.103496
Received 3 September 2020; Received in revised form 19 December 2020; Accepted 21 December 2020
Available online 28 December 2020

Throughout Europe, the variations, and differences of the loess domains are the results of a complex interplay of changing paleoenvironmental conditions and related geomorphologic processes, controlling dust sources, transport, accumulation, preservation, pedogenesis, alongside erosional and reworking events. Climatic, paleoclimatic, and pedoclimatic gradients are on the continental scale an additional important factor, since there are e.g. latitudinal differences of permafrost and periglacial processes, an increase in continentality from west to east and in aridity from northwest to southeast and south, strongly affecting regional sedimentary and geomorphic dynamics.

We propose three main depositional regimes for loess formation in Europe: (1.) periglacial and tundra loess formation with periglacial processes and permafrost in the high latitude and mountainous regions; (2.) steppe and desert margin loess formation in the (semi-)arid regions; and (3.) loess and soil formation in temperate and subtropical regions. Loess deposits of (1.) and (2.) show coarser, sandier particle distributions towards the glacial and desert regions. In the humid areas (3.) forest vegetation limited dust production and accumulation, therefore, there is an increase in finer grain sizes due to an increase in weathering.

1. Introduction and general approach

Loess is one of the most extensively distributed Pleistocene sedimentary deposits in the northern hemisphere and represents the main archive of glacial periods in Europe (Bertran et al., 2016; Haase et al., 2007; Marković et al., 2015; Rousseau et al., 2013). The so-called loess-paleosol sequences (LPS) are composed of the alternation of loess and buried soil (paleosol) horizons developed in response to climatic changes, and are key-archives in order to unravel paleoclimates (e.g. Gallet et al., 1996; Obreht et al., 2017; Torre et al., 2020), paleoenvironments (e.g. Hatté et al., 2013; Liu and Liu, 2017; Schaetzl et al., 2018; Schatz et al., 2011), and paleolandscapes (e.g. Hughes et al., 2010; Lehmkuhl et al., 2016; Leonova et al., 2015). The fertile topsoils of loess landscapes are heavily employed in agricultural practices with highly specialized past to present agricultural use of the loess lowlands commencing already during the Neolithic, 7000 years ago (Bellwood, 2005; Whittle and Whittle, 1996). The Late Pleistocene loess steppe and loess tundra also play an important role in understanding early modern human migration and the colonisation of Europe (Chu, 2018; Haesaerts et al., 2004; Hauck et al., 2018; Neugebauer-Maresch et al., 2014; Obreht et al., 2017; Zeuner, 1956). Stratigraphic and pedostratigraphic records across European LPS exhibit a more or less constant pattern including sedimentary marker horizons (especially paleosols and paleosol complexes) that can be followed over long distances (Antoine et al., 2019; Antoine et al., 2016; Haesaerts et al., 2004). These patterns demonstrates, that LPS are formed in response to at least supra-regional climatic forcing at various time-scales from glacial-interglacial (Bronger, 2003; Kukla, 1977) to millennial-scale cycles (e.g. Dansgaard-Oeschger cycles, Antoine et al., 2009a; Moine et al., 2017; Rousseau et al., 2007, 2011; Zeeden et al., 2018). To understand the environments under which loess deposits form, it is crucial to know their occurrence and distribution, the geomorphological setting they formed in, and the climate conditions which influenced their formation and characteristics (e.g. Pécsi and Richter, 1996; Smalley and Leach, 1978). To comprehend and analyze these environments, maps of the distribution of Quaternary aeolian sediments in Western Eurasian mid-latitudes show not only their regional abundance, but also their distance to potential source areas, alongside their relationship to elevation and relief (Lehmkuhl et al., 2018a, 2018b; Lindner et al., 2017). As early as the first half of the 20th century, the climatic importance of Scandinavian and Alpine ice sheets for loess deposits in Europe was understood and implications for a zonal distribution of various loess facies were proposed (e.g. Zeuner, 1937). Generally, the distribution of loess and especially the development of LPS in Europe were controlled by relief, climate, and the distance to large river systems, but past continental ice sheet dynamics and shifts in the exposed shelf area of the North Sea may have been additional key factors (Antoine et al., 2016; Lehmkuhl et al., 2016).

Maps highlighting the distribution of Quaternary aeolian deposits are an important tool to understand paleoenvironments in a spatial manner and context, and to deduce source and sink relationships at greater geomorphological scales. Maps are also useful tools in paleoecology and to reconstruct the past relief constraints on human dispersal and societal complexity. The first loess maps at the European scale were produced by Grahmann (1932) and Fink et al. (1977). Later, a digital European Loess Map was published by Haase et al. (2007). More recently, Bertran et al. (2016) generated a map of European Pleistocene aeolian deposits based on topsoil textural data from the Land Use and Cover Area frame Statistical survey database (LUCAS, Orgiazzi et al., 2018; Tóth et al., 2013). Lastly, Li et al. (2020) presented global distribution maps of provenance and transport pathways of major loess areas and discussed their genesis. Although several examples of loess maps exist, most mapping approaches encounter difficulties related to scale and availability of geodata. The choice of scale depends on the research question at hand. Most maps are either detailed on a local scale or are presented at a larger scale and lack precision. Combining several national or regional maps can circumvent this problem but this often leads to artificial spatial breaks within the geodata, which can only be amended by evaluation and generalization of the geodata sets (e.g. Lehmkuhl et al., 2018a, 2018b).

While gathering and processing continent-wide geodata for an updated, seamless map of aeolian sediments in Europe, we already compiled three regional-scale maps. The loess map of Hungary and western Romania is based on geological and pedological data (Lindner et al., 2017). The subsequent map of the entire Carpathian Basin, combines geodata sources from ten different countries (Lehmkuhl et al., 2018a). Several cross-border problems arose due to different terminologies and definitions of loess and related sediments, which are a consequence of the complex genesis of loess sediments and the fundamental lack of representative genetic formation models (Lehmkuhl et al., 2018a; Smalley et al., 2011; Sprafke and Obreht, 2016). Such difficulties are not only restricted to national borders, but are sometimes even present within one country, as shown in the map of loess and other Quaternary sediments in Germany (Lehmkuhl et al., 2018b). Due to the federal system in Germany, artificial breaks between different states could only be avoided by combining loess and loess derivates in one mapping unit (Lehmkuhl et al., 2018b).

The present study builds upon this experience and uses continent-wide geodata to present a map of the distribution of Late Pleistocene aeolian sediments for the entire European continent. We follow a two-pillar approach, in which the mapping based on multi-national geodata forms the starting point of a conceptual model of loess genesis. The continent-wide spatial synthesis of loess distribution provides the genetic basis of our geographically and geoecologically derived loess formation and distribution model. We are aware that a map always represents a snapshot of a given spatial situation. However, in a given time interval geographical distributions of sedimentary units are subjected not only to spatial but also temporal variability leading to a superposition of contrasting facies at a given point. As already done for our previous publications, this map presents late last glacial conditions,

mainly referring to Last Glacial Maximum (LGM sensu lato ~30–17 ka; Lambeck et al., 2014) environments (e.g. ice sheet margins, permafrost boundary, alluvial plains, dry shelves) to comprehend the complex conditions during the last main period of loess formation in Europe. During LGM s.l. interstadial soil formation in LPS in Europe is either weak or even absent (Fischer et al., 2021; Obreht et al., 2017; Sprafke et al., 2020), which allows for comparing loess depositional milieus without the bias of post-depositional alterations. Nevertheless, climatic conditions were never constant and there is always a certain degree of spatial and temporal variability that cannot be disentangled in a cross-continental map. We divided the map into six domains and 17 subdomains of different loess regions to differentiate depositional environments and areas. Finally, we visualize our analysis using cross-sections and 3D images. To place the loess map into a climatic context and give an overview of the present day environmental setting, Fig. 1 depicts the modern climatic conditions of the European loess covered regions (after Karger et al., 2017).

We demonstrate and discuss the influences of topography, the distance to ice margins and potential source areas, as well as paleoclimatic patterns, such as the distribution of continuous and discontinuous permafrost on the distribution and depositional facies of loess deposits in Europe, based on a compilation of different LPS across the continent. In addition, the data will be compared to the existing maps of Haase et al. (2007) and the approach by Bertran et al. (2016). Finally, we propose a conceptual model of loess genesis with three main deposition (paleoenvironmental) regimes. We envisage our approach will have strong implications in assessing the distributions and importance of aeolian and especially loess deposits in Europe, enhacing their paleoclimate, geoecological, and chronostratigraphic relevance.

2. Material and methods

2.1. Source maps, spatial data, and processing

Spatial geodata from 27 different European countries was compiled, processed, and unified to create a seamless map of the distribution of Late Pleistocene aeolian sediments and their potential sources. In most cases, this included georeferencing and vectorizing printed national and regional geological, pedological, and geomorphological maps. The source maps were chosen on a case-by-case basis, depending on the respective availability, issue date, and quality of the maps, e.g. in respect to the differentiation between Quaternary sediments in geological maps. In general, only sediments with thickness of >2 m are mapped in geological maps, while pedological and geomorphological maps also include thinner sediment cover as well (e.g. for Poland, Ukraine, Moldova, Italy). A detailed description of the used source data is presented in the Supplement and summarized in Supplementary Table S1. A short summary is given in the following.

The published map of Quaternary sediments in the Carpathian Basin (Lehmkuhl et al., 2018a; Lindner et al., 2017) combines harmonized soil, geomorphological, and geological data from 10 countries (**Austria, Bosnia and Herzegovina, Croatia, Czech Republic, Hungary, Romania, Serbia, Slovakia, Slovenia** and **Ukraine**). The map of loess and other Quaternary sediments for **Germany** uses geological data of 16 federal geological surveys and data from the Federal Geological Survey (Lehmkuhl et al., 2018b). The geodata of these published maps are used without major changes in the new European loess map. Only the geodata from Austria and Croatia were re-evaluated and altered in comparison to Lehmkuhl et al. (2018a) (see details in the supplement). For easier cross-border comparison, we unite loess and loess derivates in one class. In contrast to the map published by Lehmkuhl et al. (2018a), we differentiate between sandy loess and aeolian sands in the new European map.

The loess sediments in the **United Kingdom** are based on a national loess map (Catt, 1985). The source map differentiates between various loess thicknesses. For the European map, only loess with a thickness greater than 1 m from Catt (1985) was used to ensure the different data sets are comparable. The alluvial fill and fluvial deposits are based upon superficial deposits in the BGS Geology 625 k map (scale 1:625,000), with the permission of the British Geological Survey (2013). For **Belgium**, the national soil map (scale 1:500,000) was used to map both aeolian sediments and potential sediment sources (Marechal and Tavernier, 1970). The distribution of aeolian sediments and sediment sources in the **Netherlands** is based on the geological map (scale 1:600,000; Zagwijn and Van Staalduinen, 1975). It distinguishes between loess, dunes and coversands. For **France**, a map of loess and other aeolian sediments (Antoine et al., 1999a; scale 1:1,000,000) based on various geological and geomorphological maps, initially compiled in the 1970s for the first INQUA loess map of Europe (Fink et al., 1977), was digitized. For **Switzerland**, the national general geological map (Christ, 1944; Christ, 1942; Christ and Nabholz, 1950) was used as the most recent terminologically consistent country-wide representation of loess (scale 1:200,000). In this case, georeferenced raster files were available from which a map unit representing loess and loess derivates was vectorized. The geodata for **Spain** contain information about the spatial distribution of loess, aeolian sand and alluvial plains for central and northeastern Spain (Wolf et al., 2019) and is based on the geological maps (scale 1:50,000; de San José Mancha, 1973) and the work by Balasch et al. (2019). The minimum thickness of this approach is 2 m.

For **Italy**, the loess distribution – considered as 'loess derivates' for the European loess map – is based on data collected by many scholars and summarized in Cremaschi (2004, 1990a, 1987), Zerboni et al. (2018), Antonioli and Vai (2004), Costantini et al. (2012) and Badino et al. (2019), with a minimal mapped thickness of 50 cm (see also the supplement file for details). For **Romania**, the national geological maps (Ovejanu et al., 1968, scale 1:200,000; Săndulescu et al., 1978, scale 1:1,000,000) albeit distinguishing between several loess chronostratigraphic units, do not always show a very good lateral representation of loess. Therefore, the approach by Lindner et al. (2017), that investigated the loess cover in western Romania, was extended to the whole country. For **Bulgaria**, the geological map of Bulgaria (Cheshitev et al., 1989, scale 1:500,000) was vectorized.

National soil maps were digitized for **Poland** (Dobrzański et al., 1974), **Moldova** (Krupenikov et al., 1969a), and **Ukraine** (Sokolovsky et al., 1977a). For the loess distributions for Belarus and western Russia, the European loess map by Haase et al. (2007) was modified to fit the improved accuracy and scale. For this purpose, the map was compared to the ALOS digital surface model (JAXA EORC, 2016). The loess distribution was aligned to the Pleistocene terraces and other geomorphological features determined via the elevation data. Afterwards, the area between these presumably loess-covered terraces was vectorized as alluvial fill and fluvial deposits.

In addition to the national data sets, pan-European data sets for potential Pleistocene source areas for aeolian sediments were evaluated and added to the map to substitute missing and deficient national datasets. This includes inter alia Late Pleistocene and Holocene fluvial deposits, derived from the EUSR5000 soil map with a scale of 1:5,000,000 (BGR [Bundesanstalt für Geowissenschaften und Rohstoffe], 2005). In addition to alluvial fill and fluvial deposits, the dry continental shelf during the LGM (modified after Willmes, 2015), which represents a main source for aeolian sediments in northern Central Europe, was added to the map. Paleochannels were extracted using bathymetric data from the Eureopean Marine Observation and Data Network (EMODnet, 2019). As additional important paleoenvironmental factors we inserted the LGM northern timberline (mod. acc. to Grichuk, 1992), the LGM boundaries of continuous and discontinuous permafrost (Andrieux et al., 2016; Ruszkiczay-Rüdiger and Kern, 2016; Vandenberghe et al., 2014a), the modified ice extent during the LGM (Ehlers et al., 2011), and recent courses of the major rivers (adapted from www.naturalearthdata.com). However, especially the limits of permafrost and the northern timberline are estimates and their accuracy is still a matter of debate. For example, a careful and comprehensive revision of paleoclimate proxies and periglacial features suggests that

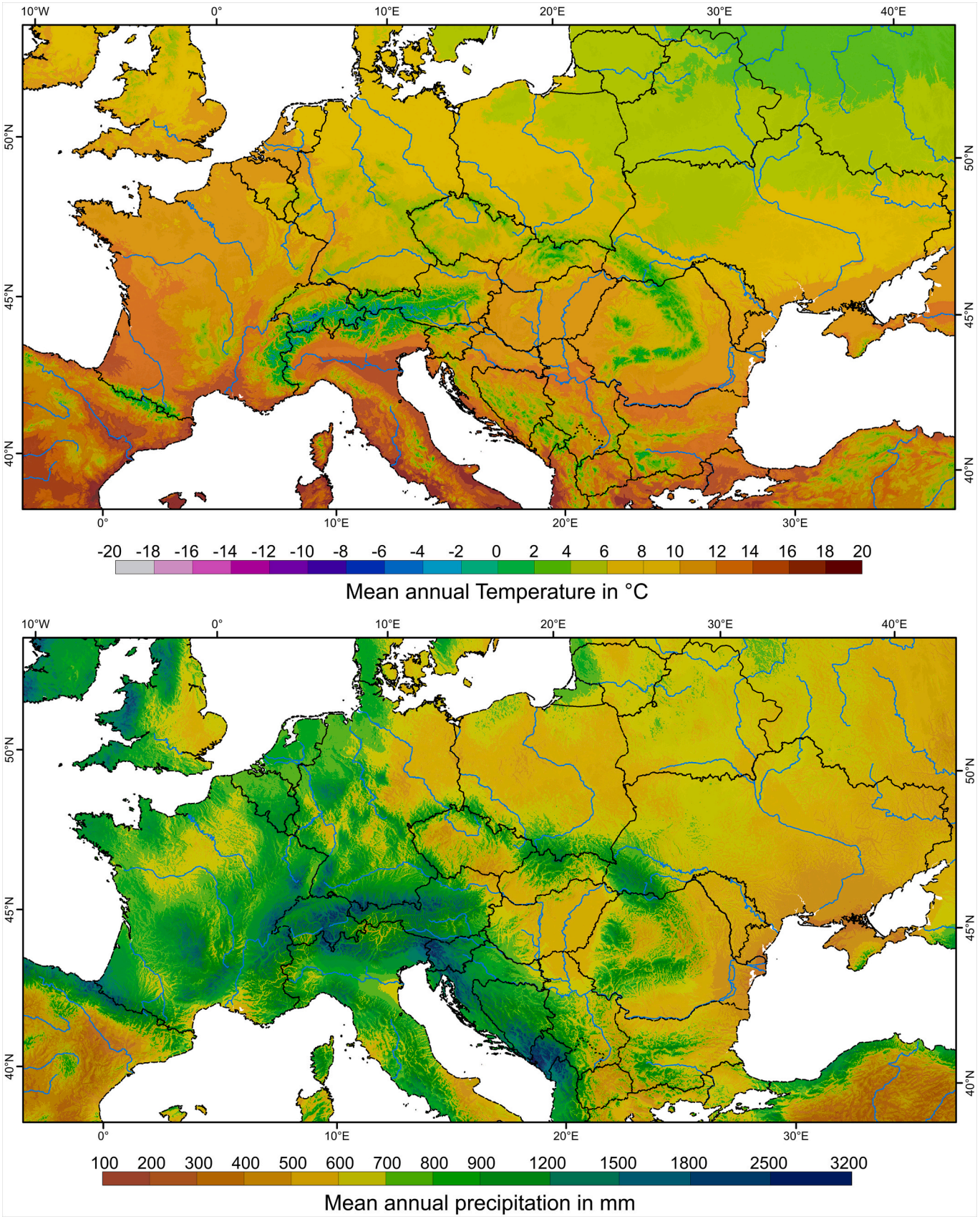

Fig. 1. Modern climatic conditions in Europe. Mean annual air temperature on the upper panel, annual precipitation on the lower panel. Data adapted from Karger et al. (2017).

the lowland territory of the Carpathian Basin (or Pannonian Basin) was not influenced by continuous permafrost, even during the most severe climatic phases of the late Quaternary (Ruszkiczay-Rüdiger and Kern, 2016). In addition, Andrieux et al. (2016) show through the mapping of the existence of ice wedge pseudomorphs in France that the line of continuous permafrost is further north than previously believed in western Europe. Therefore, we corrected the permafrost boundaries published by Vandenberghe et al. (2014a) in France in orientation to the southernmost distribution of ice wedge pseudomorphs as proposed by Andrieux et al. (2016) and in the Carpathian Basin as suggested by Ruszkiczay-Rüdiger and Kern (2016). Furthermore, it should be noted that the Last Permafrost Maximum (LPM) proposed by Vandenberghe et al. (2014a) is dated to 31 to 24 ka and therefore slightly older than the LGM. We also note that the LPM boundaries represent transitional zones of these past environmental factors and therefore a boundary is variable in space and time. The LPM boundaries are an orientation for the past influence of periglacial processes and features as seen in LPS. They fit the pan-European scale scope of our study overview but are no references for national or regional scale studies.

To harmonize and generalize the combined national and regional data sets, an automated tool was used. The tool is similar to the one used in Lehmkuhl et al. (2018b) and was applied to address cross-map-problems like misalignments that can occur due to different scales and mapping approaches in the used maps. The tool consists of a 5-step-algorithm for aggregation, simplification, and smoothing and was adjusted to fit an average national mapping scale (see scheme in Supplementary Fig. S1).

The result of this approach is a seamless map of Late Pleistocene aeolian sediments and potential sediment sources in Europe. Since it is mostly based on national and regional maps and data sets, the final resolution and accuracy is very high for a pan-European approach. A detailed table of the sources and a statistical analysis for each mapped country can be found in the Supplementary Material (Supplement Table S1).

2.2. Visualization: Cross sections and 3D images

In order to outline the influence of the topography on the distribution of Late Pleistocene aeolian sediments, four north-south running cross sections were derived using the new map and the ALOS digital surface model (JAXA EORC, 2016). To do so, polylines were interpolated based on the elevation data. The interpolated lines were superelevated by the factor 100 and intersected with the sediment distribution, glacial extents as well as the boundaries of (dis-)continuous permafrost and the northern timberline. Moreover, six block diagrams (3D images) were created using ESRI ArcScene 10.6.1. The different 3D images were superelevated with varying factors of 1 to 20, depending on the topography of the visualized region. The distribution of all mapped sediments was rasterized and superelevated to gain spatial and topographic impressions of selected areas within the differentiated loess domains. In some 3D images, a further distinction of the mapped sediments as e.g. Late Pleistocene fluvial deposits and Holocene alluvial fill or loess and loess derivates is shown. Key sites and major cities were displayed for orientation purposes.

2.3. Statistics

To analyze the distribution of loess in Europe, we also extracted information on the surface and height distribution. For the area statistics, the area of each mapped unit in each (sub-)domain was calculated via the 'calculate geometry'-function in ArcMap 10.6.1 (see Table 1). This was also done for each country in order to estimate the proportion of the national data sets (see Supplement Table 1).

The ALOS digital surface model (JAXA EORC, 2016) was clipped by the shapefiles representing 'loess and loess derivates' as well as 'aeolian sand' and 'sandy loess'. The resulting raster data sets were analyzed using the 'Zonal Statistics as Table' and the 'Zonal Histogram' tool with the vectorized (sub-) domains as feature zone data. The zonal histograms were used to calculate the relative surface percentage of each respective sediment unit at each elevation in meters above sea level (m a.s.l.). The outputs of the 'Zonal Statistics as Table' tool were used to calculate statistical parameters such as minimum, maximum, mean, and median of the elevation distribution. In addition to the zonal statistics and histograms, the attribute tables of each clipped raster were exported for further analysis via RStudio. The data was then used to create whisker plots that illustrate the elevations at which the corresponding sediments are distributed. To exclude extreme outliers, the upper and lower limit in the whisker was set to 1%. These outliers are probably related to misalignments between the loess shapefiles and the DEM, the scale of the source data or the smoothing process.

Table 1
Surface statistics of the distribution of loess and selected Late Pleistocene sediments in Europe (Fig. 2) per domain and subdomain.

Domain & subdomain	Surface area [km^2]			
	Loess & loess derivates	Sandy loess	Aeolian sand	Alluvial fill & fluvial deposits
I	248,379	2005	12,764	137,794
Ia	1875	2005	12,764	59,735
Ib	246,504	0	0	78,059
II	453,713	6115	14,341	116,767
IIa	46,718	5780	10,942	27,067
IIb	18,813	335	1289	9180
IIc	21,316	0	0	15,776
IId	351,082	0	509	54,865
IIe	15,784	0	1601	9878
III	53,249	10,084	5479	79,232
IIIa	3295	0	0	10,936
IIIb	9955	0	987	10,131
IIIc	7297	0	92	18,182
IIId	29,075	10,059	4187	33,952
IIIe	3626	26	213	6031
IV	60,428	12,616	4526	36,754
V	245,978	0	1578	45,810
VI	17,916	0	2843	81,887
VIa	2532	0	2843	45,323
VIb	13,276	0	0	28,245
VIc	2108	0	0	8319
Total	1,079,663	30,820	41,532	498,244

3. Spatial distribution of European loess landscapes

The new map shows that loess is widely distributed in Europe (Fig. 2). It spreads along the southern limit of the Pleistocene British and Fennoscandian ice sheets, spanning from southern England, through northern France, Germany, Poland and the Carpathian Basin to the Eastern European Plain. Within the Baltic part of Russia and northern Belarus, some loess patches can be found which overlap with the LGM ice extent. These patches are part of the late glacial sheets of aeolian sands and silts deposited after the ice receded. Several intramontane basins of the Central European low mountain ranges (German: Mittelgebirge), the valleys of large river systems such as the Rhône, Po, Rhine and Danube, and the lowlands of the Middle and Lower Danube Basin and the northern shore of the Black Sea are important loess regions. Some smaller and more isolated loess patches are found within the Mediterranean part of Europe and the Balkan Peninsula. The new map also depicts major alluvial and fluvial deposits. Here, the delta regions of the Rhône, Po, and Danube rivers show an extremely wide Late Pleistocene and Holocene alluvial fill. These vast fluvial accumulations are the result of sea level rise after the deglaciation period and thus contain late glacial to Holocene deposits (e.g. Bruno et al., 2020).

As the last glacial cycle comprises the last period of major loess deposition (Marković et al., 2015), we focus on that time period and added to our map the LGM extent of glaciers (modified according to

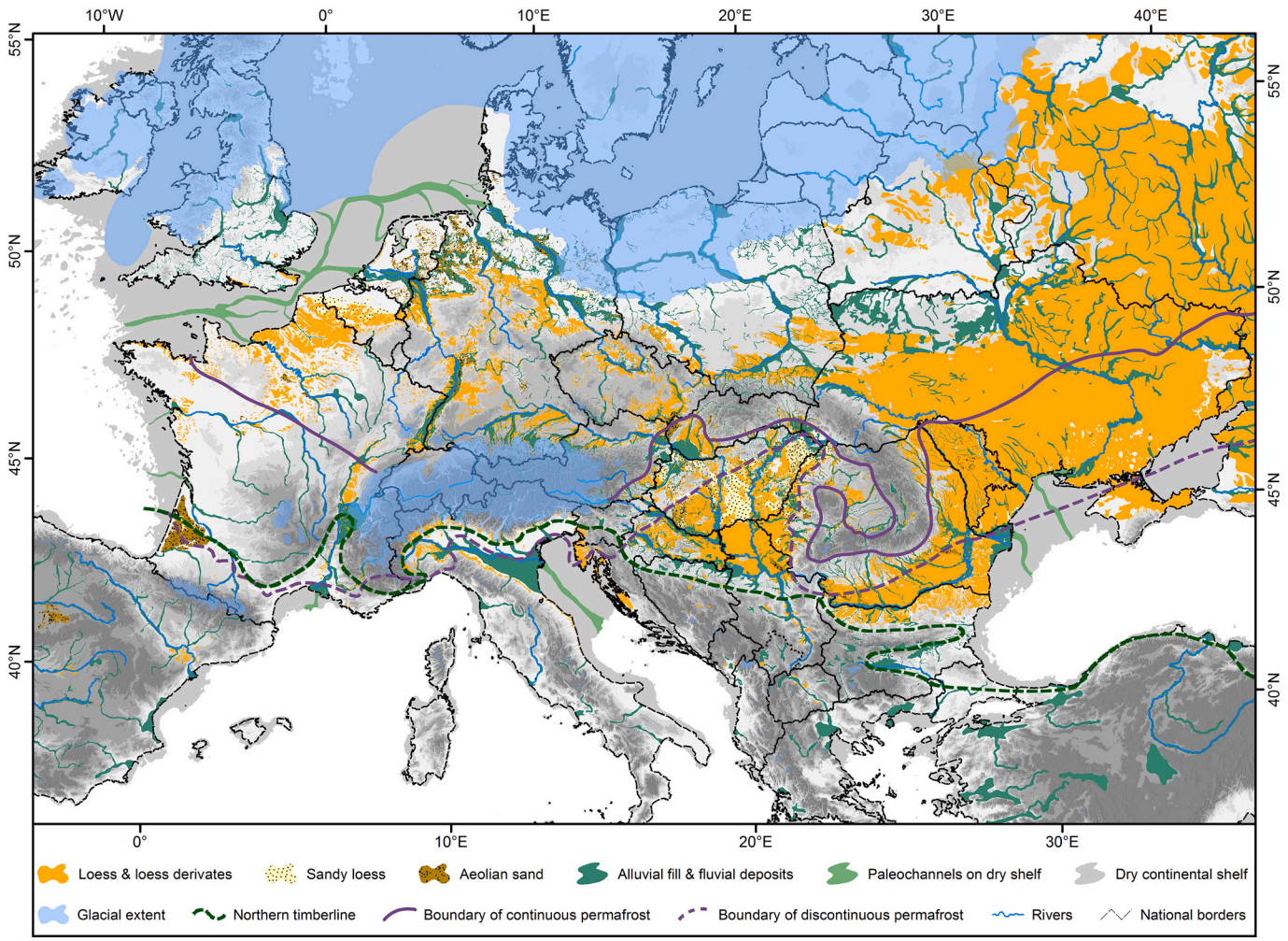

Fig. 2. Distribution of loess and selected Late Pleistocene sediments in Europe. The LGM extent of glaciers (Ehlers et al., 2011) and dry continental shelves (modified after Willmes, 2015), as well as the northern timberline (modified after Grichuk, 1992) and the boundaries of continuous and discontinuous permafrost (Andrieux et al., 2016; Ruszkiczay-Rüdiger and Kern, 2016; Vandenberghe et al., 2014a) are also mapped.

Ehlers et al., 2011), the contemporaneously dry continental shelves (modified according to Willmes, 2015), as well as the northern timberline (modified after Grichuk, 1992) and the boundaries of continuous and discontinuous permafrost (Andrieux et al., 2016; Ruszkiczay-Rüdiger and Kern, 2016; Vandenberghe et al., 2014a, Fig. 2).

We divided the European loess distribution in six major domains and 17 subdomains (Fig. 3). For the differentiation, we used the following criteria that determine the loess facies: (1) Influence of potential silt production areas (North European / Alpine ice sheets with glacial grinding and periglacial areas with frost weathering vs. drylands with soluble salts and prevailing insolation weathering). (2) Catchment areas, as rivers are very important regional silt transport agents and river valleys act both as sinks and sources of sedimentary particles. (3) Paleoenvironmental factors influencing the formation, preservation and transformation of loess deposits, such as past periglacial activity with its characteristic overprinting of the primary deposits.

The six major domains are (I) the Weichselian marginal or protogenetic zone; (II) the northern European loess belt; (III) the loess adjacent to Central European high altitude mountain ranges (northern fringe of the Alpine ice sheets and Carpathians); (IV) the Middle Danube Basin loess; (V) the eastern (Pontic) European loess; and (VI) the Mediterranean loess. Here we use the term **'loess facies'** to describe its properties and define characteristics more or less specific to each domain. This term should be seen in particularly in context of proximity to source as well as the type and intensity of weathering processes. Loess facies characteristics e.g. are influenced by factors such as the parent material of the deposits, distance of transport, and (post-) depositional milieus (Pécsi and Richter, 1996). There are large variations between loess deposited proximally or more distally to ice margins. Loess formation and preservation are among others factors strongly influenced by the environment. In western Europe, for example, loess layers occur which show characteristics of laminated niveo-aeolian deposits (e.g. Antoine et al., 2016; Antoine et al., 2001; Haesaerts et al., 2016), while in southeastern Europe, loess formation was rather homogeneous and more continuous sedimentation took place (Marković et al., 2015; Obreht et al., 2019; Zeeden et al., 2016). Although it seems generally accepted that less hiatuses occur in the loess deposits of domains VI and V, one should mention that most study sites are usually chosen in order to avoid visible sedimentation discordances. However, it is also crucial that works reporting age gaps rely on several lines of chronological evidence, alongside sedimentological data (i.e., trends in magnetic susceptibility, grain-size, etc.) that would allow to critically evaluate such data in light of stratigraphic constraints. Different potential major sources of aeolian deposits are the outwash plains of the British and Fennoscandian ice sheets, of alpine glaciations and the alluvial deposits of river systems. Sources and loess facies can also vary on a local scale. In southern Germany for example, we distinguish between loess linked to sources from the Swiss Alps (Upper Rhine Plain or Graben, subdomain IIIb) and from the Black Forest and the Eastern Alps (Upper Danube, subdomain IIIc). The most important (paleo-) environmental factors

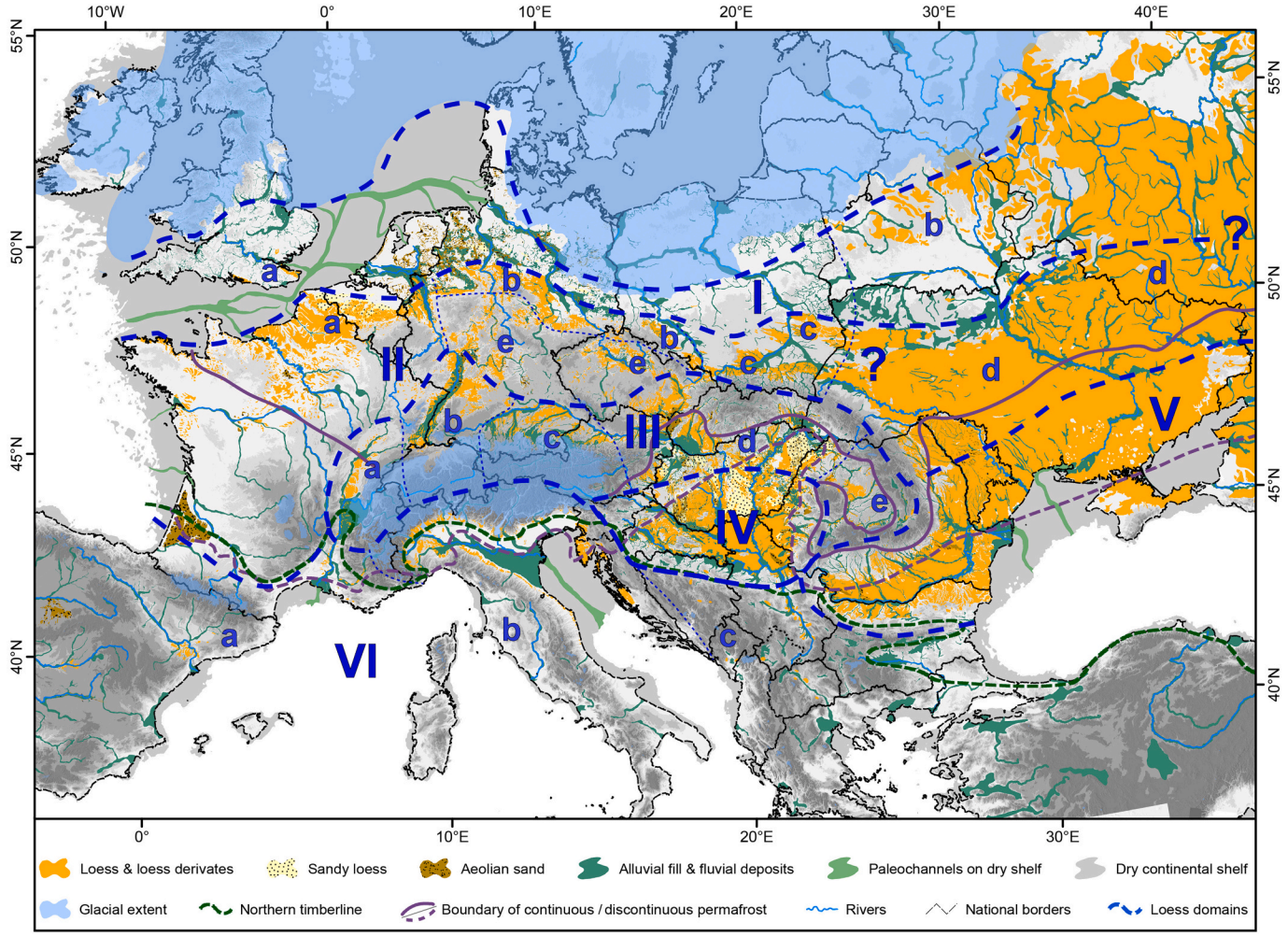

Fig. 3. Major domains (roman numerals) and subdomains (lowercase letters) of loess and loess derivates for the LGM loess landscapes as shown in Fig. 2.

dividing the subdomains are (1) the boundaries of (dis-) continuous permafrost, which strongly influences the preservation of loess, and (2) hydroclimatic factors, especially continentality which generally increases from west to east and strongly changes the chemical weathering and pedogenesis intensity, mainly during interglacials and interstadials. Both processes result in syndepositional/early diagenetic decalcification, hydromorphic overprinting, and decomposition of organic compounds in humid and cold areas. On the contrary, in semi-arid regions, the preservation of dry, calcareous loess composed of almost pristine silty mineral dust dominates. Regarding pedogenesis, Chernozem-like (paleo-) soils are formed in the steppic areas, Greyzems (grey forest soils) in forest-steppe zones and more rubified (paleo-) soils (e.g. chromic Cambisols or Terra Rossa) are found in areas under the Mediterranean climatic influence, whereas under Atlantic and boreal climatic environments Luvisols and Cambisols (brown soils) are predominant (European Soils Bureau Network, 2005).

In the following, the six major domains and 17 subdomains are explained in detail to display the differences in aeolian sediment dynamics during the Late Pleistocene. The domains are described roughly from north to south. Fig. 4 provides four loess landscape transects that visualize the interplay of relief and loess in the various suggested subdomains across Europe (more information given in Chapter 3.2). In addition, we show a map with selected European loess sections as an orientation for the reader to locate the given examples in the text in Supplementary Fig. S2. The figure is accompanied by Supplementary Table S2, which lists the referenced loess sections.

3.1. Loess domains and subdomains

3.1.1. I: Weichselian marginal or protogenetic zone

Following the suggestion by Łanczont and Wojtanowicz (2009) and Gozhik et al. (2014), we call the northernmost domain 'Weichselian marginal or protogenetic zone'. However, this term and especially the associated genetic interpretation is used differently as stated by Łanczont and Wojtanowicz (2009), who suggest that silty and silty-sandy deposits in this zone were created mainly as a result of cryogenic weathering. We use the geographical attribution and the name and interpret this as protogenetic transport and accumulation zone. Loess and loess derivates in this domain cover an area of ~ 248,000 km^2. This domain comprises patches of sandy loess and coversands (total ~ 15,000 km^2). The domain is divided further into two subdomains: Ia the western and Ib the eastern protogenetic subdomain.

3.1.1.1. Ia: Western protogenetic subdomain. This subdomain is located between the former margins of the British and Fennoscandian Weichselian ice sheets and the northern European loess belt and stretches from southern England to the main drainage divide between the Vistula (Wisła) and Dnieper rivers. In southern England loess deposits are usually found in rather thin covers with a maximum thickness of 4 m in local sedimentary traps (Catt, 1985; Catt, 1977). The new map only shows mapped loess deposits >2 m thick in Kent, Hampshire, and Essex. For southern England such loess and loess derivates are described by Antoine et al. (2003). A recent review concerning loess in England is given in Assadi-Langroudi (2019). Stevens et al. (2020) showed that

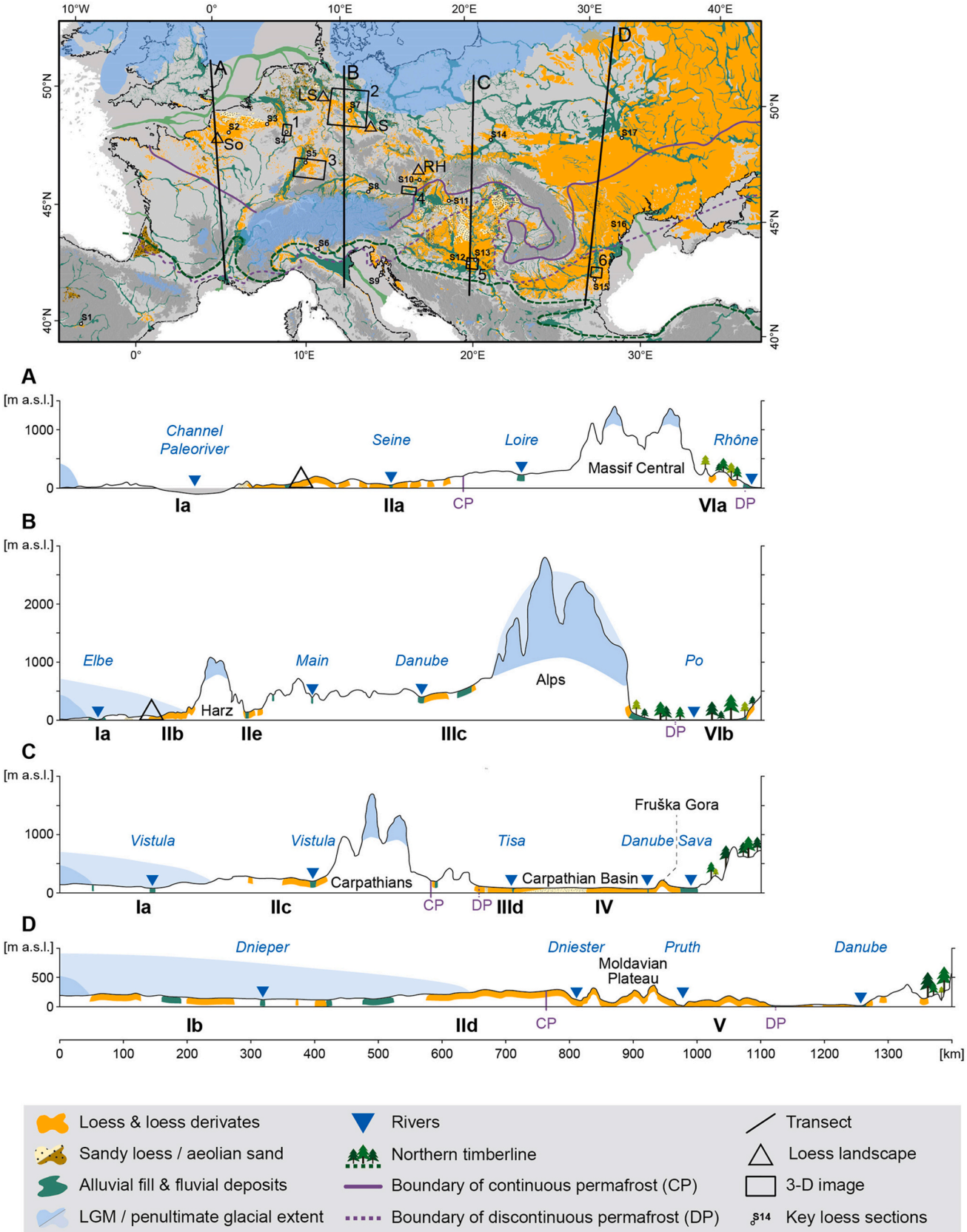

Fig. 4. N-S transects showing four exemplary loess landscapes across Europe. The location of the transects, the 3-D images (Figs. 8, 9, 11, 12, 14, 15), and the meso-scale loess landscapes is shown in the top map. Key loess sections (S1-S17) are illustrated in Fig. 6. Meso-scale loess landscape: Valley sections (So = Somme, Northern France Fig. 7 and RH = Red Hill, Czech Republic, Fig. 13) loess-edge ramp (LS = Lower Saxony, S = Saxony, both Germany, Fig. 10). (For interpretation of the references to color in this figure legend, the reader is referred to the web version of this article.)

loess accumulation in southeast England started at c. 25 ka and highlighted the interplay between the ice sheets, Atlantic storm tracks, and the topography and drainage of the exposed North Sea, which had an crucial influence on dust dynamics and accumulation.

Sandy deposits form a belt spanning from Belgium, through the Netherlands, Germany, Poland up to northwestern Ukraine. Kozarski and Nowaczyk (1991) reported a relatively frequent occurrence of isolated loess and sandy loess patches in the lower Oder (Odra) and Warta regions (northwestern Poland). Within this belt, the aeolian sediments reach various thicknesses, up to several meters. However, quite many of these regional sand sheets have thicknesses less than 2 m. As our data is mainly based on geological maps, cover sediments with a thickness of less than 2 m are not included in our map. For Poland, Ukraine, and Moldova we use soil maps (Dobrzański et al., 1974; Krupenikov et al., 1969b; Sokolovsky et al., 1977b) which did not allow to differentiate the origin of sand (glacial, glacio-fluvial, fluvial or aeolian). For Russia we only include sandy loess from the Haase et al. (2007) map, without additional data on aeolian sands. Therefore, there is an underestimation of aeolian sand in our map especially for this domain. Research showed that the grain size decreases with increasing distance from the Weichselian ice sheets, with aeolian sand and sandy loess found in close proximity to the source areas (e.g. in Germany east of Hamburg and south of Berlin, respectively), whereas loess and loess derivates can be found in distal positions further south (domain II). There are also aeolian sand covers that are overlapping with the maximum extent of the Weichselian glaciation. This indicates a post-LGM sedimentation during the late glacial or even early Holocene (Hilgers et al., 2001b; Koster, 2005; Küster and Preusser, 2010; Zeeberg, 1998). Vandenberghe (in Schaetzl et al., 2018) gives a summary of these periglacial aeolian sands and their transition to loess. Most of the loess deposits in this subdomain can be found at elevations between ~ 30 m and ~ 100 m a.s.l., with a maximum at around 230 m a.s.l. (cf. Chapter 3.3).

3.1.1.2. Ib: Eastern protogenetic subdomain. Subdomain Ib comprises the loess deposits on the plains of Belarus and Russia. Loess is found in elevations up to 285 m a.s.l. The southern border of this domain is the border between continuous and discontinuous loess mantle as suggested by Velichko (1990) along the line from Lviv through Kyiv to Ryazan. North of this line towards the limits of the Valdai (Weichselian) ice sheet, loess occurs rather sporadically (subdomain Ib) with the largest patches found near the cities of Minsk, Smolensk, Moscow, and Vladimir. South of this line the loess forms an almost continuous mantle (domains II and V) stretching up to the coasts of the Black and Azov Seas (cf. Gozhik et al., 2014).

The discontinuous loess of subdomain Ib was deposited mainly during the Late Pleistocene (Velichko et al., 2006). The key loess sections in this area contain pedogenic marker horizons in the form of two well developed paleosol complexes assigned to Marine Isotope Stage (MIS) 5 and MIS 3, respectively, and are stratigraphically comparable to other marker paleosol complexes in European loess areas (Little et al., 2002; Rutter et al., 2003; Velichko, 1990). However, the particular feature of loess sequences in this subdomain are stratigraphically consistent and frequently repeating periglacial features indicating the impact of permafrost conditions and changing hydroclimate of the last glacial period (Morozova and Nechaev, 1997; Velichko et al., 2006). Loess deposits in this subdomain are found up to ~ 280 m a.s.l., with a median of 199 m a.s.l. (cf. Chapter 3.3).

3.1.2. II: Northern European loess belt

The northern European loess belt preserves the most diversified pedo-sedimentary records in Europe. These deposits were strongly influenced by periglacial processes and environments and thus show a complex stratigraphy including erosional unconformities and permafrost features such as ice wedge pseudomorphs or cryoturbation features as well as thermokarst erosion processes. This domain extends from western France through Belgium, Germany, and Poland to Ukraine and Russia. Geochemical results and heavy mineral signatures show that most material has its origin in northern Europe delivered by the British and Fennoscandian ice sheets and contains also recycled material (Nawrocki et al., 2019; Rousseau et al., 2014; Skurzyński et al., 2020). In addition, there is a redistribution of the particles by periglacial braided rivers in the southern North Sea and eastern Channel, far from the original zones of production by glacial grinding, which are glacial fronts and glaciofluvial outwash plains (Antoine et al., 2009a). We divided this domain into five subdomains: three (IIa-c) from west to east along the front of the Central European low mountain ranges stretching to western Ukraine and gradually passing on towards subdomain IId in northern Ukraine and the Russian uplands. In subdomain IId there is a gradual transition towards domain V with no or less influence of permafrost and periglacial features towards the south. The last subdomain (IIe) includes basins within the Central European low mountain ranges with elevations between 200 and 600 m a.s.l.. Loess and loess derivates occur here rather in isolated patches covering mostly wide river terraces, which are usually older than the last glacial cycle.

In some parts, especially in Belgium and Germany, the northern limit of sandy loess in the northern European Loess Belt coincides with the southern limit of the coversands as shown by Zeeberg (1998) and Bertran et al. (2016). Due to the North Atlantic influence, loess in northern Europe has a rich stratigraphy that is generally similar within the whole domain from Normandy to Ukraine (Antoine et al., 2013, Antoine et al., 2009b; Buggle et al., 2009; Jary and Ciszek, 2013; Lehmkuhl et al., 2018b, Lehmkuhl et al., 2016; Rousseau, 1987; Rousseau et al., 2017, see Fig. 6). There is a gradual transition from the subdomains IIa to IIc due to enhanced continentality and less humidity towards the east. In addition, the distance to and extent of the last and penultimate Fennoscandian ice sheets influence the loess facies and thickness in these subdomains. The accumulation of aeolian sediments was shifting throughout the Pleistocene. Especially during the Middle Pleistocene, sediment dynamics were strongly influenced by a more southward extension of the ice sheets and by the occurrence of large ice marginal lakes. Fig. 5 indicates the extent of the Saalian and Elsterian ice sheets in the northern part of Europe modified according to Ehlers et al. (2011). The extent of Elsterian and Saalian ice sheets was more than 100 km further south in England and more than 300 km further south in the North Sea west of Denmark when compared to the Weichselian ice sheets. Such extent of ice sheets also influenced the different loess domains, especially domain II, since larger areas were covered by ice (such as IIb and partly IIc) and glacial lakes and thus the dust deflation and accumulation areas shifted further south. Especially the larger extent of ice might be the main reason for the limited accumulation of loess in domain II during the time of older glaciations. Both, ice extent and (glacial) lakes reduced the dust production areas during the Middle Pleistocene in the protogenetic domain (I) and thus they also reduced the potential for loess accumulation in domains II and III.

This domain mainly contains loess that was deposited during the last glacial cycle. During this period, environmental conditions were highly variable and included also erosive processes (slope wash, deflation, desert pavements) and periglacial processes (solifluction, involution, permafrost; Vandenberghe et al., 2014a; Zens et al., 2018). As a result, the thickness and temporal resolution of LPS can vary locally as well as between different loess regions (from <2 to more than 10 m for the same time span). However, if such erosion features appear at supra-regional scale in response to global climate events they also offer strong marker levels for correlation (Antoine et al., 2016; Schirmer, 2016; Zens et al., 2018). In our map, loess deposits in domain II cover an area of ~454,000 km^2, while sandy loess and aeolian sand are mapped on ~6100 km^2 and 14, 300 km^2, respectively (see Chapter 3.3).

3.1.2.1. IIa: Western European maritime (Atlantic) subdomain. This subdomain contains the loess deposits in northern France, Belgium, the

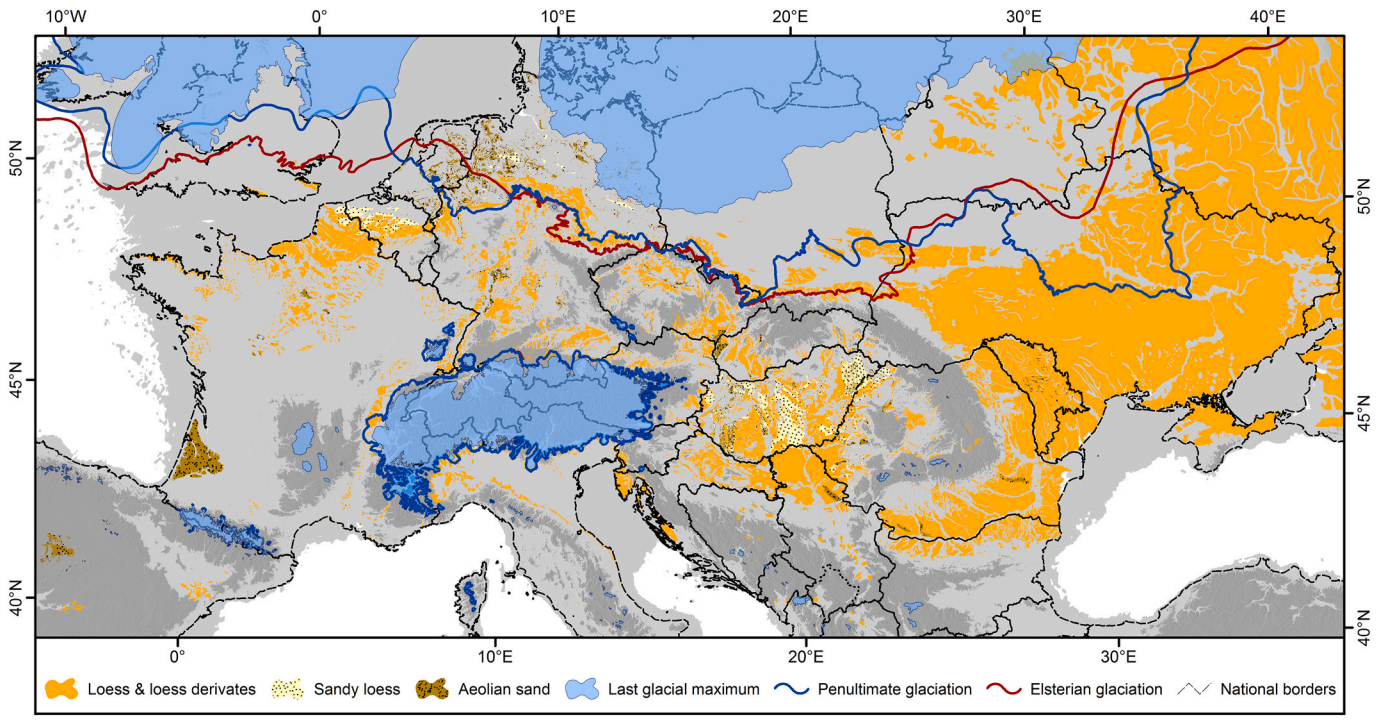

Fig. 5. Loess map and extent of Middle Pleistocene glaciation (Saalian / Rissian; Elsterian) according to Ehlers et al. (2011).

Netherlands, and the Lower Rhine Embayment in western Germany. Since the 1950s several loess stratigraphies based on paleosols and specific sedimentary units were developed for the different regions of this subdomain. The latest updates were recently published for central Belgium by Haesaerts et al. (2016), and for the Lower Rhine Embayment by Schirmer (2016), Lehmkuhl et al. (2016), and Fischer et al. (2019). A recent summary of the loess sequences in northern France and Belgium is given by Antoine et al. (2016). The studies include detailed descriptions of single units, their most important sedimentological characteristics, and their chronostratigraphic position.

In northern France, the Weichselian loess cover is represented by a semi-continuous mantle up to 8 m in thickness in favored sediment traps such as leeward slopes or fluvial terraces (cf. Fig. 7; Antoine et al., 2016). The LPS from the last interglacial-glacial cycle exhibit a particular pattern, including well-identified pedological and periglacial marker horizons that can be followed throughout Belgium and towards western Germany (Antoine et al., 2016). Loess characteristics within one location can be quite variable, where laminated decalcified loess that formed during the coldest parts of the glacial is replaced by homogenous, bioturbated, calcareous loess in the latest glacial phase. In this Atlantic subdomain, more humid conditions enhanced the erosive periglacial processes, but also led to better preservation in favorable accumulative settings (Antoine et al., 2016; Lehmkuhl et al., 2016).

For the whole area from Northern Brittany to Belgium the general stratigraphy of the last glacial period (115–11.7 ka) can be summarized as follows (Antoine et al., 2016; Antoine et al., 2001; Zens et al., 2018). The Weichselian sequence starts above the truncated last interglacial brown leached soil complex (Rocourt / Elbeuf I) and can be further subdivided by four main chronoclimatic phases: (1) Early glacial (115–72 ka) consisting of a phase with grey forest soils (early glacial A) and a phase with steppe-like soils (early glacial B); (2) Lower Pleniglacial (LPG, ≈70–58 ka): First typical homogeneous loess deposits marking the first occurrence of typical periglacial conditions; (3) Middle Pleniglacial (MPG, ≈58–32 ka): Loess deposition was strongly diminished and frequent phases of erosion reduced the resolution of MPG sediments in most LPS (Antoine et al., 2001). As a result of the relocation, the older units are redeposited in colluviums. A brown soil complex and very thin aeolian deposits have been preserved only in positions less affected by erosion; (4) Upper Pleniglacial (UPG, ≈32–15 ka): Characterized by a drastic increase in loess sedimentation and the formation of tundra-gley horizons and large ice wedge pseudomorphs, especially between 30 and 23 ka (Antoine et al., 2016; Zens et al., 2018).

The Belgian and Dutch parts of Limburg are partly covered by loess (van Baelen, 2017; Zagwijn and Van Staalduinen, 1975) and the deposits have a continuous thickness of 2 to 6 m (Antoine et al., 2003; Antoine et al., 1999a; Henze et al., 1998; Kels, 2007; Meijs, 2002). Both, Weichselian and Saalian loess deposits have been preserved (van Kolfschoten et al., 1993; Meijs et al., 2013; van Baelen, 2017; Vancampenhout et al., 2013). The LPS Romont (cf. Fig. 6), located south of Maastricht in Belgian Limburg (Haesaerts et al., 2011) is defined as a stratotype in Belgium because the sequence is the type locality of the Eben-Zone (Schirmer, 2003) and the Rocourt tephra (Juvigné et al., 2008).

The Lower Rhine Embayment shows clear differences in the presence and properties of loess related to the (meso-) relief. Loess sections in plateau-like positions are usually shorter and more affected by erosion than sections in depressions, paleochannels, on stretched slopes and slope toes. The latter ones are characterized by reworked sediments of older paleosols redeposited as heterogeneous, finely laminated colluvium (Lehmkuhl et al., 2016; Schirmer, 2016 and references therein). After the Eemian interglacial, Chernozem-like humic soils were formed under steppe-like environmental conditions. This was followed by a transition to colder and more continental conditions, which are reflected in the respective loess stratigraphies (e.g. Haesaerts et al., 2016; Schirmer, 2016; Semmel, 1998). The first phases of the last glacial loess successions are characterized by redeposited, finely laminated sediments while the loess packages contain several thin and weakly developed tundra gleys and humic soils (cf. Fig. 6; Zens et al., 2018). The most recent loess layer in this subdomain can be divided into two sedimentary facies: the niveo-aeolian (cold-humid) and the homogenous (cold-arid) loess. They were termed Hesbaye and Brabant loess in Belgium and the Lower Rhine Embayment (e.g. Haesaerts et al., 2016; Schirmer, 2016) and can be also observed in northern France (Antoine et al., 2016). While most sections in the Lower Rhine Embayment show considerable

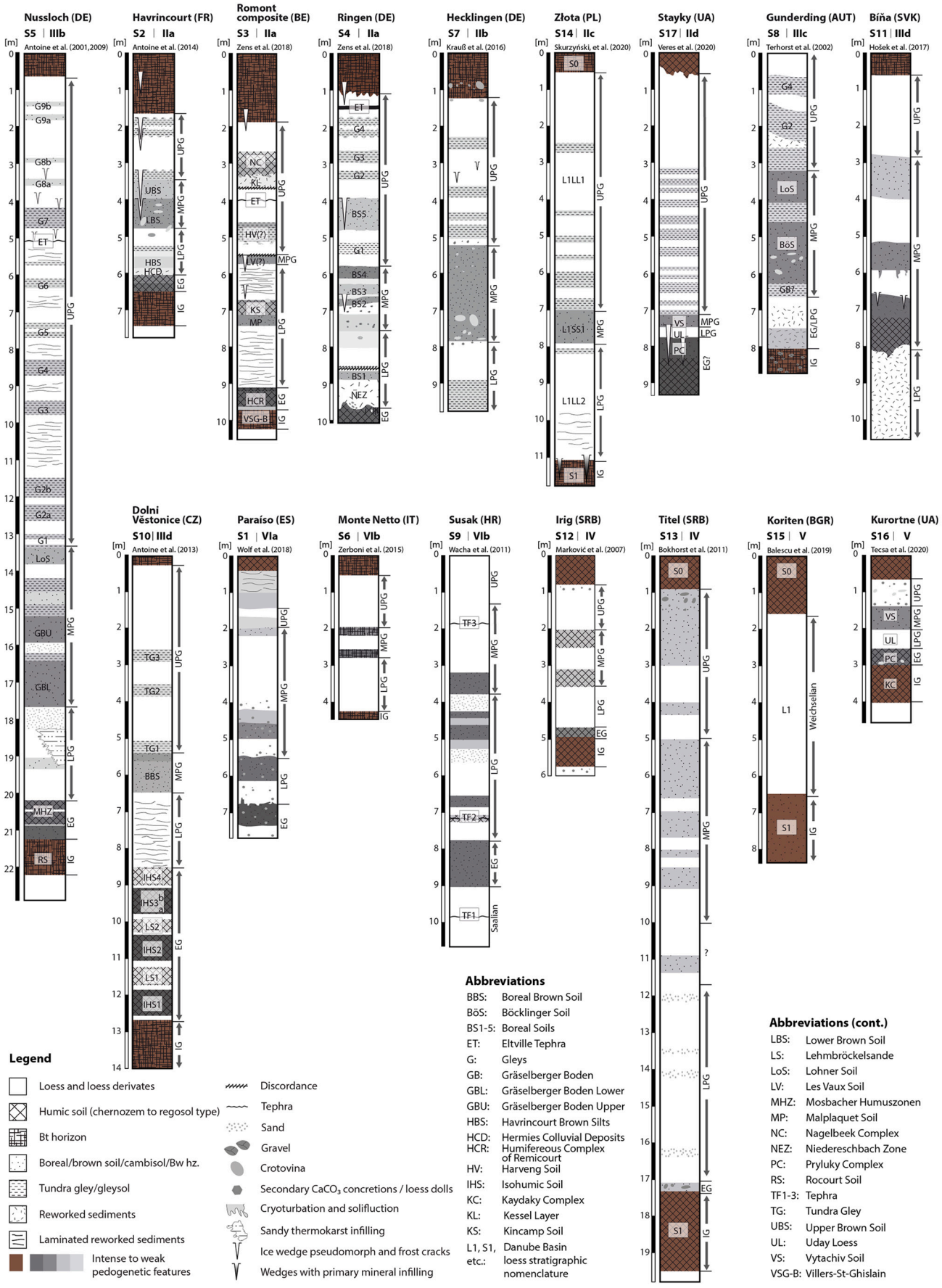

(caption on next page)

Fig. 6. Transect of 17 selected LPSs from northern France to Ukraine, which span the last glacial cycle in the respective subdomains. For correlation, all sections schematically divided in chrono-climatic units of European loess sequences (Haesaerts and Mestdagh, 2000; Antoine et al., 2013): Saalian, Interglacial (IG), Early glacial (EG), Lower Pleniglacial (LPG), Middle Pleniglacial (MPG) and Upper Pleniglacial (UPG). The interglacials are shown in brown and the glacials in grey scales. The hatchings indicate the soil types. The individual OSL ages can be obtained from the references given above the sequences; countries and loess subdomains are given as abbreviations. The locations of the LPSs are given in Fig. 4. Danube Basin loess stratigraphic nomenclature follows Marković et al. (2015). Sections were chosen to cover all subdomains based on available documentation and chronological data. (For interpretation of the references to color in this figure legend, the reader is referred to the web version of this article.)

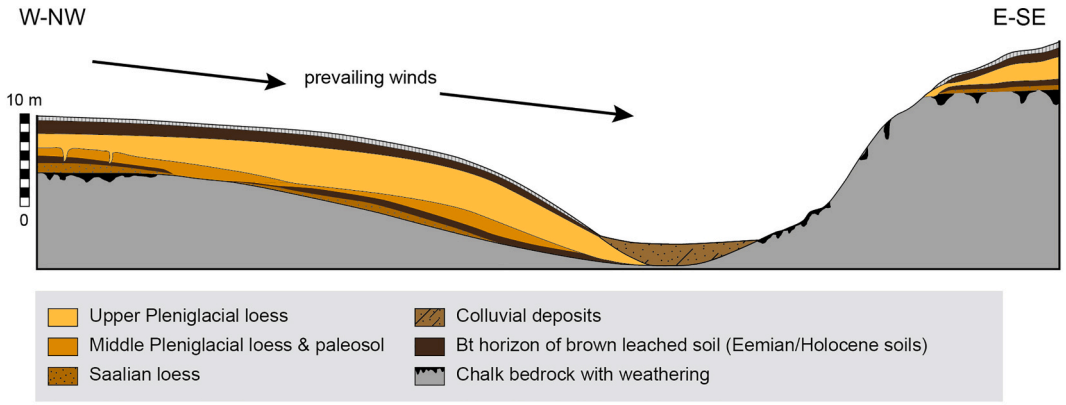

Fig. 7. Loess stratigraphy in northern France (subdomain IIa) controlled by asymmetric valley topography (modified according to Antoine et al., 2016).

variations in the presence and properties of loess related to the (meso-) relief, the LPS Remagen in the Middle Rhine valley reveals the most detailed sequence throughout the entire last glacial cycle reflecting millennial to centennial North Atlantic climate oscillations (Fischer et al., 2021; Vinnepand et al., 2020). For the northern European Loess Belt if not for entire Europe, the recent study on the LPS Remagen by Fischer et al. (2021) provides a so far unprecedented stratigraphically complete and precisely dated Late Pleistocene loess record embedded in a temporal/spatial 4D-reconstruction.

Fig. 8 shows the clear boundary of loess from the lowlands in the southern part of the Lower Rhine Embayment against the northern margins of the Eifel Mountains as part of the Rhenish Massif. Its restriction to lower elevations in the foreland is a typical feature for this subdomain. Loess in this subdomain is distributed at elevations up to ~ 320 m with a median at 117 m a.s.l. (cf. Chapter 3.3).

3.1.2.2. IIb: Western European continental subdomain. The subdomain IIb is situated in northern Germany on the northern margin of the Central European low mountain ranges from the foreland of the Rhenish Massif east of the Rhine River towards the eastern part of the foreland of

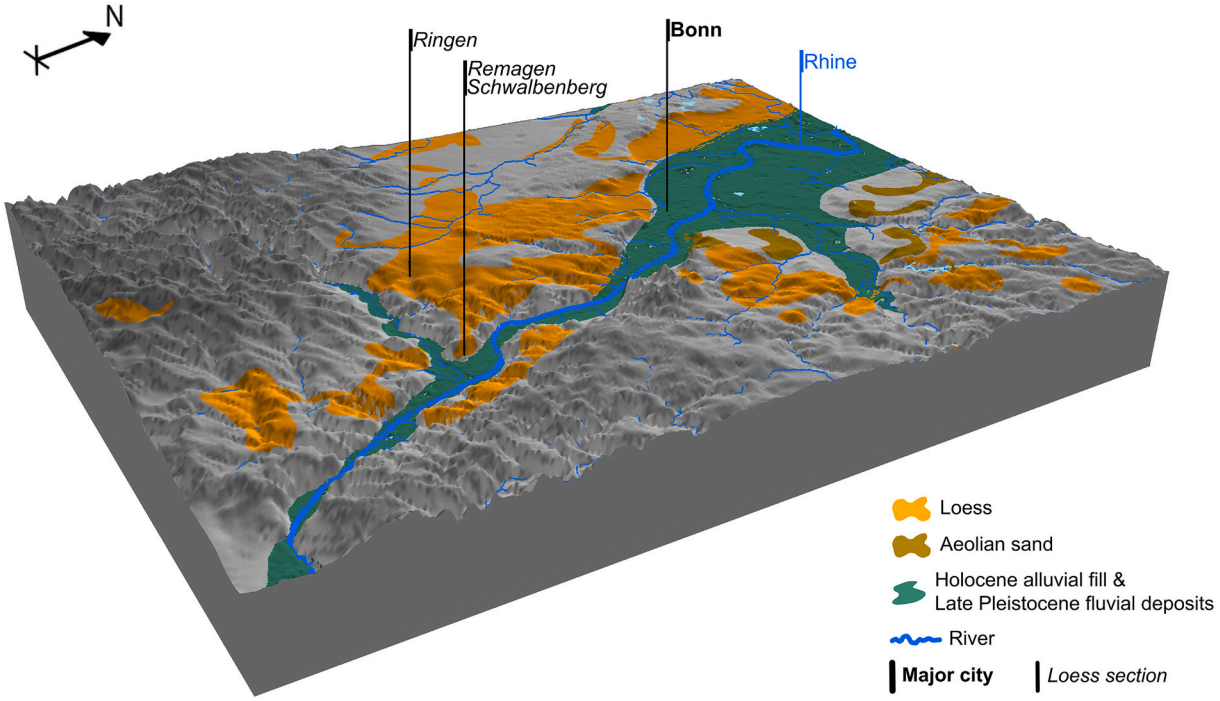

Fig. 8. 3D image of the distribution of loess, sandy deposits, and the Late Quaternary floodplain in the southern part of the Lower Rhine Embayment (No. 1 in Fig. 4). The size of the 3-D image is 40 × 55 km. Superelevated by factor 1 (no superelevation).

the Harz Mountains close to the Elbe River. Further to the east, it includes the loess region of Saxony north of the Ore Mountains, the northernmost part of Bohemia in the Czech Republic, and parts of western Poland up to the Odra (Oder) River. Thick loess sequences are mainly preserved in the eastern part of this subdomain, especially in Saxony. In the western parts, e.g. in the foreland of the Harz Mountains, a more undulating relief developed on bedrock is covered with a generally thin loess cover. This is due to the advances and fluctuations of the ice sheet margin during the Saalian glacial period into this region that resulted in the absence of older LPS (Fig. 5). Lehmkuhl et al. (2016) summarized the differences and similarities of LPS in the transition from more humid areas in the Lower Rhine Embayment towards drier areas in the east. In the foreland of the Harz Mountains, more continental climate conditions led to less intensive periglacial slope processes and solifluction, which is expressed by more complete preservation and less pronounced erosional discordances (Lehmkuhl et al., 2016). Fig. 9 shows a 3D visualization of the loess distribution surrounding the Harz Mountains including the two selected sections of Hecklingen and Zilly. Recent studies provide a summary of selected sections in the northern foreland of the Harz Mountains (Krauß et al., 2016; Lehmkuhl et al., 2016). A typical site stratigraphy is depicted in Fig. 6.

The northern margin of the loess in this subdomain is in some areas a sharp, rectilinear boundary. Sections at this loess boundary show a distinct succession of loess, sandy loess, and loess with sand layers, which were later modified by aeolian and cryogenic processes (Gehrt, 1994; Gehrt and Hagedorn, 1996). In Fig. 10, the general composition of the so-called loess-edge ramp (Leger, 1990) (German: 'Lössrandstufe') and the stratigraphy in both Lower Saxony and Saxony is summarized (redrawn and modified according to Gehrt (1994), personal communication by E. Gehrt (2020) and Haase et al. (1970)). Luminescence dating from sections of the loess-edge ramp in Lower Saxony leads to the assumption that the latest, northernmost loess formation occurred until the late glacial period. The time span covered by luminescence ages indicates sedimentation starting at ~28 ka and ending with the accumulation of sandier sediments from about 15 until 8 ka, but mainly around ~11 ka. These findings confirm earlier suggestions that the northernmost loess deposits in Germany can be linked to the return of strong aeolian processes (westerly winds) under cold and dry conditions during the late glacial that shaped this northern loess boundary (Hilgers et al., 2001a).

In Saxony, the thickness of the loess deposits increases from south to north and reaches a maximum of around 8–12 m close to the northern boundary. Northwards, there is an abrupt change from loess deposits to coarser-grained aeolian, glacial, or glaciofluvial sediments (Haase et al., 1970; Meszner et al., 2014; Meszner et al., 2013). This loess-edge ramp, comparable, but still distinct to those in Lower Saxony, marks a clear northern boundary. With a step of around 10 m, it is significantly higher than the one in Lower Saxony (Fig. 10, redrawn and modified according to Haase et al., 1970). Meszner et al. (2013) concluded from sedimentological patterns and grain size distributions that dominantly westerly winds delivered the deposited dust.

Loess in southwestern Poland is distributed in several isolated patches differing in sediment thickness, stratigraphy, and basic physical properties (Jary, 2010; Jary, 1996; Jary et al., 2016; Jary et al., 2002). Its aeolian origin was recognized early by Orth (1872). Thin, discontinuous patches of loess and loess-derived sediments prevailed but there are also thick loess covers up to 10–15 m with a well-defined stratigraphy exhibiting the last glacial period (Jary, 2007; Moska et al., 2019; Moska et al., 2012; Moska et al., 2011). Aeolian silt was derived and deposited within a relatively narrow corridor between the Weichselian Ice Sheet and the Sudetes Mountains. The loess material was presumably redistributed by the Great Odra Valley fluvial system (Badura et al., 2013) and then blown to the surroundings by strong winds from the northwest. The loess-edge ramp occurs both on the left and right side of the Oder (Odra) river valley confirming the role of the river as a main transport and redistribution medium before the final aeolian event. Loess in this subdomain is distributed at elevations up to ~380 m with a median of 160 m a.s.l. (cf. Chapter 3.3).

3.1.2.3. IIc: Central European continental subdomain. The third subdomain of domain II (IIc) is the continuation of the northern European loess belt to the east in the area of the Vistula (Wisła) basin stretching within the widening corridor between the Carpathian mountain ranges in the south and the protogenetic zone in the north towards western Ukraine (Badura et al., 2013). There is a gradual shift from subdomain IIb to more continental conditions within subdomain IIc. This also

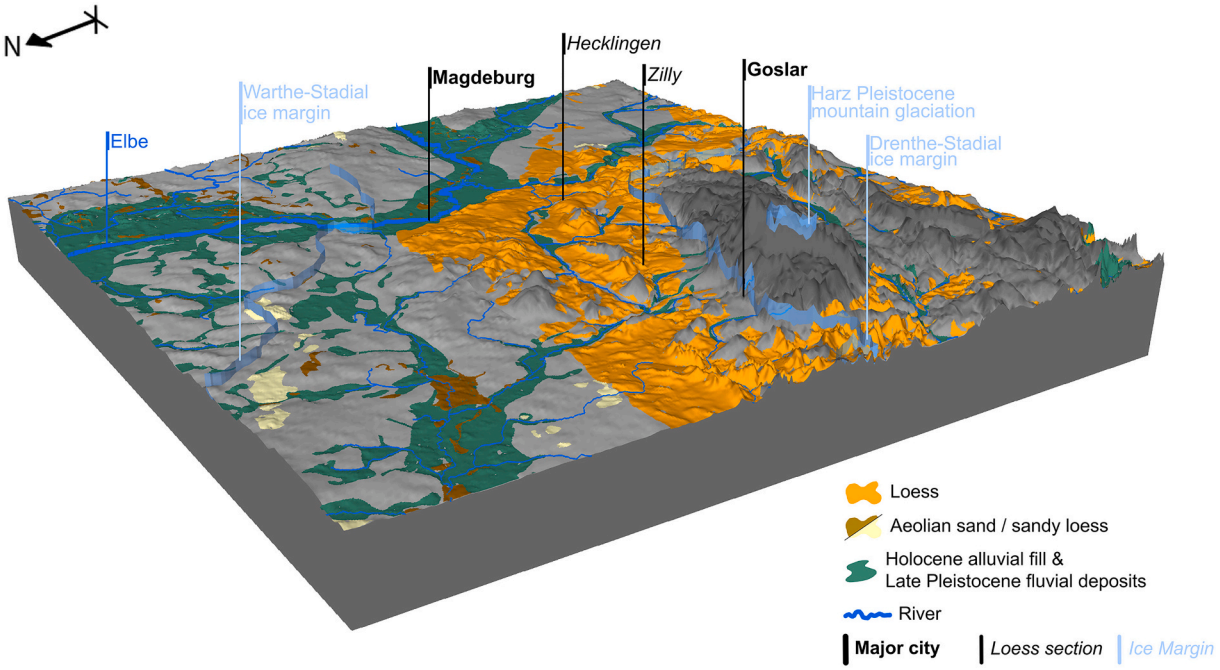

Fig. 9. 3D image of the distribution of loess, sandy deposits, and the Late Quaternary floodplains surrounding the Harz Mountains in northern Germany (No. 2 in Fig. 4). The size of the 3-D image is 180 × 190 km. Superelevated by factor 20.

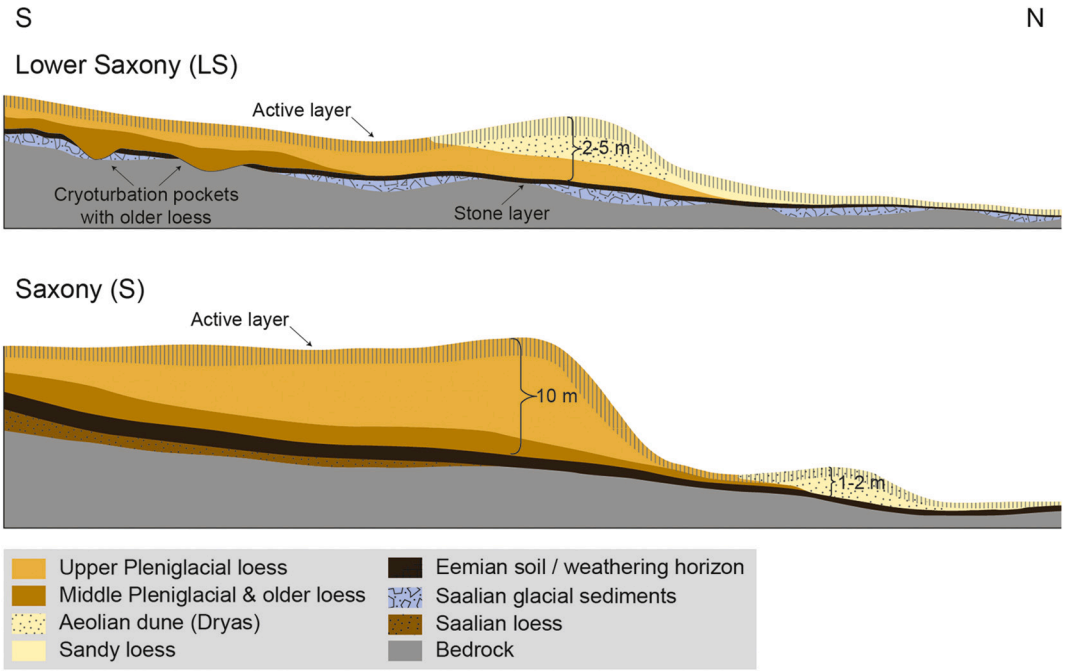

Fig. 10. Loess-edge ramp ("Lößrandstufe") in Germany: Examples from Lower Saxony (redrawn and simplified according to Gehrt (1994) and personal communication by E. Gehrt, 2020) and Saxony (redrawn and modified according to Haase et al., 1970).

affected the periglacial processes with more frequent cryoturbation horizons and larger ice wedge pseudomorphs in the east (Jary, 2009; Jary and Ciszek, 2013). Compared to subdomain IIb this area has a greater distance to the Weichselian ice sheet and due to the absence of Saalian ice in most parts pre-Weichselian loess deposits occur. Close to the border between Poland and Ukraine there is a transitional area to the eastern European continental subdomain (IId). We draw this eastern boundary at the main drainage divide between the rivers that drain towards the Baltic Sea and those that drain towards the Black Sea. In addition, the maximum extent of the Saalian ice sheet is also close to this boundary (Fig. 5). This subdomain includes also lowlands (~ 270 m a.s.l.) of the Oder (Odra) River basin in the northeastern part of Czech Republic (south Silesia, the vicinity of Ostrava city) where up to 15 m thick Middle and Upper Pleistocene LPSs are preserved in isolated patches (Macoun et al., 1965). In comparison with the southerly situated loess cover of the Morava Valley (domain III), the loess is usually completely decalcified and signs of periglacial processes are more frequent. In many sites, textural and structural features of loess (e.g. significant laminated structure or abundant redoximorphic features) together with the specific combination of wetland and aquatic mollusc assemblages indicate an ephemeral swamp or limnic environment, in which dust was deposited (so-called 'swamp loess' or German 'Sumpflöss'). This facies corresponds to large proglacial lakes and wetlands existing in the region during the Saalian and Elsterian glaciations.

For Poland, Maruszczak (1991, 1985) distinguishes three regions of loess occurrence within the southern Polish upland region (in the vicinity of Kraków, Sandomierz, and Lublin) and two foothill regions in the foreland of the Sudetes (subdomain IIb) and the Carpathians (subdomain IIc). A typical feature of the Polish loess areas is their occurrence as isolated patches and their transitional position between subdomains IIb (SW Poland) and IIc (SE Poland). Many authors claimed that the loess covers in Poland reflect present and past regional climatic conditions: continental in the east and more oceanic in the west (Cegła, 1972; Jersak, 1973; Maruszczak, 1991). The thickness, continuity and stratigraphic differentiation of loess cover increase towards the east (Jary, 2009; Jary and Ciszek, 2013). These isolated loess patches are composed of units of different ages; Late Pleistocene loess, however, predominates in the area of loess occurrence. In eastern Poland, loess of several glacial cycles formed thick sequences, locally up to 40 m thickness. A fundamental rule of loess arrangement in Poland is the connection of these deposits with a specified hypsometric level of 180–300 m a.s.l.. Locally, the lower limit drops to 150 m whereas the upper limit of loess occurrence may exceed 400 m a.s.l. (Jersak, 1973; Maruszczak, 1991; Maruszczak, 1985; Maruszczak, 1969). The thick loess mantles are often limited by distinct morphologic margins controlled by primary accumulation. The main dust sources for loess formation in Poland are usually related to the Pleistocene Fennoscandian ice sheets (e.g. Jahn, 1950; Jary and Kida, 2000; Smalley and Leach, 1978; Tutkovsky, 1899). However, some authors stress the role of local sources (e.g. Malicki, 1950; Maruszczak, 1991) and/or the significance of fluvial processes delivering material for aeolian deposits through the Vistula River and its tributaries (e.g. Jersak, 1973; Maruszczak, 1991). Most of the loess in this subdomain is found at elevations between ~ 220 and ~ 290 m a.s.l., with a minimum and maximum at ~ 170 m and ~ 440 m a.s.l., respectively (cf. Chapter 3.3).

3.1.2.4. IId: Eastern European continental subdomain. Loess in eastern Europe stretches from northern Russia and Belarus towards Ukraine, Romania, and Bulgaria in the south, until the shore of the Black Sea, and covers more than one million square kilometers including domain V and the Volga loess outside of our map. This loess field gradually transitions eastwards into the (Central) Asian steppe belt. South of the latitude of Kyiv, a virtually continuous and thick loess cover begins (Gozhik et al., 2014). We separated this subdomain from domain V because of the decreasing influence of periglacial processes (and Middle Pleistocene glacial deposits) and the increasing dust deposition towards the south. A recent example for Late Pleistocene loess in the Central Russian Upland is given in Sycheva et al. (2020).

Important source areas of this subdomain and also for domain V were the alluvial and lacustrine plains that formed in front of the advancing and retreating Pleistocene ice sheets (Buggle et al., 2008; Makeev, 2009; Velichko, 1990; Velichko et al., 2006). The outwash material was transported by north-south flowing rivers (e.g. Dnieper, Dniester, Don, or Volga) or by frequent northerly winds. The loess cover in this

subdomain is thick (usually 10–20 m, Haase et al., 2007; Li et al., 2020 report local occurrences up to 50 m). In this area, dust accumulated mainly under tundra-like environments. In some regions there are older glacial tills from the maximum extent of the Elsterian (Oka) and Saalian (Dnieper) glaciations intercalated into the loess deposits. Especially the deposits of the Dnieper glaciation in the Middle Dnieper Basin are an important stratigraphic marker horizon, that is found approximately as far south as the latitude of Dnepropetrovsk (Gozhik et al., 2014). They occur either at the base of the loess cover or as an intercalated layer within loess sequences (cf. Fig. 6; Rousseau et al., 2011). In addition, periglacial features are visible in the sections of this region (Veres et al., 2018). There is a gradual transition between this subdomain and domain V following the permafrost boundary. This transition is gradual because of the fluctuation of the ice margins and permafrost distribution during the Pleistocene. Most of the loess in this subdomain is distributed at elevations between ~ 140 m and ~ 230 m a.s.l. with maximum of ~ 370 m a.s.l. (cf. Chapter 3.3).

3.1.2.5. IIe: Central European low mountain ranges and basins subdomain. The fifth subdomain of the northern European loess belt is located in basins of the German and northern Czech low mountain ranges. As described by Lehmkuhl et al. (2016, 2018b), there is a topographic limitation of these basins and the distribution pattern of their deposits is rather fragmentary. Exceptions are the lowlands of Lower Franconia (Germany) east of Frankfurt am Main (e.g. Roesner, 1990) or the Wetterau as a part of Hessian basin between Frankfurt am Main and Gießen (see stratigraphy in Fig. 6; Steup and Fuchs, 2017). We attributed the loess downstream of the Alps in the eastern vicinity of the Rhine River in southwestern Germany to subdomain IIIc.

The loess sections further to the east in Bohemia (western part of Czech Republic) have more similarities with sections of the northern European loess belt (domain II) than those in South Moravia (the southeastern part of the Czech Republic (domain III)), as apparent e.g. from geochemical and rock magnetic investigations conducted on reference Late Pleistocene LPS (Hošek et al., 2015). The data reveal stronger leaching of central Bohemian compared to South Moravian loess and paleosols suggesting more humid conditions in the more northwesterly situated Bohemia. Consequently, these findings suggest that the transitional zone between the two climate regions of the Late Pleistocene climate in central Europe could be quite narrow. Bohemia was and is under the direct influence of Atlantic cyclones whereas South Moravia belongs geographically to the Pannonian forest steppe landscapes, which were marked in the Late Pleistocene by continuous dry continental climate conditions, under the fluctuating influences of a temperate sub-Mediterranean climate (Krolopp and Sümegi, 2002; Marković et al., 2007). In addition, the region benefits from its rain shadow position in the southeast of the Bohemian Massif and its proximity to the Carpathian Basin where dry and warm air masses can penetrate. Therefore, we attribute the Bohemian area to IIe and the Moravian loess to the subdomain IIId. Most of the loess in this subdomain is distributed at elevations between ~ 230 m and ~ 330 m a.s.l. with a minimum and maximum of 125 m and 480 m a.s.l. (cf. Section 3.3).

3.1.2.6. Marker features and horizons allow correlation in domains II and III. The complexity of the pedosedimentary and stratigraphical evolution of the last glacial cycle loess is particularly high in subdomain IIa and decreases eastwards, while the loess thickness increases on average (Fig. 6). By using pedostratigraphical units as markers, a correlation over the whole European loess area is possible. During phases of strong erosion (visible by unconformities) in the LPG and UPG, especially but not exclusively on slope sites, the interglacial and MPG soil complexes were eroded. Romont (compare Fig. 6) shows the incomplete stratigraphic record of some profiles whereas Remagen and Nussloch areis rather exceptions concerning preservation conditions allowing for high-resolution paleoenvironmental reconstruction and enabling millennial-scale correlation to North Atlantic climatic fluctuations (DO-Cycles etc.).

Marker features such as the Eltville Tephra, or the Eben unconformity allow an inter-section correlation of individual profiles, and the correlation between subdomains and domains, especially between domains II and III. In these domains, the homogenous uppermost loess package often starts above a periglacial marker horizon: the Nagelbeek tongue horizon (Haesaerts et al., 1981) or Nagelbeek Complex (E4 Soil, Haesaerts et al., 2016; Schirmer, 2016, Schirmer, 2003). This important marker horizon follows a major unconformity (Eben unconformity) which is continuously traceable in the western and central European loess regions (Krauß et al., 2016; Pouclet and Juvigne, 2009; Zens et al., 2018; Zens et al., 2017). The niveo-aeolian laminated loess below contains several tundra gleys (Gelic Cryosols) and the Eltville Tephra (Pouclet and Juvigne, 2009; Zens et al., 2017), which also allows correlation beyond different domains (Zens et al., 2017). This laminated loess is a marker-facies found from western France to Belgium and even to the Czech Republic in Dolní Věstonice (Antoine et al., 2013; Fuchs et al., 2013; Kukla, 1977) for the period between about 28–23 ka (Moine et al., 2017). For the MPG, the main pedostratigraphic pattern allowing for lateral correlation (Fischer et al., 2021; Zens et al., 2018) is the occurrence of various interstadial soils with varying intensities and pedogenetic characteristics. They are labeled as Saint-Acheul-Villiers-Adam (Antoine et al., 2003) or Lower and Upper Brown Soils (Antoine et al., 2016) in France, Les Vaux Soil in Belgium (Haesaerts et al., 2016); Lohne Soil, Böcking Soil, Boreal Soil 2 and 4 (Zens et al., 2018; Zöller and Semmel, 2001), Remagen-1 to 5 Soils (Frechen and Schirmer, 2011), and Boreal Brown Soil (Antoine et al., 2013; Fuchs et al., 2013) in Germany and Czech Republic. Due to low sedimentation rates, the MPG soils are often condensed to a polygenetic brown soil complex, which represents the entire period. However, in the Remagen LPS of the Middle Rhine Valley a detailed millennial-scale record provides a detailed stratigraphy of MPG soil and loess intercalations (Fischer et al., 2021). During the Lower Pleniglacial, the earliest Weichselian loess deposit (MIS 4, 60–70 ka) can be considered as a very good marker-level for correlation throughout the area (Haesaerts et al., 2016). Below this loess layer follows a Boreal brown soil called Havrincourt Brown Silt in France (cf. Fig. 6; Antoine et al., 2014), Boreal Soil 1 (Zens et al., 2018) or Malplaquet Soil in Belgium (Haesaerts et al., 2016), and Jackerath Soil (Regosol-Cambisol) in the Lower Rhine Embayment (Schirmer, 2016). Finally, a characteristic humic soil complex, namely the Humiferous complex of Remicourt (Haesaerts et al., 2016), Saint-Sauflieu Soil Complex (Antoine et al., 2016), Mosbacher Humus Zone (cf. Fig. 6, Zens et al., 2018), Isohumic Soil (Antoine et al., 2013), Pryluky complex (Rousseau et al., 2011; Tecsa et al., 2020; Veres et al., 2018 and references therein) developed under early glacial conditions and includes up to four distinct horizons. It is traceable from northern France towards Ukraine (Antoine et al., 2013; Haesaerts et al., 2016; Haesaerts and Mestdagh, 2000). Due to its widespread distribution this soil complex serves as one of the major marker units of the last glacial (Fig. 6).

The preservation of the sedimentary markers, especially the tephra layers, is often achieved by high aeolian accumulation rates at the time of their deposition. Therefore, for example at Ringen five individual bands of the Eltville Tephra can be differentiated (Zens et al., 2017).

3.1.3. III: Loess adjacent to Central European high-altitude mountain ranges (northern Alps and Carpathians)

This domain comprises the western, northern, and northeastern margins of the European Alps, the northern part of the Carpathian Basin and Transylvania and the adjacent basins and catchments. During the LGM this domain was influenced by periglacial activity indicated by tundra gley soils and cryogenic features. The resulting subdomains are located in the valleys of the Saône and Rhône rivers, the Upper Rhine graben and the upper reaches of the Danube including adjacent areas. Additionally, we enclose the northern part of the Carpathian Basin (southern slopes of the Western Carpathians) and Transylvania, as

periglacial processes also affected loess deposits in these areas. These areas are strongly impacted by major rivers, originating in the Alps (Rhône and Rhine), the Black Forest (the Danube), the central Alps (major tributaries of the Danube such as the Inn River), and the Carpathian Mountains (e.g. Tisa, Somes, Mures), which are responsible for the silt transport from the Pleistocene alpine glaciers and mountainous regions influenced by physical weathering such as frost shattering. All these areas were influenced by periglacial conditions during loess accumulation and therefore the LPS of this domain are usually comparable with those from the northern European loess belt (domain II). A west-east trend in increasing climate continentality, modulated by regional topographic variations, can be recognized in the character of the intercalated interglacial and interstadial paleosols. Our map shows ~53,000 km^2 loess, ~5500 km^2 aeolian sand, ~10,100 km^2 sandy loess, and ~ 79,000 km^2 alluvial fill and fluvial deposits in this domain (Table 1).

3.1.3.1. IIIa: Saône to lower Rhône subdomain. This subdomain in the Saône and lower Rhône catchments in southeastern France stretches from the confluence of the Rhône with the Saône River northward towards the Vosges. The source of the Rhône is close to the Pleistocene Rhône paleoglacier and other smaller alpine glaciers along the western margin of the Alps. The climatic conditions along this north-to-south trending region represent a gradient from a humid-temperate to a Mediterranean climate today or warmer temperate climatic condition without permafrost during the LGM, respectively. Because the area south of Valence (~45°N) has been strongly influenced by the Mediterranean climate conditions we categorized this part to subdomain VIa (Bosq et al., 2018, 2020a). Recent studies investigate the Pleistocene loess of these areas, highlighting the Rhône River as the major dust source in the area. The (paleo-)wind direction in the southern part, the Rhône graben, is north-south since air masses are channelled and concentrated by the topography. The more Mediterranean influenced loess sequences of the southern Rhône Valley and the Provence seem to have their source area more in ophiolitic areas of the Alps (Bosq et al., 2020a). Most of the loess in this subdomain is distributed in elevations between ~ 200 m and ~ 270 m a.s.l. with a minimum and maximum of ~ 130 m and ~ 520 m a.s.l. (cf. Chapter 3.3).

3.1.3.2. IIIb: Upper Rhine subdomain. This subdomain comprises loess in the Upper Rhine Plain (Graben) and adjacent areas, such as the Kraichgau and Neckar Basin to the east. Common features of this subdomain are (1) the Pleistocene glaciations of the Alps and the higher mountains of Jura, Vosges, and Black Forest as proximal areas for glacial silt production, (2) periglacial silt production and regional sediment transport of the Rhine River and its tributaries until the northern end of the Upper Rhine plain and aeolian transport from the wide Pleistocene braided river plain, and (3) features of periglacial overprinting of the LPS.

Switzerland was largely covered by ice during the last glaciations. Loess deposits of few meters in thickness are present on high terraces and hills in the lowlands close to Aarau and along the Rhine River (Christ, 1944; Christ, 1942; Christ and Nabholz, 1950; Gouda, 1962). In the Upper Rhine Plain, the Rhine developed a large braided river system during the Pleistocene providing abundant material for mineral dust deflation. In the marginal hills of the southern Upper Rhine Plain and at the Kaiserstuhl, loess reaches in places thicknesses of more than 25 m (Guenther, 1987). Fig. 11 indicates locations of important LPS in the Rhine-Neckar region, including the European reference LPS Nussloch located in a loess greda (dune-like morphology), characterized by an exceptional high last glacial dust accumulation rate (see Fig. 6; Antoine et al., 2009b; Antoine et al., 2001; Moine et al., 2017 and references therein). Fig. 11 illustrates the distribution of alluvial fill and aeolian sediments from the middle Upper Rhine Graben and the adjacent eastern shoulders with elevations between 300 and 600 m a.s.l. (e.g. the Kraichgau and Neckar Basin). Aeolian sands are located close to the Rhine, indicating their local transport by westerly winds. Further east widespread loess covers suggest large-scale silt transport from the dry riverbeds of the Rhine, with a clear Alpine contribution (Bosq et al., 2020a). Antoine et al. (2009a) further assume significant deposition of dust from the English Channel and northern France in the region close to Heidelberg. Upstream the Neckar and its tributaries we assume next to the contribution from the glaciated Black Forest regional periglacial silt sources. Loess formation in subdomain IIIb occurred mainly under the cold and dry periglacial condition in a cold tundra environment (recent publications and references therein: Kadereit et al., 2013; Krauß et al., 2017; Zens et al., 2018). The lowlands in this region were slightly drier

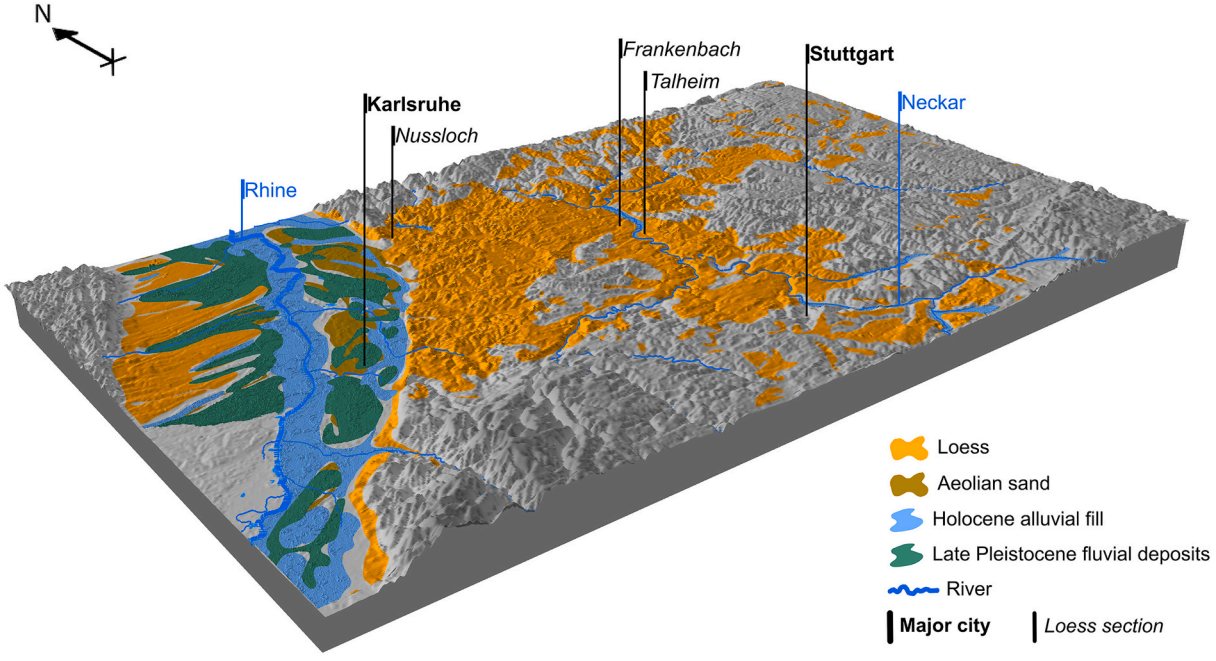

Fig. 11. 3D image of the distribution of loess, sandy deposits, the Late Pleistocene fluvial deposits and Holocene floodplain in the Upper Rhine Graben, the Kraichgau and Neckar Basin (No. 3 in Fig. 4). The size of the 3-D image is 95 × 155 km. Superelevated by factor 1 (no superelevation).

compared to the neighboring regions in the north and west, but there are also a lot of similarities to the northern European loess belt including tundra gley soils (Gelic Cryosols) and some of the same marker soil horizons.

Swiss LPS are few and poorly studied. Most known is probably the c. 17 m thick Middle to Late Pleistocene section formerly exposed in the brickyard of Allschwil near Basel (Zollinger, 1991). 23 km upstream the Rhine, drillings revealed more than 6 m thick last glacial loess deposits, recently studied by Gaar and Preusser (2017). Close to Freiburg, at Heitersheim and Riegel, 20 to 30 m of loess contain one or more interglacial Bt horizons (Guenther, 1987). There are also thick loess sequences on the western side of the Rhine River in France; the most prominent site is Achenheim, including three interglacial paleosols along a more than 30 m thick LPS, which also contains Paleolithic findings (see Rousseau and Puisségur, 1990 and references therein). The LPS of the Rhein-Neckar region are shown in Fig. 11 (see also Bibus, 2002). The 23 m thick Nussloch LPS (see Fig. 6) is well known as highly resolved Upper Pleniglacial loess record of central Europe (Moine et al., 2017; Prud'homme et al., 2016). At Mainz-Weisenau, at the northern end of the Upper Rhine Plain, thick LPSs are exposed, for example the last interglacial soil and three early glacial humus zones (e.g. Bibus et al., 2002). Most of the loess in this subdomain is distributed in elevations between ~ 190 m and ~ 350 m a.s.l., with a minimum and maximum of ~ 110 m and ~ 580 m a.s.l. (cf. Chapter 3.3).

3.1.3.3. IIIc: Northern margin of the European Alps subdomain (upper Danube). Subdomain IIIc comprises loess in southern Germany and northeastern Austria, which stretches mainly along the Danube River and its southern tributaries. These are primarily the water and sediment laden rivers draining the Alps, respectively the front of the alpine Würmian ice margin. Loess deposits are mainly found directly next to the (glacio-)fluvial source areas and are widely distributed on terraces older than the last glacial cycle. Very little silt contribution comes from the non-glaciated highlands north of the Danube (Swabian-Franconian Alb, Bohemian Massif). This subdomain ends at the southern end of the Bohemian Massif, where the Danube tributaries are no longer draining former glaciated areas. Furthermore, the Bohemian Massif acts as a barrier for moisture brought by the Westerlies, resulting in a change of loess facies. Carbonate-bearing loess in subdomain IIIc is largely restricted to the thickest last glacial deposits and the lowest altitudes of this region, whereas loess sediments in subdomain IIId usually have high carbonate contents (Fink, 1965). Closer to the Alps, with increasing moisture, the decalcified loess shows redoximorphic features, which corresponds to the brown loess and dust loam facies, respectively (Fink and Nagl, 1979). Most of the loess and loess derivates in subdomain IIIc are located at elevations between ~ 380 m and ~ 490 m a.s.l., with minimum and maximum values of ~ 290 m and ~ 640 m a.s.l. (see Chapter 3.3).

Upper terrace gravel pits expose up to 5–10 m thick last glacial LPS, for example Bobingen in southwestern Bavaria (Mayr et al., 2017) or Gunderding in northeastern Austria (Terhorst et al., 2015). LPS of 10–15 m thickness reaching back into the Middle Pleistocene (with several Bt horizons) can be found in loam pits, usually on older Terrace levels (German 'Deckenschotter') and in the Neogene Alpine molasse hills, e.g. at Hagelstadt in Central Bavaria (Strunk, 1990) or Wels-Aschet in northeast Austria (Terhorst, 2013).

3.1.3.4. IIId: Eastern margin of the European Alps and northern Carpathian Basin (including adjacent basins) subdomain. This subdomain comprises the loess in the eastern parts of the Bohemian Massif, the eastern and southeastern margin of the Alps and the widespread loess covers east of the uplands reaching from northeast Austria and southeast Czech Republic (Moravia) into the northern part of the Carpathian Basin (southern Slovakia, northern Hungary, and Romania). The importance of the Danube alluvium as a sediment supplier for dust deflation in subdomain IIId is widely accepted. The conceptual study by Smalley and Leach (1978) was supported by provenance studies using heavy minerals (Újvári et al., 2013; Újvári and Klötzli, 2015). However, these studies also highlight the importance of spatially constraint sediment transport pathways. The loess deposits of Upper Austria show significant input from detrital material derived from the Eastern Alps, which was primarly reworked by fluvial activity. Further east, detrital zircon ages of loess deposits near Krems point to influences of material eroded from geological units of the nearby Bohemian Massif (Újvári et al., 2013; Újvári and Klötzli, 2015). Detrital material from the Bohemian Massif is also of special importance for loess deposits of Moravia and Silesia (Lisá, 2004; Lisá and Uhler, 2006). Generally, the influence of the Danube as a sediment supplier in this subdomain decreases with increasing distance to the river, as local sources gain more importance (Schatz et al., 2015a). Additionally, regions far downstream from the Alps, especially towards domain IV, contain significant proportions of reworked older loess, remobilized by wind and river erosion (Smalley and Leach, 1978).

In northeast Austria, loess sediments are widespread along the higher terraces of the Danube and adjacent hills (Fig. 12) locally reaching almost 40 m thickness at Krems, where the Danube leaves the narrow valley cutting through the Bohemian Massif (Wachau). Within the Wachau and at the eastern margin of the Bohemian Massif loess deposits are highly variable in age and thickness and often contain fragments of local rock mixed in by slope processes (Sprafke, 2016; Sprafke and Obreht, 2016). A high carbonate content (c. 20–25%) and loess-like structure made Vetters (1933) map these silt-dominated deposits as loess, whereas decalcified aeolian silts in northwestern and southeastern Austria remain largely ignored on geological maps (see section 2). Thick loess deposits in northwestern Austria and Moravia can be found in the lowlands of the larger tributaries of the Danube (Morava/Thaya), but on the eastern side of these rivers at the border to the Slovakian Republic, large deposits of aeolian sand accumulated, which indicates that the wind mainly deflated dry floodplain deposits from western directions. Notable loess covers of variable thickness are present in the rolling hills between the larger rivers, but the highest altitudes between Danube and Thaya remain free of loess (Fig. 12).

LPS close to the Bohemian Massif and in the hills of northeastern Austria are variable in age and stratigraphic resolution. Interglacial paleosols in the Krems region are often polygenetic or missing completely because of reworking or differential erosion, especially at late phases of interglacials, which renders pedostratigraphical approaches rather difficult (Sprafke, 2016). The classical LPS of Krems-Schießstätte (shooting range) and Stranzendorf are unique loess records of the Early Pleistocene paleoclimatic cycles (Fink and Kukla, 1977; Kukla and Cílek, 1996). The LPS Paudorf and Göttweig near Krems expose Middle Pleistocene to last interglacial pedocomplexes (Sprafke et al., 2014; Thiel et al., 2011b). Thick calcified last glacial loess packages in the Wachau and Krems region are also famous for Upper Paleolithic cultural layers, e.g. at Willendorf (Wachau; Nigst et al., 2014), Krems-Hundsteig (Neugebauer-Maresch, 2008), Krems–Wachtberg (Einwögerer et al., 2006; Sprafke et al., 2020), and Stratzing (Neugebauer-Maresch, 1993; Thiel et al., 2011a).

Cumulative loess thickness can reach up to 50 m in South Moravia, especially towards the Bohemian Massif foothills (Hošek et al., 2017, Hošek et al., 2015; Lehmkuhl et al., 2018a; Zeman et al., 1986, 1980). The famous LPS Červený Kopec (Red Hill) at Brno (southeastern edge of Bohemian Massif) is an exclusive example of such accumulation. This classical loess section, intercalated by fourteen pedocomplexes, provides the most complete record in central Europe, covering the last 1 Ma, i.e. MIS 25 – MIS 2 (Kukla, 1975). Fig. 13 shows the Červený kopec section with the terraces CK 1–5 covered with LPS (redrawn and modified sketch from Kukla, 1978, 1977).

In southwestern Slovakia, Middle and Late Pleistocene loess covers a vast area of Danube and Záhoří lowlands, reaching up to 40 m in thickness (Šajgalík and Modlitba, 1983). To the north (higher elevation along the western Carpathians) and the east (East Slovakian lowlands),

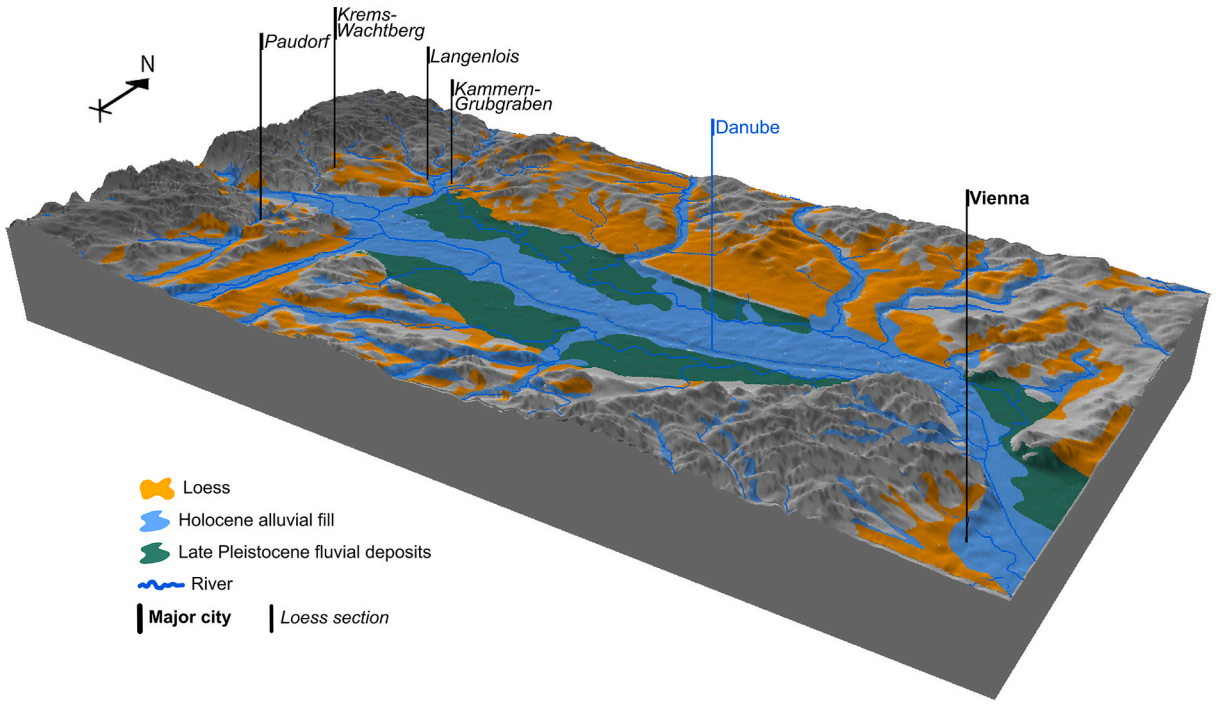

Fig. 12. 3D image of the distribution of loess, sandy deposits, the Late Pleistocene fluvial deposits and Holocene floodplain in Lower Austria (No. 4 in Fig. 4). The size of the 3-D image is 35 × 70 km. Superelevated by factor 1 (no superelevation).

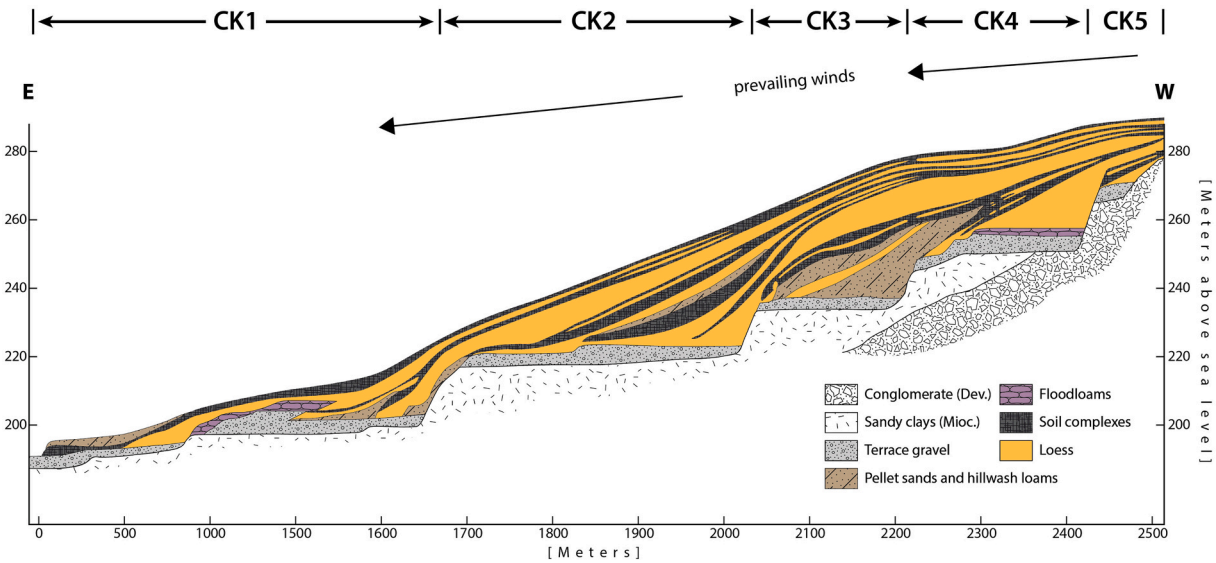

Fig. 13. Redrawn and modified sketch from Kukla (1977, 1978) showing the Červený kopec (Red Hill) section at Brno Czech Republic with the terraces CK 1–5 covered with LPS. The section was exposed in an excavation front of a brickyard pit and in boreholes. (For interpretation of the references to color in this figure legend, the reader is referred to the web version of this article.)

loess becomes coarser than in southwestern Slovakia and is mainly decalcified and polygenetic exibiting strongly (pseudo)gleyed paleosols (Košťálik, 1989; Lehmkuhl et al., 2018a; Šajgalík and Modlitba, 1983; Vaškovský, 1977). Some smaller patches of loess and loess derivates can also be found in the Carpathian foothills in western Ukraine, which also belong to this subdomain.

Loess and its derivates and coarser variants, as well as aeolian sand, are widely distributed in (northern) Hungary (Pécsi, 1987) and northwestern Romania. Loess deposits are distributed along the Danube and Tisa rivers. Several famous loess sections are part of this subdomain such as the LPS Basaharc (Sümegi et al., 2011), Mende (Borsy et al., 1979; Frechen et al., 1997; Marton, 1979; Wagner, 1979), Albertirsa (Novothny et al., 2002), and Süttő (Fig. 6; Barta, 2014; Koeniger et al., 2014; Novothny et al., 2011, Novothny et al., 2009; Profe et al., 2018a; Rolf et al., 2014). Most of the investigated loess sequences are located within the basin along the major rivers, but also in northeastern Hungary two sites were recently investigated in detail: Bodrogkeresztúr and Tokaj (Bösken et al., 2019; Schatz et al., 2015a, 2015b; Schatz et al., 2012; Schatz et al., 2011; Sümegi et al., 2016b; Sümegi et al., 2000). These sites highlight the more humid paleoenvironmental conditions at the Carpathian foothills with regard to the center of the Carpathian Basin.

Geomorphological processes in the northern part of Carpathian Basin were controlled by strong northern and northwestern winds during glacial times (Sebe et al., 2011). Most of the loess in this subdomain is distributed in elevations between ~ 130 m and ~ 260 m a.s.l. with a minimum and maximum of ~ 80 m and ~ 540 m a.s.l. (cf. Chapter 3.3).

3.1.3.5. IIIe: Transylvanian subdomain. Loess is distributed in one greater area in the western Transylvanian Plateau and several small, isolated patches along the rivers in the rest of the basin. Due to the high elevations and the proximity to the (partly) glaciated Carpathian Mountains, the relatively steep slopes resulting from significant basin-wide neotectonic activity (including salt and gas diapirism), the Quaternary sediments were strongly influenced and overprinted by permafrost and periglacial features (Pendea et al., 2008). Additionally, the sequences in Transylvania are often disturbed by slope processes, resulting in colluviated loess and loess derivates (Jakab, 2007; Pendea et al., 2009). These deposits are an archive for the landscape evolution of the area, but it is challenging to use them as paleoclimate archives. Most of the loess in this subdomain is distributed in elevations between ~ 330 m and ~ 460 m a.s.l. with a minimum and maximum of ~ 210 m and ~ 710 m a.s.l., in thicknesses up to 20 m, especially along the Aries and Mures river cuesta (cf. Chapter 3.3).

3.1.4. IV: Middle Danube loess

The loess domain of the Middle Danube Basin has seen a long tradition in loess research (Marković et al., 2016; Obreht et al., 2019) and contains some of the thickest European loess sequences (at least >50 m in outcrops and approx. >100 m recorded from drillings; Koloszar, 2010; Sümegi et al., 2018), preserving a quasi-continuous paleoenvironmental record extending back to the Early Pleistocene (Buggle et al., 2013; Marković et al., 2011, 2015; Schaetzl et al., 2018). In this domain we include the central and southern part of the Carpathian Basin (Middle Danube Basin). The southern limit of the extensive spatial loess distribution in this domain follows the valley of the Great Morava River and is bounded to the south by the foothills of the Dinaric and Carpathian-Balkan mountain ranges. South of these areas, loess distribution is characterized by many isolated deposits that essentially originate from local sources (see subdomain VIc).

The loess deposits of the Carpathian Basin and adjacent areas are not as homogeneous as one might expect. In the western part of domain IV between southeastern Austria and Croatia the distinction between Neogene Pannonian Basin silts and loess is not always clear, which is complicated by redoximorphic features overprinting these sediments, i.e. dust loam according to Fink and Nagl (1979) and pseudogleyed loess derivates according to Rubinić et al. (2018). Yet, these poorly mapped and investigated loess deposits can reach 10 m in thickness at the northern side of the Mur River draining the Alps. There is a gradual transition towards the southern part of domain IV that is reflected in slight shifts in (paleo-)vegetation and environment from periglacial conditions with tundra and forest-steppe towards drier steppe conditions. Thus, loess from the central and southern part of the Carpathian Basin does not belong to the same loess facies as the northern part (i.e. Moravia, the eastern parts of Austria and the northern Hungarian plain). Loess deposits from domain IV share more commonalities with the loess deposits of the Lower Danube Basin (domain V). However, modern and Pleistocene climate conditions differed between the Carpathian Basin (Middle Danube Basin) and the Lower Danube Basin: Both are rather continental but the aridity is more pronounced in the latter one (Botti, 2018; Obreht et al., 2017).

Generally, LPSs in the Middle Danube Basin reflect typical loess plateau deposition (e.g. Marković et al., 2018a). Characteristics of these LPS also indicate a paleoclimatic gradient towards warmer and drier conditions from northwest to southeast (Sümegi and Krolopp, 2002). Drier conditions indicated better preservation of more complete LPS in the southeastern part of the Carpathian Basin (Marković et al., 2015; Marković et al., 2008) and also higher sedimentation rates (Antoine et al., 2009a; Bokhorst et al., 2009; Sümegi et al., 2013; Újvári et al., 2017; Újvári et al., 2010). The domain is positioned in an important geographic location, being close enough to the Atlantic Ocean to record its weakened influence, but at the same time isolated inland by surrounding mountains and partly protected from intensive cold Arctic air masses. Because of the geographic setting, climate and environmental conditions in the southeastern Carpathian Basin region were more stable than those elsewhere, as indicated by paleoclimate records from other European late Pleistocene LPSs (Antoine et al., 2001; Antoine et al., 1999b; Rousseau, 2001; Rousseau et al., 1998; Vandenberghe et al., 1998). The mechanisms behind dust accretion in loess plateaus seem to be restricted to steppe environments in which seasonal droughts during late summer and early autumn occur (Buggle et al., 2014; Buggle et al., 2013). In those climates of Cfb to Cfa type (Walter, 1974) biological loess crusts and mats played an important role serving as dust traps and possibly also facilitating loessification and transforming the semi-continuous accretion of dust to stable LPS (Svirčev et al., 2019). Together with the flora of the semi-desert to steppe environments the biocrusts effectively protect LPS from erosion and deflation leading to plateau deposits which record Pleistocene environmental history since the late Lower Pleistocene at least.

The loess plateaus of domain IV are mainly located between the floodplains of the Danube River and its major tributaries, such as Tisa, Drava, Sava and Timis/Tamiš. Loess plateaus are remarkably thick at the confluences of the rivers, where deflatable material from both sides was deposited (Fitzsimmons et al., 2012; Marković et al., 2008). This indicates that the Danube River and its tributaries were important source areas during the Pleistocene, at least for the relatively coarse-grained silt and sand fractions (Bokhorst et al., 2011; Buggle et al., 2008; Smalley and Leach, 1978; Újvári et al., 2012; Újvári et al., 2008), while smaller particles potentially can be of far-distance origin (Varga et al., 2019; Zeeden et al., 2016). Fig. 14 provides an overview of different loess landscapes and loess sections along the Danube in the southern part of the Carpathian Basin and their geomorphological situation. Loess and loess derivates are distinguished according to Lehmkuhl et al. (2018a). The lowermost and youngest terraces of the Tisa, Sava, and Danube rivers and their tributaries are covered by loess-like sediments and loess derivates and are therefore often referred to as loess terraces. The famous Titel loess plateau, which is situated in the Danube-Tisa-interfluve, can be clearly distinguished in the figure. Next to the Titel LPS (Bokhorst et al., 2009), also the 20 m thick Surduk LPS on the opposite bank of the Danube exhibits a very detailed record of the last interglacial-glacial cycle (Antoine et al., 2009a; Fuchs et al., 2008). Surduk is located at the edge of the Srem loess plateau, which has been formed between the Danube and Sava rivers at the southern and eastern slopes of the tectonically uplifted Fruška Gora Mountains. These mountains are surrounded to the south by a system of loess covered alluvial fans, with decreasing loess thickness upslope. This geomorphic situation influences e.g. the stratigraphic succession and the characteristics of paleosols (Vandenberghe et al., 2014b). Whereas the upslope section of Irig shows pure aeolian set-up, the downslope section of Ruma comprises a loess facies also characterized by intense sediment relocation (Marković et al., 2007; Marković et al., 2006; Pötter et al., 2020; Vandenberghe et al., 2014b). The plateaus continue west of the Fruška Gora Mountains in eastern Croatia, where loess is regarded as generally pure or unaltered.

Quaternary limnic, alluvial, and marshy sediments are overlain by aeolian deposits in the Croatian part of the Carpathian Basin (e.g. Marković et al., 2009; Galović et al., 2011). Loess and loess derivates continue into the Slavonija-Srijem/Srem region in Croatia, along the Danube-Drava-Sava interfluve where several LPS were described. This region can be regarded as the southernmost border of loess in the Carpathian (Middle Danube) Basin. Loess mostly covers alluvial river terrace sediments and forms smaller plateaus in the river interfluve. There are several LPS described, e.g. Šarengrad, Vukovar, Erdut, and

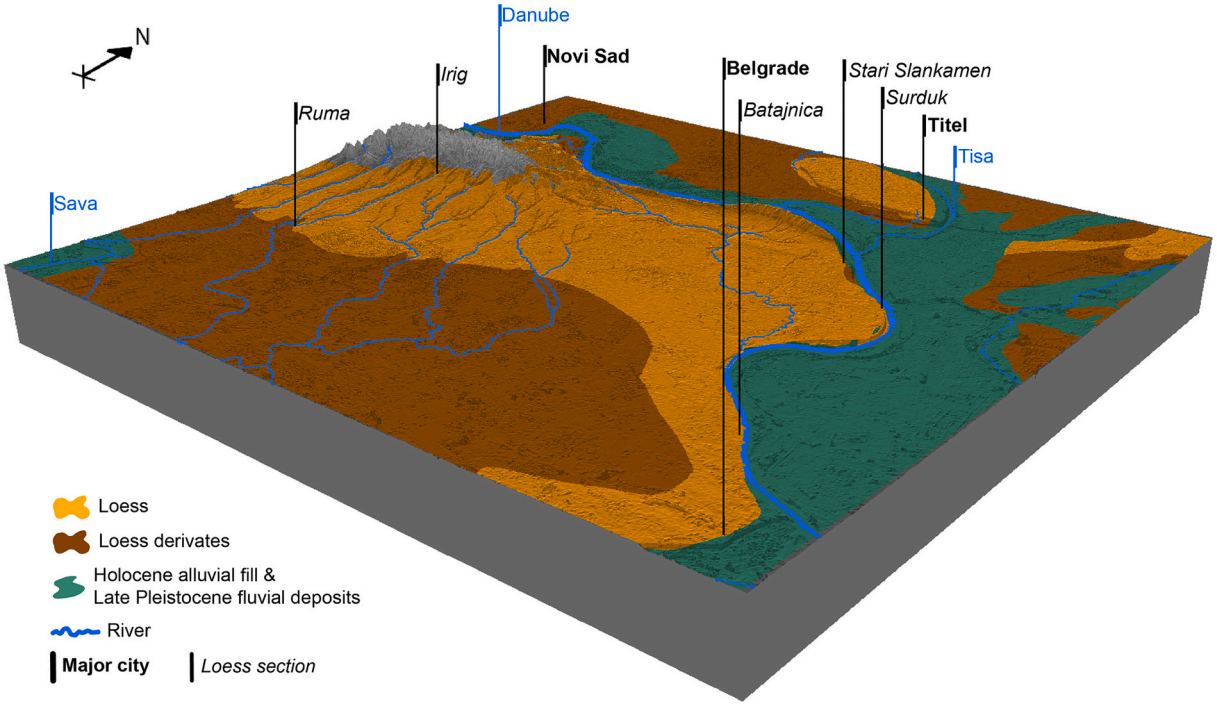

Fig. 14. 3D image of the loess landscape in the Vojvodina (northern Serbia) showing the distribution of loess, loess derivates, the Late Quaternary floodplain and numerous investigated loess sequences (No. 5 in Fig. 4). The size of the 3-D image is 53 × 57 km. Superelevated by factor 1 (no superelevation).

Zmajevac (Banak et al., 2016; Fenn et al., 2020; Galović et al., 2009; Wacha et al., 2013; Wacha and Frechen, 2011). The paleosols intercalating the loess are mostly Chernozem-type soils and brown forest Cambisol-type forest soils (Bronger, 2003). The provenance of the material is similar to the Carpathian Basin region with an evident, more local influence from southern provinces (e.g. Sava River tributaries originating from the Dinaride Ophiolite Zone; Galović, 2016). A gradual increase in humidity is observed in the loess sequences from across the Pannonian region of Croatia towards the west. This increase persisted throughout all (or most) climatic shifts from the late glacial to today (Rubinić et al., 2018). A particularity of paleosols (mainly Stagnosols) in the western part of the Pannonian region in Croatia is that the increased distance to the source allowed pedogenesis to outcompete loess accumulation, so that no unaltered loess can be found in this area. Rubinić et al. (2018) concluded that Croatian pseudogleys could be considered as soils that had reached their quasi-equilibrium stage thousands of years ago and they have continued to form throughout the Holocene. Loess in this domain is distributed in elevations up to 393 m a.s.l. with a median of 98 m a.s.l. (cf. Chapter 3.3). The map shows ~ 60,500 km^2 loess and loess derivates, ~ 12,600 km^2 aeolian sand, ~4500 km^2 sandy loess, and ~ 37,000 km^2 alluvial fill and fluvial deposits (Table 1). Most of the loess and loess derivates are located in elevations between ~ 80 m and ~ 140 m a.s.l., with a maximum of ~ 290 m a.s.l.

3.1.5. V: Pontic East European domain

Domain V consists of the vast and laterally continuous aeolian deposits of southern Ukraine, Russia, Moldova, the Moldavian Plateau, and the Lower Danube Basin in Romania and Bulgaria, including the Dobrogea. The most comprehensive studies of LPS in eastern Europe are located in this domain and they contain a rich archive of paleoclimatic changes for at least the Middle and Late Pleistocene (Antoine et al., 2019; Buggle et al., 2013; Chen et al., 2020; Haesaerts et al., 2003; Liang et al., 2016; Lomax et al., 2019; Necula et al., 2015a; Obreht et al., 2017; Rousseau et al., 2020; Rousseau et al., 2013; Rousseau et al., 2001; Tecsa et al., 2020; Tsatskin et al., 1998; Velichko et al., 2009; Zeeden et al., 2018). In this area, there are no indications of permafrost and loess deposits developed under forest steppe and steppe conditions. This is also reflected in the distribution of modern topsoils, with recent Luvisols in the former forest steppes and Chernozems in the steppe areas (e.g. Velichko, 1990). Loess deposits are strongly influenced by the Danube River, the Carpathian Mountains, and the Black Sea, but also the Dniester, Dnieper, Don, and Volga run through this domain. Another relevant dust source are the drylands around the Caspian Sea and further east and dust might have been transported by the Easterlies to domain V (see e.g. Obreht et al., 2017 and references therein). This loess domain covers different bioclimatic zones: Continental conditions in the Lower Danube Basin, sub-Mediterranean Black Sea and Sea of Azov coasts, and more semi-arid and desert conditions towards the east. Similar to domain IV, the dominating depositional mode is the accretion of dust in plateau deposits over the entire Pleistocene. At the western and northern shores of the Black Sea, the Sea of Azov, and the Caspian Basin loess deposits are influenced by desert margin conditions with dust input from the east including endorheic basins and alluvial fans at the foot slopes of mountain ranges which both delivered deflatable silt (Vandenberghe et al., 2006). Interestingly, thicknesses of paleosol and loess intervals are similar and grain sizes are getting finer in this area indicating continuous and steady input of far traveled dust (Chen et al., 2020). Towards the Caspian Basin, the loess cover gets generally thinner. The shelf of the Black Sea is not a dominant source area as LPS are thinning towards the coast (Jipa, 2014). This domain shows features which are commonly found in more arid landscapes e.g. in Central Asia, such as alkaline lakes, which are frequent in the rain shadow of the Carpathian Mountains in the Lower Danube Basin and even north of the Black Sea coast.

The southern part of this domain is dominated by the Lower Danube Basin (LDB) and the Dobrogea uplands. The LDB is strongly influenced by the Danube River and its tributaries draining the Eastern and Southern Carpathians, as well as the Balkans. The basin is characterized by vast aeolian plateaus nested between major river valleys, and can be subdivided into the Wallachian Plain, the Bulgarian Plain, the forelands of Carpathians and Balkans, the Moldavian Plateau as well as the Dobrogea uplands (Jipa, 2014). The plains are usually covered with thick (tens of meters) Quaternary loess mantles, smoothing the

landscape. In these areas the sediment covers are dissected by rivers forming loess bluffs at their banks (e.g. LPS Vlasca, Fig. 15). In contrast, the Dobrogea uplands consist of a Cretaceous to Tertiary limestone plateau in the south and a Mesozoic to Paleozoic Dobrogea orogen in the north with a dendritic fluvial system, which is mostly covered by loess deposits in variable thickness. Here, the thickest sections are usually accessible in abandoned quarries (e.g. LPS Mircea Voda and Urluia, Fig. 15) or also as loess bluffs along valleys (e.g. LPS Rasova, Fig. 15) or even in cliffs along the Danube and the Black Sea coast. In general, the studied sequences of the LDB show a broad variability in thickness and age (Costinești, Constantin et al., 2014; Mostiștea, Necula et al., 2015b; Urluia, Obreht et al., 2017) reflecting mainly profile accessibility. Albeit loess records in the region are laterally very consistent chronostratigraphically, thicknesses of different loess beds can also vary significantly. Additionally, several LPS preserve tephra layers (Italian, Carpathian and Caucasian), in places in considerable thickness (Anechitei-Deacu et al., 2014; Antoine et al., 2019; Constantin et al., 2012; Lomax et al., 2019; Obreht et al., 2017; Veres et al., 2013; Zeeden et al., 2018).

In addition to the paleoenvironmental preconditions, the Carpathian Bending area is also influenced by tectonic subsidence, leading to thick sediment fillings, e.g. in the Focşani Basin comprising up to 7 km thick Pliocene-Pleistocene fluvial and aeolian deposits (Matenco et al., 2016). The map shows ~ 246,000 km^2 loess and loess derivates, ~1600 km^2 aeolian sand, and ~ 46,000 km^2 alluvial fill and fluvial deposits. Most of the loess deposits are found in elevations between ~ 50 m and ~ 140 m a.s.l. with a maximum of ~ 310 m a.s.l. (cf. Chapter 3.3).

3.1.6. VI: Mediterranean loess

This domain comprises loess and loess-like sediments in the Mediterranean area. Periglacial processes are limited to discontinuous evidence of soil freezing and ice lensing recorded at the margin of the Po Plain (Cremaschi et al., 2015; Cremaschi et al., 1990; Cremaschi and Van Vliet-Lanoë, 1990). Recent studies suggest that Pleistocene loess covers vast areas in the (*peri*) Mediterranean regions (Boixadera et al., 2015; Bosq et al., 2020a; Wacha et al., 2018; Wolf et al., 2019; Zerboni et al., 2018). Loess in these regions does not reach the thickness of loess in central and eastern Europe and is often preserved as (relocated and weathered) loess-derivates. We present three subdomains: The western Mediterranean subdomain (VIa), the northern Mediterranean subdomain (VIb), and the eastern Mediterranean subdomain (VIc). A possible source for aeolian material besides globally distributed dust are the rivers (such as Ebro or Po), glacial and pro-glacial systems at the margin of the southern Alps, and glacial grinding from several paleoglaciations in the Mediterranean (Ehlers et al., 2011), especially on the Iberian Peninsula (summary in Oliva et al., 2019) and in the Dinaric mountain ranges (e.g. Hughes et al., 2011). Moreover, periglacial weathering processes in the mountains and regional desert-like conditions and insolation weathering in the lowlands produced silt-sized particles. Dry emerged shelves are a further source of loess along shorelines. The map shows ~18,000 km^2 of loess and loess derivates, ~1600 km^2 of aeolian sand and ~ 82,000 km^2 alluvial fill and fluvial deposits in this domain (see Chapter 3.3).

3.1.6.1. VIa: Western Mediterranean subdomain. Loess in southwestern Europe is mostly concentrated on the Iberian peninsula (e.g. Bertran et al., 2016). Aeolian deposits can be found in the lower Ebro Basin in northeastern Spain (Boixadera et al., 2015) and the upper Tagus Basin in central Spain (Wolf et al., 2019; Wolf et al., 2018). Boixadera et al. (2015) reported loess deposits in the Ebro Basin that are generally 3–4 m thick and consist of well-sorted fine sands and silts, i.e. coarser than typical loess. Loess in central Spain is distributed along the upper Tagus River in elevations between 500 and 700 m a.s.l., covering fluvial terraces and depressions nearby. The Tagus loess reaches thicknesses of around 8 m and reveals high contents of calcium carbonate (between 30 and 40%) and soluble salts (~10%) indicating that Tagus River deposits and weathered local marls were important loess sources during the Pleistocene (Wolf et al., 2019). In contrast to other European loess areas, paleosols generally show reddish colors and can be rated as Mediterranean Cambisols. In addition, there are some areas in the southern part of the lower Rhône and Rhône delta region, which can be attributed to this subdomain (see IIIa). Especially in the region of Provence, Mediterranean influences on loess derivates lead to indicative soil formation such as Terra Rossa (Bosq et al., 2020a). Loess in this subdomain is distributed

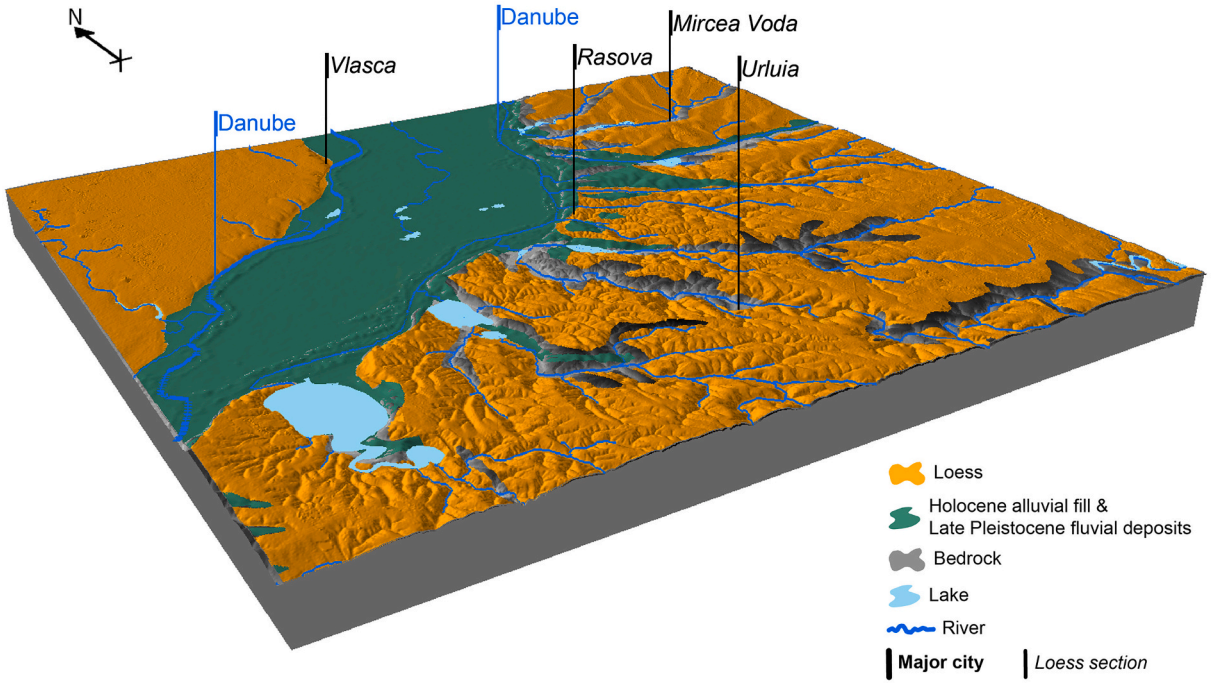

Fig. 15. 3D image of the distribution of loess and Late Quaternary floodplain deposits in the Lower Danube Basin (No. 6 in Fig. 4). The size of the 3-D image is 50 × 55 km. Superelevated by factor 1 (no superelevation).

in elevations up to ~ 710 m a.s.l., with a median of 286 m a.s.l. (cf. Chapter 3.3).

3.1.6.2. VIb: Northern Mediterranean subdomain. In this subdomain, loess formation is widely recorded along the margins of the Po Plain (Cremaschi et al., 2015) and the coastline of the northern and eastern Adriatic Sea and on the islands of Croatia (Cremaschi, 1990a; Wacha et al., 2011b, 2018). These deposits are summarized as the Po Plain loess basin (Cremaschi, 2004; Cremaschi, 1990a; Cremaschi, 1987; Peresani et al., 2020; Zerboni et al., 2018). Moreover, loess is discontinuously distributed along the shorelines of the southern Adriatic, where it is mostly preserved at the top of limestone plateaus (eventually recycled by pedogenesis) and within caves and rock shelters (Cremaschi, 2004; Cremaschi and Ferraro, 2007) and was occasionally described along the Tyrrhenian shorelines (Boretto et al., 2017). Loess in Italy originates from the deflation of the Upper Pleistocene fluvioglacial and fluvial deposits at the southern margin of the Alps, along the northern fringe of the Apennines, or the Adriatic shelf. Along the southern Adriatic and Tyrrhenian shorelines a further silt source are secondary tephra clasts that deposited along the emerged shelf and later deflated inland (Cremaschi and Ferraro, 2007; Hirniak et al., 2020). Loess here is also often overprinted by pedogenesis and thus its extent and paleoenvironmental significance were underestimated (Amit and Zerboni, 2013). A variety of soils are interbedded within loess sequences, including Chernozems, Alfisols, Cambisols, and Luvisols, and occasionally layers of reworked loess are also present. Only a few sequences of thick, unweathered loess (e.g. the Val Sorda of Torino Hill sequence) and some complex pedosequences (e.g. Monte Netto) can be found in northern Italy (Cremaschi et al., 1990; Ferraro, 2009; Forno, 1990; Zerboni et al., 2015). The Val Sorda sequence, for instance, was preserved because it was capped by glacial deposits emplaced during the latest LGM advance of the Garda Lake Glacier. The majority, however, is deposited as sheets of windblown silt. Loess deposits are recurrent at several geomorphological settings along the southern margin of the Alps and the northern margin of the Apennines. These locations correspond to dissected fluvial terraces, pre-LGM glacial deposits, uplifted isolated hills and karst plateaus (Cremaschi, 2004; Zerboni et al., 2018). Occasionally, loess bodies can be found on top of polygenetic paleosols, inside sinkholes and trapped within caves and rock shelters, and embed anthropogenic deposits (Peresani et al., 2008).

Additionally to the Italian loess deposits, this subdomain also consists of loess on the Adriatic coast of Croatia (e.g. Istrian Penisula: Zhang et al., 2018), including the islands of the Kvarner Bay (Profe et al., 2018b; Wacha et al., 2018). These deposits originate from Alpine glacial outwash plains in the Po Plain (Cremaschi, 1990a; Pavlaković et al., 2011), but are strongly influenced by Mediterranean climate (Profe et al., 2018b). The large glacio-fluvial outwash plains from the Pleistocene alpine glaciers in the northern Po Plain and the dry shelf of the Adriatic Sea provide additional dust sources. Heavy mineral assemblages of loess sequences from the two opposite sides of the Adriatic Sea (Monte Conero and Susak Island) suggest the same source of aeolian sediments, corresponding to the Upper Pleistocene alluvial plain of the Po River, today submerged by the Adriatic Sea (Cremaschi, 1990b).

Loess along the eastern Adriatic coast and on the islands directly covers the Cretaceous carbonate basement. Simulation from Ludwig et al. (2020) show that strong Bora winds flowing down slopes of the Dinaric Alps over the northern Adriatic region during the LGM played a major role in the accumulation of the local to regional dust. Here, the loess deposits are mostly coarser in grain size compared to loess in domain IV. In Susak, the loess is interfingered with rapidly deposited laterally strongly varying aeolian sands as well as three tephra layers (Wacha et al., 2011b) and the grain size is shifted towards fine sand (Wacha et al., 2018). On a more recent geological map of Croatian loess, Susak was mapped as sandy loess (Fuček et al., 2014). It contains more paleosols compared to loess in eastern Croatia (domain IV). The soils are also more reddish in color, highlighting the Mediterranean climate influence (see stratigraphy in Fig. 6). The thickness of loess and loess derivates in the Adriatic region is quite small, Susak being the exception with ca. 30 m thick loess deposits, which is why most were not presented on older maps. Their distribution is discontinuous and patchy. The loess in Istria, on the other hand, is finer grained compared to the Susak loess, and therewith more similar to typical loess in domain IV, but it also shows a higher degree of pedogenetic overprinting. The loess in the Adriatic region is mainly of last glacial age (Cremaschi et al., 2015; Wacha et al., 2011a; Zhang et al., 2018), but it is suggested that red paleosols below the loess on Susak as well as buried paleosols at Monte Netto (Delpiano et al., 2019; Zerboni et al., 2015) formed on even older loess (Durn et al., 2018). Loess in this subdomain is distributed in elevations up to ~ 700 m a.s.l., with a median of 188 m a.s.l. (cf. Chapter 3.3).

3.1.6.3. VIc: Eastern Mediterranean subdomain. There are several small patches of loess deposits in the basins and river valleys of the Balkan Peninsula, especially in Bosnia-Herzegovina, southern Serbia, Montenegro, and North Macedonia. These are scarcely described in the literature. However, these deposits exhibit unique geophysical and geochemical properties, reflecting a stronger influence of Mediterranean climate with more intensive weathering (Basarin et al., 2011; Bösken et al., 2017; Obreht et al., 2016; Obreht et al., 2014). Based on the strong geochemical fingerprints of the silt originating from mafic rocks of surrounding mountains, the most plausible major source areas are local dried river beds (Obreht et al., 2016). An illustrative example for the alternating influence of the local rivers as a dust source is the Stalać LPS (Bösken et al., 2017; Obreht et al., 2016), which lies in the vicinity of the confluence of the South (Južna) Morava and the West (Zapadna) Morava rivers into the Great (Velika) Morava River. This setting of three river basins served as local dust source, making loess accumulation possible. This makes this section exceptional since it preserves several glacial-interglacial cycles (Bösken et al., 2017; Kostić and Protić, 2000; Obreht et al., 2016), while others usually cover just parts of the last glacial cycle (Basarin et al., 2011; Obreht et al., 2014). Consequently, the occurrence of the small patches of loess deposits in this subdomain is highly influenced by the local geomorphology and the extent of glaciers in the Balkan mountain ranges (Obreht et al., 2016). Results from LPS of the region show that the central Balkans were still under the influence of the westerlies from the Atlantic Ocean, but more continental and Mediterranean climatic conditions prevailed in this region. Investigations showed that the climatic boundaries were sharp and fluctuated in the course of the Pleistocene. These fluctuations are e.g. imprinted in indicative (paleo-)soil properties (Obreht et al., 2016). However, the transitional region from the Balkan to the Carpathian Basin is characterized by loess that is similar to plateau loess in domain IV with some characteristic of Mediterranean loess, e.g. Nosak and Smedarevo (Marković et al., 2014). Loess in this subdomain is distributed in elevations up to ~ 1310 m a.s.l., with a median of 374 m a.s.l. (cf. Chapter 3.3).

3.2. Relief and loess in Europe: Visualization with four north-south transects

The north-south transects were chosen in a longitudinal distance of approx. 400 km. They were spread across Europe to visualize the interplay of relief and loess in various domains and subdomains. The geographic location of transects are depicted in the top panel of Fig. 4.

Transect A shows a cross section from the southern margin of the British Isles ice sheet, through southern England, France, and the Massif Central towards the Mediterranean coast near the Rhône delta. It depicts the broad area of the dry English Channel, which acted together with the exposed North Sea shelf during glacial periods as deflation area and therefore major source of aeolian sediments deposited further south

(subdomain IIa). The nowadays French-Belgium coast in direct vicinity to the source area is characterized by aeolian sands and dunes. To the south, broad and extensive loess areas with a hilly relief adjoin. The Seine Basin, known for vast loess deposits, is also visible and it is intersected by several fluvial systems (subdomain IIa). The central uplands with the Loire Valley are free of loess and aeolian sediments. They are bounded to the south by the Massif Central. Towards the Rhône delta, just small patches of Mediterranean loess occur (subdomain VIa).

Transect B runs from the southwestern margin of the Fennoscandian ice sheet through northern Germany, the Harz Mountains, the Central European low mountain ranges, the Danube Valley, across the Alps towards the Po Plain in Italy. The protogenetic zone (subdomain Ia) is dominated in this area by broad glaciofluvial sediments and sparse aeolian sediments, mainly sands. In the foreland of the Harz Mountains, the sharp northern boundary of loess subdomain IIb (loess-edge ramp, see chapter 3.1) is visible. The foothills of the Harz Mountains are covered by a thinning loess cover, reaching up to an elevation of approx. 300 m. This area was also influenced by the advances of the penultimate (Saalian) glaciation (see Fig. 5). Thus, the loess-edge ramp at the northern loess margin covers Saalian glacial tills (Fig. 10). The glaciated mountain range is bounded to the south by the loess covered Thuringian Basin (subdomain IIe), which is adjoined by the central German low mountain ranges, where loess is only found sparsely in basins and depressions. Along the German stretches of the Danube River (subdomain IIIc), loess can be found in higher elevations and is intersected by alluvial plains of the Danube River and its tributaries, which act as local dust sources. The (glacio-) fluvial deposits from the Würmian Pleistocene glaciation of the Alps acted as additional dust sources and are mainly free of loess covers (cf. Lehmkuhl et al., 2018b). Within the transect loess distribution rapidly declines south of the LGM timberline, indicating reduced dust deposition in forested areas. Only the southern slopes of the Alps and the northern slopes of the Apennines are covered with a loess blanket (subdomain VIb).

Transect C runs from the southern margin of the Fennoscandian ice sheet southwards through Poland, crossing the Western Carpathians and their forelands, the Carpathian Basin and ends on the northern foothills of the Dinaric mountain range. The northern part (subdomain Ia) was strongly influenced by the Weichselian and especially the Saalian ice sheet advances. The latter is also true for subdomain IIb. Therefore, hardly any aeolian sediments can be found in this area. Southwards, the loess regions of southern Poland adjoin (subdomain IIc), which are bounded by the Tatra Mountains as a part of the Western Carpathians. The mountain ranges of northern Hungary, such as the Bükk Mountains, are free of aeolian sediments, which reoccur on their southern slopes. The northern Carpathian Basin is dominated by vast deposits of loess and loess derivates (subdomain IIId). Further to the south in the Danube-Tisa interfluve, the aeolian sediments are coarser, forming sandy loess deposits and large bodies of aeolian coversands and dunes. The southern part of the basin is again covered by loess (domain IV) until the foothills of the Dinaric mountain range. The timberline during the LGM did not play a role in loess distribution in the Carpathian Basin, since it was located at higher elevations. The southern Carpathian Basin acted as a refugium for several mammal species (Stojak et al., 2015) and warmth-loving gastropod taxa (Sümegi et al., 2017) and especially the mountain regions are regarded as biogeographical refugium with transitional zones in the loess steppe (Marković et al., 2018b; Marković et al., 2008; Sümegi et al., 2016a).

Transect D starts at the eastern margin of the ice sheet near the Russian-Belarusian border, going slightly tilted towards southwest through the Eastern European Plain, Moldova, southeast Romania, and northern Bulgaria to the eastern foothills of the Balkans. The northern fringe is slightly influenced by last glacial ice advances. Southwards, the vast and flat East European Plain adjoins (subdomain Ib), where loess and loess derivates are found in large extents. These are intersected by the large river system of the Dnieper. In subdomain Ib and IId, the area was strongly influenced by ice advances of the penultimate glacial (MIS 6, see Fig. 5). The loess sequences in this area show in some cases intercalations of glacial sediments (Lindner et al., 2002). The Moldavian Plateau south of the Dniester is heavily intersected by fluvial erosion. It was still influenced by discontinuous permafrost during the LGM and shows a hilly relief. Further to the south, the Lower Danube Basin with its flat topography and vast extents of aeolian deposits is located (domain V). Within the foothills of the Balkans, loess only occurs in patches within depressions and basins.

3.3. Statistical analysis

In Europe more than 1 million km^2 are covered by loess and loess derivates, ~41,500 km^2 are covered by aeolian sand, ~31,000 km^2 by sandy loess deposits, and ~ 500,000 km^2 in the map shows alluvial fill and fluvial deposits (Table 1). Loess and loess derivates cover vast areas of subdomains Ib, IId, and domain V, while most of the aeolian sand and sandy loess is shown in domains Ia, IIa, IIId, and IV, while in other subdomains none are mapped. Large areas of alluvial fill and fluvial deposits cover domains I, IId, IIId, V, and VI.

Fig. 16 indicates that loess and loess derivates are distributed up to an elevation of 1307 m a.s.l.. While half of the loess in each subdomain is clustered in a narrow elevation band for most domains, the subdomains of domain VI show very broad distributions. Especially the upper limit was often very far from the mean values, which is a reason why we only show 98% of the distribution (considering that small misalignments between the loess distribution and the digital surface model with a resolution of ~30 m might lead to big differences in steep terrain). The highest elevation is found in domain VIc with 1307 m a.s.l..

It is evident from Fig. 17 that the loess and aeolian sediments are not normally distributed in their height. While some subdomains such as domain IV show a very narrow height distribution, most of the loess is spread over several hundred m a.s.l. The broadest spectrum is observed in domain VI where loess and loess derivates are found between 25 m and 1307 m a.s.l.. Domain IV shows a very sharp lower boundary of loess distribution that is likely related to the flat landscape in the Carpathian Basin. In domain II, subdomains IIa and IIb show a similar distribution, as do IIc and IIe. Some subdomains can be almost distinguished by their elevation (e.g. Ia and Ib), but usually there is quite some overlap (IIIa, IIIb, IIIe).

4. Discussion

4.1. Comparison to other methodological approaches

Maps of the distribution of aeolian sediments in Europe, either on a regional or continental scale, were compiled for almost a century (e.g. Antoine et al., 2003; Bertran et al., 2016; Fink et al., 1977; Fink and Nagl, 1979; Flint, 1971; Grahmann, 1932; Haase et al., 2007; Lehmkuhl et al., 2018a, 2018b; Lindner et al., 2017; Zerboni et al., 2018). Especially the pan-European approaches are widely recognized and used as a basis for geospatial analysis and interpretation (e.g. Buggle et al., 2013; Buggle et al., 2008; Fitzsimmons et al., 2012; Franc et al., 2017; Iovita et al., 2012; Lehmkuhl et al., 2016; Nawrocki et al., 2018; Sprafke and Obreht, 2016). Besides mapping approaches based on geological and pedological data or field observations, potential dust emission and deposition areas can be determined using numerical models (Ludwig et al., 2020; Schaffernicht et al., 2020; Sima et al., 2009). In the following subchapters, we compare our map to the most widely used European loess map by Haase et al. (2007), which combined several existing data sets and a more recent approach by Bertran et al. (2016), where the distribution of aeolian sediments was derived from topsoil data. Finally, we discuss our data with the results of the model-simulated dust deposition by Schaffernicht et al. (2020).

4.1.1. Comparison with the map of Haase et al. (2007)

One of the most commonly used maps of European loess is the one

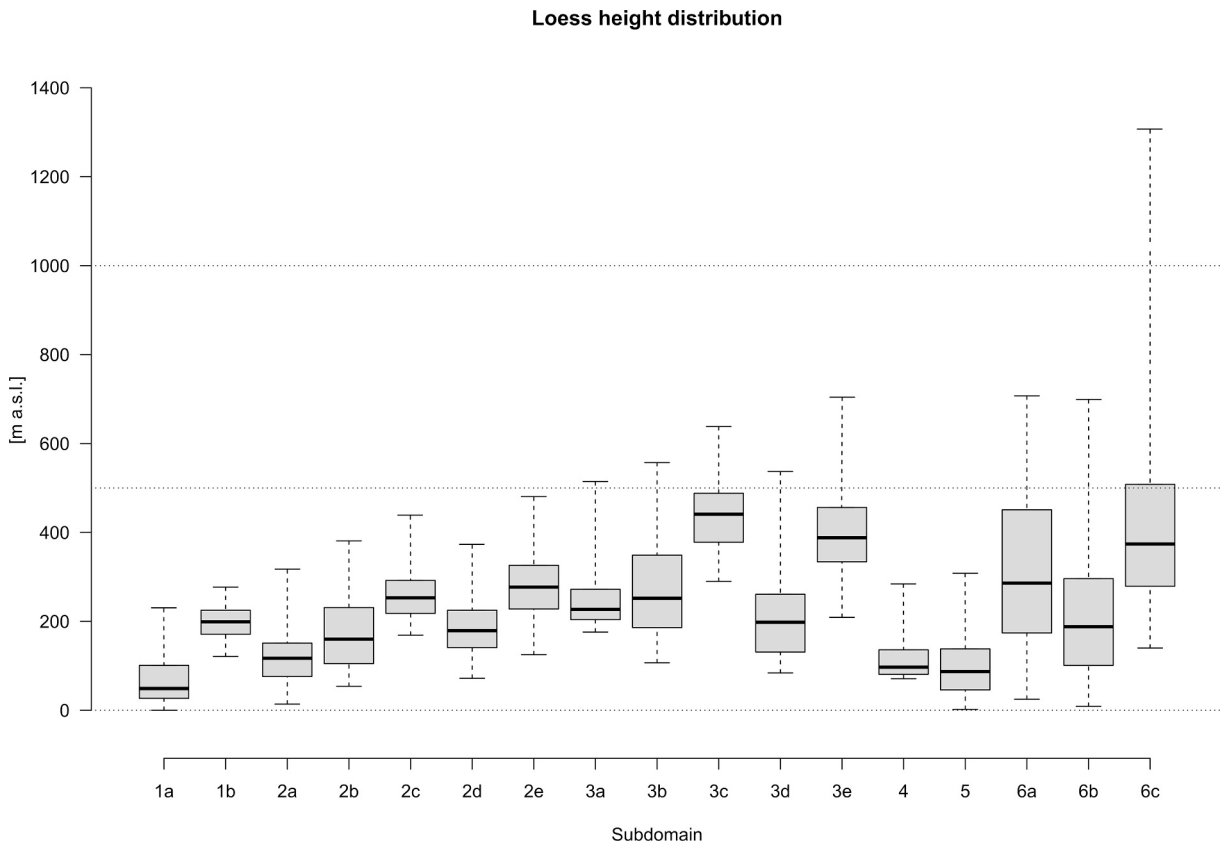

Fig. 16. Whisker plot of the elevation (ordinate) of loess and loess derivates in Europe per subdomain (abscissae). To exclude extreme outliers, the upper and lower limit in the whisker was set to 1% (cf. Supplementary Table S3).

provided by Haase et al. (2007). This map has a scale of 1:2,500,000 and is based on data compiled in the 1970s, 1980s, and the 2000s. This collaborative effort was carried out by the INQUA Loess Commission under guidance of J. Fink. Similar to our approach, the Haase et al. (2007) map is based on digitized paper maps from numerous authors. This led for example to artificial breaks along borders, and the persistence of locally separated loess classes such as the alluvial loess in Hungary. Additionally, important loess areas, such as the whole Paris Basin, were not mapped by this approach. Fig. 18 includes different categories of aeolian sediments and compares the results of this study with the well-established map of Haase et al. (2007). Differences occur for example in north-central France, where some sandy loess and loess derivates are mapped that are not included in our new map. A possible explanation for these discrepancies is the fact that in France loess with a minimum thickness of one meter was mapped. For our study, the minimum thickness usually was two meters. These differences are also observed in southern Germany, Austria, and Slovenia. Haase et al. (2007) included discontinuous and thin loess sediments in their map (cf. Fink and Nagl, 1979), leading to a more widespread loess distribution. Furthermore, some sandy loess and loess derivates in eastern Germany and southwestern Poland are mapped by Haase et al. (2007), which do not occur in our map. In these areas, loess is often incorporated within loamy and sandy sediments. These polygenetic deposits were not mapped by our approach.

In the southwestern Carpathian Basin, striking differences between the two mapping approaches are visible. This may be due to the uncertain data situation for the area. Most Quaternary deposits are mapped as “Quaternary in general” in the geological map of former Yugoslavia (Federal Geological Institute, 1970), without further differentiation (see Lehmkuhl et al., 2018a). This data was used in prior mapping approaches. Our new map includes the newest data from the Croatian Geological Survey (2009), which have not been available during data acquisition for the map compiled by Haase et al. (2007). This might explain the differences between the two data sets. Minor differences are found in the southern Lower Danube Basin, as well as the western parts of Ukraine and Crimea.

Areas that are mapped in our loess map that are not present in the map by Haase et al. (2007) are a consequence of different source data in our map. This includes areas in Spain, southern France, Italy, and coastal Croatia, which were not mapped before due to their small extent (Haase et al., 2007). Aeolian sediments in Great Britain and the Netherlands have not been mapped by Haase et al. (2007) but have been included here. Some differences occur in the Central German low mountain ranges, Czech Republic, and southern Poland. These areas are influenced by, e.g., slope processes, which can rework loess. We excluded data concerning reworked loess deposits (see Lehmkuhl et al., 2018b), since regional differences hamper a consistent mapping of these sediments. In Romania, loess deposits were not mapped in detail in geological maps. Therefore, the map presented here is based on an approach that uses pedological maps (Lindner et al., 2017) and thus shows different loess distribution patterns. Further, Haase et al. (2007) used a global stream network based on the grid cell boundaries of the GLOBE DEM (Hastings et al., 1999) to extract alluvial plains from the loess distribution. Since this DEM has a resolution of 1 km it is less precise than the pedological map we used for Ukraine (Sokolovsky et al., 1977b), leading to differences between both maps. Generally, we propose that our new map is more precise because in some areas updated maps were used, local experts critically checked all data, and our map relies on a higher analytical resolution. Nevertheless, it remains challenging to generate absolutely accurate maps since it is impossible to validate the loess distribution in all regions in the greatest of detail.

4.1.2. *Comparison with the mapping approach of Bertran et al. (2016)*

Since this study is based on a multitude of geological,

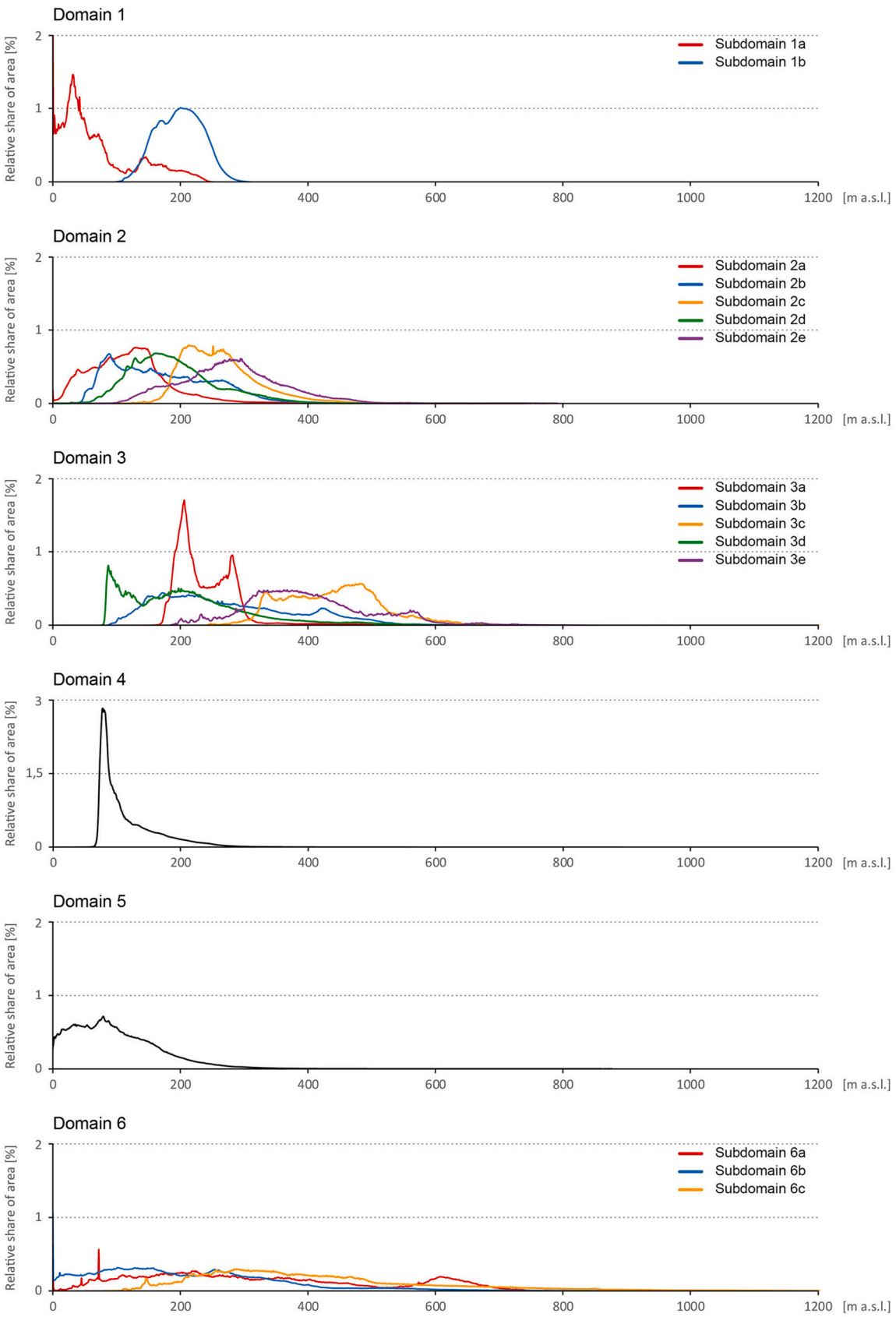

Fig. 17. Frequency distributions of the elevation of loess and loess derivates per main and subdomain. The ordinate shows the relative proportion of each elevation that is depicted on the horizontal axis. A color legend is given for the subdomains. Note that the ordinate of domain IV uses a different scale.

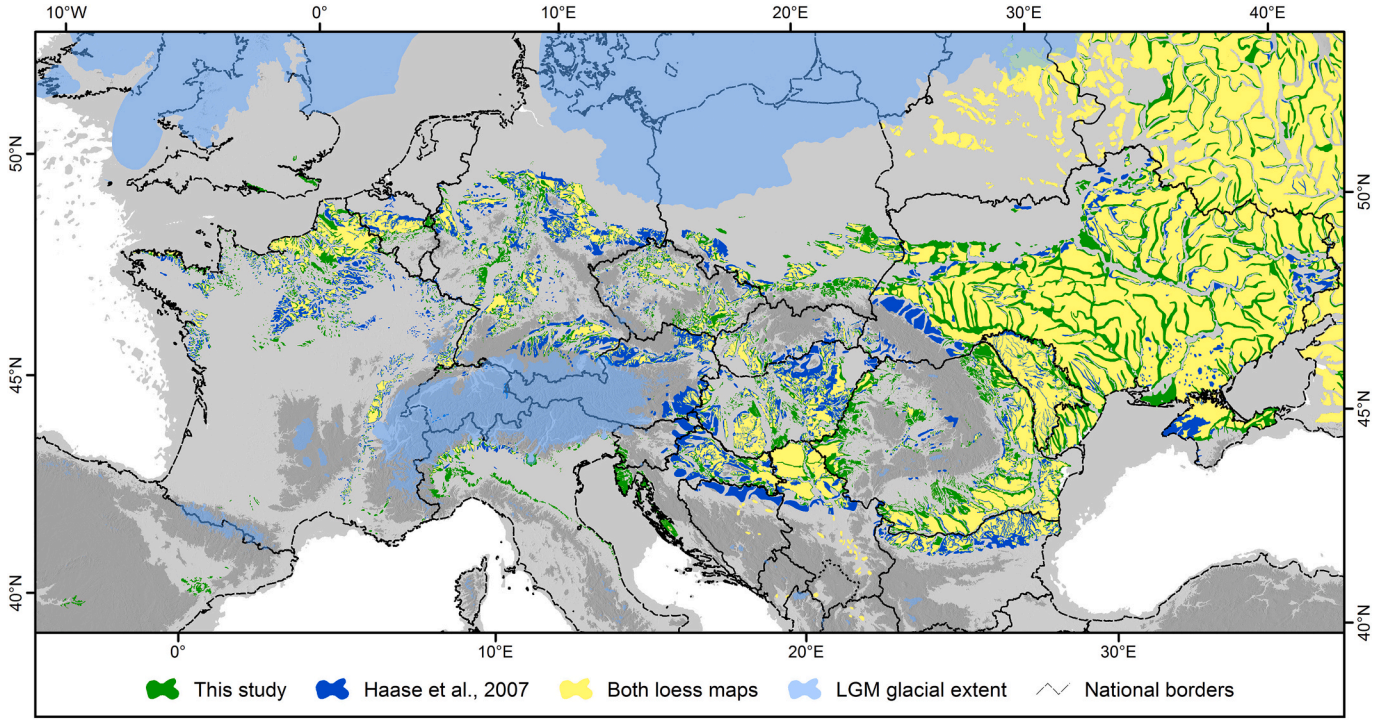

Fig. 18. Comparison of our new European loess map to the mapping approach from Haase et al. (2007). Similarities are shown in yellow. The distribution of loess, sandy loess, aeolian sand, and loess derivates that are only evident in our map is depicted in green, while the distribution of loess, loess derivates, sandy and alluvial loess that are only present in the Haase et al. (2007) map are shown in blue. The extent of glaciers (Ehlers et al., 2011) and the dry continental shelves (modified after Willmes, 2015) during the LGM are also depicted. (For interpretation of the references to color in this figure legend, the reader is referred to the web version of this article.)

geomorphological, and pedological maps (see Chapter 2.1), the detection, removal, and smoothing of artificial breaks was one of the main issues. Other recent approaches to map aeolian cover sediments used continuous, European Union wide data. Bertran et al. (2016) used the topsoil textural data from the Land Use and Cover Area frame Statistical survey database (LUCAS, Orgiazzi et al., 2018; Tóth et al., 2013) to extract information about the grain size distribution within the soils and therefore their parent material. The information about clay, silt, and sand content were extracted, set in relation and validated for various areas in France and Belgium (Bertran et al., 2016). As a result of the processing of the LUCAS data set, Bertran et al. (2016) classified aeolian sediments in Europe in four categories: loess, colluviated loess, silty sand, and sands. These categories were set by combining the different grain size classes from the data set. The thresholds for these categories of aeolian sediments are based on textural data for loess deposits in Northern France. The differing classification of aeolian sediments by this approach compared to our study hampers a direct comparison of all classes. Therefore, we only compare the classes loess and colluviated loess from Bertran et al. (2016) with the class loess and loess derivates from our study.

In general, the result of our study is comparable to the approach by Bertran et al. (2016). It is, however, obvious that the aeolian sediments mapped by Bertran et al. (2016) cover larger areas. This is especially the case in northwestern France, northern Belgium, the Central German low mountain ranges, southeastern Austria, eastern Slovakia, Transylvania, the eastern Carpathian foreland, southwestern France, northern Spain, and the Po Plain (Fig. 19).

The differences between the two approaches are due to manifold reasons. One of them is the differing mapping approaches. While the LUCAS database is based on data from top soil samples (Orgiazzi et al., 2018; Tóth et al., 2013), this study is based inter alia on geological maps. Geological maps usually exclude the uppermost one to two meters below the surface. Therefore, this approach can be expected to miss some of the thin loess and sand covers thinner than one or two meters. This is the case in subdomains Ia and IIa, especially in northern Germany (cf. Lehmkuhl et al., 2018b).

Vast covers of colluviated loess are mapped in some areas, such as basins within the Central European low mountain ranges (Fig. 19). Colluviated loess is also mapped in, e.g., geological maps in Germany (so-called 'Umlagerungsbildungen' or 'Schwemmlöss'; Lehmkuhl et al., 2018b), but their nomenclature is not consistent throughout Europe. Additionally, colluviated loess is usually not mapped in soil maps. To avoid issues and inconsistencies, we disregarded the direct mapping of every form of relocated aeolian sediments. Nevertheless, the class is included in the comparison since it overlaps largely with loess derivates in many regions.

The differences are most striking in the Central European mountain ranges and the Transylvanian Basin. The foothills of, e.g., the Ore Mountains, the Sudetes, the Tatra, and the Carpathians are affected. Within these regions, the differences are mostly due to mapped colluviated loess, or colluviated fine-grained Neogene deposits, as we observed over most of Transylvania and parts of the Moldavian Plateau. In eastern Slovakia, however, there are vast areas of loess mapped by topsoil data, which were not included in geological maps. There are some areas where the mapped colluviated loess is congruent with loess and loess derivates. The loess deposits of these areas, e.g., the Moldavian plateau and the upper reaches of the Danube River, were mapped as colluviated loess by Bertran et al. (2016) and as loess and loess derivates in this study. Generally, the areas of colluviated loess according to Bertran et al. (2016), correspond to areas in which the loess deposits are located in high elevations, compared to their surroundings.

Some inconsistencies between this study and Bertran et al. (2016) are noticeable especially within the Mediterranean realm and the coasts of Normandy and Brittany in northern France. In the Ebro Basin in northern Spain and the Po plain in northern Italy, large areas of (colluviated) loess were mapped. This may be due to substrates with a

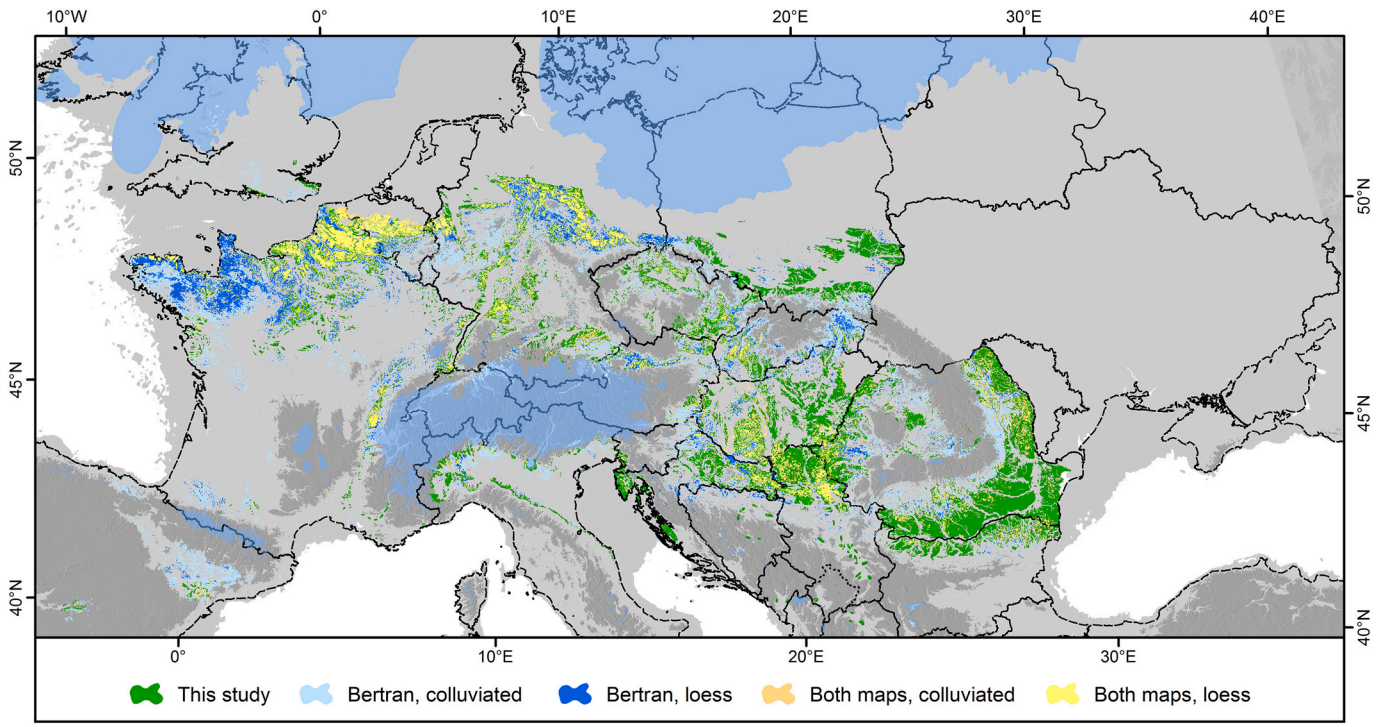

Fig. 19. Comparison of our new loess map to the mapping approach from Bertran et al. (2016). Please note that only data from the European Union was included due to the extent of the base data. The extent of glaciers (Ehlers et al., 2011) and the dry continental shelves (modified after Willmes, 2015) during the LGM are depicted.

similar granulometric signature as loess, such as weathered marls (Bosq et al., 2018). In studies following Bertran et al. (2016), the thresholds for loess mapping were therefore adjusted (Bosq et al., 2018).

4.1.3. Comparison of the new European loess map with an atmospheric LGM dust model of Schaffernicht et al. (2020)

Here, we compare our map with the recent work by Schaffernicht et al. (2020) that presents an LGM dust cycle model of Europe. According to this study, most of the dust emission occurred in a zone between the Alps, the Black Sea, and the southern margin of the ice sheets. Within this zone, the highest deposition rates were located near the southernmost ice sheet margins in domain I and II. Westwards relocation via dust plumes resulted in high modeled deposition rates in western Poland, northern Czech Republic, the Netherlands, the southern North Sea region, and northern and central Germany (Fig. 20). Relatively high dust production occured mainly in domain I in front of the ice sheet margin, while dust accumulation occurred mainly in domain II suggesting the role of higher vegetation density southwards in trapping dust particles.

Fig. 20 compares the atmospheric dust deposition of the dust cycle model (Schaffernicht et al., 2020) with the loess distribution and main domains established by this study. Dust emission and deposition were modeled using a regional climate-dust model. The modeled deposition rates for the entire LGM from Schaffernicht et al. (2020) show differences and commonalities to the observed thicknesses of the loess deposits (Fig. 20). The thickest loess deposits occur in central-eastern and southeastern Europe and not in the areas with the highest modeled rates. These differences can probably be explained by the degree of preservation. Differences in domain I could be due to insufficient vegetation cover to effectively trap dust in the direct vicinity of the ice margins. Reworking, erosion and relocation of sediment was also enhanced in the periglacially influenced regions of northern Europe. The model also indicates high deposition rates for high mountain areas, which is due to the consideration of only fine silt; coarse silt is rarely transported to higher elevations by wind. On the contrary, the model results for single wind directions show some commonalities to the reconstructed sediment pathways for European loess deposits. The proposed increased influence of easterly wind systems during the LGM, and therefore enhanced emission of dust on the margin of the ice sheet, is in accordance to evidence from a dust record of the Dehner Maar lake in Germany (Römer et al., 2016). Easterly winds also correspond to high deposition rates in the Lower Danube Basin, due to the increased influence of the exposed shelf of the Black Sea (Schaffernicht et al., 2020). This pathway was reconstructed for loess deposits of northern Bulgaria (Avramov et al., 2006; Jordanova et al., 2007), but it contrasts with the heavy mineral distribution and grain-size characteristics of the Lower Danube loess in the Danube Plain and Dobrogea (Jipa, 2014) indicating finer grain sizes and progressively reduced thicknesses of LPS, from the Danube valley towards the Black Sea. High modeled dust emission rates from the eastern margin of the continental ice sheet (Schaffernicht et al., 2020) correspond to the continental glacier provenance-river transport (CR) mode sensu Li et al. (2020), which was reconstructed for, e.g., the loess deposits of Central Ukraine (Buggle et al., 2008; Veres et al., 2018).

The atmospheric dust modeling approach took only (far traveled) dust with small-sized particles of up to 20 μm diameter (fine to medium silt) into account, while loess deposits mainly contain coarser silt particles. Nevertheless, the model can be used to understand the atmospheric circulation patterns and the preservation potential of the different domains, although numerical models, due to their limitations cannot yet reconstruct complex natural process chains such as the uptake, transport, and deposition of aeolian dust in appropriate spatial and temporal resolution. Large-scale models cannot display for example short term shifts in atmospheric circulations or sediment availability, which are indeed crucial factors in dust deposition, preservation, and loess formation (Antoine et al., 2009b).

In contrast to the current climatic situation, during the LGM winds from northeast, east, and southeast and cyclonic regimes prevailed over central Europe (Schaffernicht et al., 2020). While potentially a lot of dust was deposited within domains I-III, the preservation potential especially in domain I was very low. The continentality and aridity, presumably coupled with appropriate dust traps (e.g., certain vegetation types) in domains Ib, IId, IV, and V probably led to the loess preservation

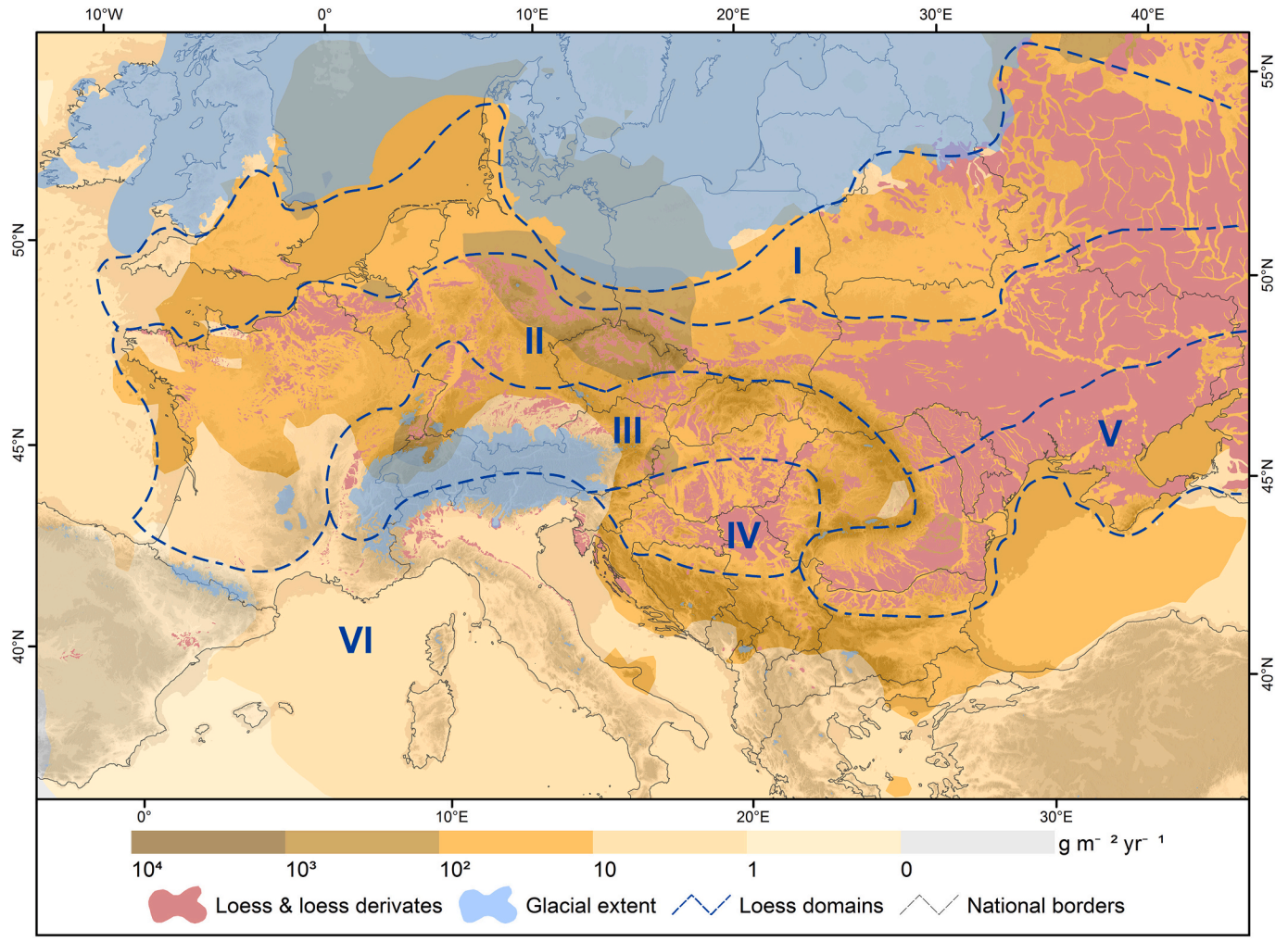

Fig. 20. Dust deposition rates for the LGM according to modeled data from Schaffernicht et al. (2020). The dust deposition rates comprise particles of up to 20 μm diameter (FD20) using a dynamic downscaling (FD20 DD). Distribution of loess as well as the boundaries of the main loess domains are given for comparison.

we see in those regions today. However, it should be emphasized that in most climate models the coarse dust as observed during dust fall (Goudie, 1983; Jarke, 1960; Schütz, 1980) is not considered (Adebiyi and Kok, 2020). Additionally, the dust cycle model by Schaffernicht et al. (2020) only includes atmospheric variability during the LGM, whereas dust deposition occurred quasi-continuously during the last interglacial-glacial cycle, while hydroclimatic conditions, and therefore dust availability and regional dust cycling fluctuated significantly.

4.2. *Discussion of the distribution of loess in Europe*

Loess, loess derivates, sandy loess, and aeolian sands are widely distributed throughout Europe. In domain I, between the ice sheets and the northern boundary of the European loess belt, patches of loess-like sediments, sandy loess, and widespread sand sheets (coversands) occur. The boundary between the protogenetic zone and the northern European loess belt is in most regions clearly marked by the transition of sandy loess or sand sheets towards loess. Transitional zones can be found in northern France, Belgium, or the Lower Rhine Embayment in Western Germany (subdomain IIa; see Vandenberghe in Schaetzl et al., 2018). In the central parts of domain II, a sharp and clear boundary of the loess distribution occurs - the loess-edge ramp (subdomain IIb, see Fig. 10). These marginal steps vary in spatial distribution and shape among others due to the influences of and distance to the extending ice sheets. The main distribution of loess within domain II is located at the northern front of Central European low mountain ranges mainly between 105 and 231 m a.s.l. (subdomains IIb). Domain II and III are strongly influenced by periglacial processes and permafrost. The loess accumulation took place in many cases at downwind positions, creating asymmetric valleys (e.g. Fig. 7) and covering fluvial terraces (e.g. Fig. 13). The influence of periglacial processes gradually diminishes southwards and finally ceases. For example, in the Rhône area of subdomain IIIa there is a gradual transition towards domain VIa, where Mediterranean conditions prevailed (Bosq et al., 2020a, 2020b). A similar shift occurs in the Carpathian Basin between domain IIId and IV as well as further east between subdomain IId and domain V in the Eastern European lowlands. These transitions are characterized by increasing temperate to humid subtropical climate conditions with more intensive weathering and soil development in southwestern and southern Europe and to a more semi-arid desert margin environment with lack of humidity in the eastern and southeastern parts of Europe, respectively. In domains IV and V, dust accumulation occurred predominately in plateau situations. Due to the local depositional conditions and relatively extensive erosional processes, these plateaus are incised by lowland rivers and are nowadays preserved between the alluvial plains of these rivers. They represent the most complete records of Quaternary paleoclimate and paleoenvironment in Europe besides a few lake records. These plateaus are described in the literature (e.g. Marković et al., 2016; Smalley et al., 2011) and their genesis is discussed e.g. by Florea (2010).

The distribution of sand and sandy loess in the domains I and II differs from those in other domains. Generally, aeolian sands are transported by strong wind systems over short distances. In domains I

and II, however, sands are deflated from the outwash plains and other sandy sediments related to Middle Pleistocene (Saalian and Elsterian) ice extents, as well as (Early) Weichselian deposits. In other loess domains, such as the peri-alpine river valleys (IIIa-c) or eastern Europe (V), aeolian sands originate from the deposits of larger rivers (e.g. Rhône, Rhine, and Danube in subdomain III and VI; Dnieper and Dniester in domain V). The Danube River and its tributaries in the Carpathian Basin provide large quantities of silty and (fine) sandy material. When this material is deflated and subsequently deposited, a complex sedimentary pattern of loess, sandy loess, and aeolian sands develops. In this pattern, it is often difficult to distinguish between aeolian sand and sandy loess. Nevertheless, one needs to be aware that this is not the case in domain I, e.g. in northern Germany, where sands, sandy loess, and loess are clearly separated. Aeolian sands occur parallel to the ice margin, whereas the northern boundary of loess distribution is further south. Between these two boundaries, sandy loess is found.

Throughout Europe, loess is mostly distributed in the basins and lowlands (northern France, Belgium, Germany, Czech Republic; Middle and Lower Danube Basins, in general up to 600 m a.s.l.), the foothills of the Central European low mountain ranges (e.g. Central German low mountain ranges, Carpathian promontory, Fruška Gora Mountains, mainly below 200 m a.s.l.), and in favorable geomorphological settings, e.g. the larger valleys of the Rhône River and upper Rhine River (mainly below 300 to 400 m a.s.l.). In higher elevations, silt-sized particles of aeolian origin are usually mixed with periglacial cover beds building the upper cover bed (Lehmkuhl et al., 2016; Semmel and Terhorst, 2010). In the European Alps, Gild et al. (2018) used the term drape for aeolian mantles in the western part of the Northern Limestone Alps. They described drapes as aeolian covers of a few decimeters in thickness covering different bedrock and older Pleistocene sediments. They are slightly modified by initial soil formation and of late glacial in age. These drapes have also been described along valleys of the Italian Dolomites (Cremaschi and Lanzinger, 1987; Cremaschi and Lanzinger, 1984). Usually no or only very limited typical loess deposits occur in the Pleistocene polar deserts in northern Europe of domain I, high-mountain areas, or south of the Pleistocene timberline.

The distribution of aeolian sediments is mainly controlled by sediment availability, the prevalent wind directions, and the presence of suitable dust traps. The sediment availability is dependent on the distance to potential source areas such as larger river systems (e.g. Smalley et al., 2009; Smalley and Leach, 1978), dry shelves (Antoine et al., 2009a), or glacio-fluvial outwash plains of ice sheet margins (e.g. Antoine et al., 2016; Lehmkuhl et al., 2016; Pye, 1995). The vegetation density in the source areas also governs the amount of dust, which can be deflated, since vegetation acts as a dust trap and fixes the sediment (Pye, 1995). It is obvious that the distribution of loess is closely linked to the distribution of these source areas (Fig. 2). The vastest and most prominent loess deposits occur south of the ice margin and along large rivers, where during the Quaternary large amounts of sediment were available for deflation, with no or very sparse vegetation cover.

The local geomorphological setting of sink areas strongly influenced the distribution, preservation, and thickness of loess sequences. Several depositional settings such as plateau and interfluve loess, slope loess, colluvial (slope toe) loess, and loess sedimentation in depressions and erosion channels (valley loess) were distinguished (see Lehmkuhl et al., 2016 and references therein). Higher accumulation rates are observed for example in depressions or on the lee sites of topographic barriers, following the prevailing wind direction (e.g. Fig. 7, Antoine et al., 2003). The best-developed loess sequences are generally preserved in sediment traps formed by the intersection between alluvial terraces and slopes of the stepped terraces systems such as along the valleys of Dnieper, Danube, Rhine, and other large rivers in Europe (see examples in Figs. 7 and 13; e.g. Kukla, 1977, 1978). The most thoroughly investigated loess sequences and related archeological findings in the northern parts of Europe are in slope toe or plateau situations (Lehmkuhl et al., 2016). In domains IV and V dust sedimentation on plateaus is considered continuous since the Middle Pleistocene at least (Basarin et al., 2014; Marković et al., 2015), with their sedimentological and paleoclimate characteristics allowing for close comparison with the higher resolution LPS of the Chinese Loess Plateau (Zeeden et al., 2020; Zeeden et al., 2018).

To summarize, loess in Europe was formed, preserved, overprinted, reworked, and relocated through a multitude of different geomorphological, sedimentological, and pedological processes. These variations and differences are the results of a complex interplay of regional to local paleoclimatic, paleoenvironmental, and geomorphological conditions. These conditions control dust accumulation, pedogenesis, preservation, and syngenetic or diachronous erosional events (Maruszczak, 2000; Smalley et al., 2011; Sprafke and Obreht, 2016). Additionally, there is a strong dependence on the distance to the ice sheets and local source areas ((glacio-) fluvial and alluvial sediments, dry shelves), as well as prevailing paleo-wind systems.

4.3. Discussion of the genesis of loess in Europe

There is a multitude of approaches to differentiate between the genesis modes of loess deposits. Two main directions developed within the centuries: The sedimentological (geological) approach and the pedogenetic one (e.g. Smalley et al., 2011; Smalley and Obreht, 2018; Sprafke and Obreht, 2016). Whereas mainly Pécsi (e.g. 1990) developed many criteria for a loess definition from the latter direction, others like Pye (1995), used a more simple definition for loess as wind-blown dust (see the summarizing discussion in Smalley et al., 2011). Besides the definition of loess itself, which is still under discussion (Sprafke and Obreht, 2016), different modes of loess genesis are described in literature. Muhs and his co-workers summarized, developed and focused on models of “glacial loess” (cold loess, higher latitude loess) and “desert loess” (warm loess) formation (Lancaster, 2020; Muhs, 2013; Muhs and Bettis, 2003; Schaetzl et al., 2018; Wright, 2001). Lately, Li et al. (2020) suggested three modes for the global loess genesis: Continental glacier provenance-river transport, mountain provenance-river transport, and mountain provenance-river transport-desert transition.

However, there is not only the “glacial loess” versus “non-glacial” formation in Europe. The main factors for loess formation are the amount of available dust (Crouvi et al., 2010; Maher et al., 2003) and the degree of humidity (semi-arid to semi-humid conditions) as well as its seasonality. In the more humid regions, pedogenesis dominates especially during the interglacials and amounts of incoming far-traveled dust on continental scale (cf. Lancaster, 2020; Muhs, 2013) are reduced in volume and immediately trapped and altered by soil formation processes. In the semi-arid regions, however, dust can accrete also during interglacial periods lowering but not inhibiting intensity of soil formation (Constantin et al., 2019; Tecsa et al., 2020; Varga et al., 2016). Additionally, (paleo-) environmental factors play an important role for the accumulation and especially the preservation of dust aggradations. They determine the boundaries of vegetation zones and the permafrost distribution, which in turn influence dust trapping, weathering, and erosional processes. A conceptual model of glacial loess genesis for Europe was already proposed by Zeuner (1937). Anticyclonal synoptic patterns controlled by the Scandinavian and Alpine ice sheets and their interplay with westerlies are the main element of this concept, in which strong anticyclonal winds are responsible for dust uptake and transport and tundra/steppe vegetation benefitting from humidity brought in by the westerlies controlled the trapping and embedding of dust particles. According to various authors, the trapping of dust is mostly related to the vegetation cover (e.g. Danin and Ganor, 1991; Hatté et al., 2013; Tsoar and Pye, 1987; Zech et al., 2013) or biocrusts (Svirčev et al., 2019; Svirčev et al., 2013). Beside the periglacial realm, where higher vegetation did not play any role during full glacial and stadial times, shrubs and trees and even grasses were likewise widely absent during colder and drier climatic periods also in the dry steppe landscapes of Central-East and South-East Europe, where today grasslands represent the

interglacial optimum vegetation biome (Botti, 2018; Magyari et al., 2014). Soil surfaces in these dry settings were covered by biocrusts consisting of communities dominated by lichens, algae, and fungi and act as dust traps consolidating and transforming incoming dust into loess (e.g. Svirčev et al., 2019 and references therein). Others argued that dust trapping by shrubs explains the specific characters of loess accumulations at least in the Rhône valley, France (Bosq et al., 2018). As evident from lacustrine and marine archives from southeastern Europe and adjacent Mediterranean and Black Sea areas, dust accumulates as background sedimentation during the Quaternary (e.g. Kwiecien et al., 2009; Skonieczny et al., 2019; Wagner et al., 2010). In glacial and interglacial times, south of the northern timberline, dust was and is deposited very likely in reduced rates because of the lack of local sources. Upon deposition, 'far-traveled' dust under forest is possibly effectively geochemically weathered and the weathering products were partially exported out of the system (Ronchi et al., 2015; Sommer et al., 2006). As today, there was also a lower and upper timberline in the mountains of southeastern Europe and in the Mediterranean realm during glacial times (Feurdean et al., 2012; Monegato et al., 2015; Peresani et al., 2020). Hence, loess accumulation was not only limited by the forest vegetation to the south but similarly also by the altitudinal timberline in mountain areas. Therefore, we assert that the accumulation of dust and the formation of loess is related mainly to tundra and steppe environments.

In any loess deposition, after sedimentation and initial fixation of atmospheric mineral dust particles, first post-sedimentary alteration processes occur (Berg, 1916; Pécsi, 1990; Smalley et al., 2011; Svirčev et al., 2013; Smalley and Marković, 2014). It is a matter of debate whether such processes should be strictly assigned to processes such as pedogenesis or diagenesis or to a kind of transitional processes between the two (Sprafke and Obreht, 2016). However, there is consensus that the typical structure of a loess deposit is caused by these initial alteration processes, whereby the loess differs from primary airborne dust (Pécsi, 1990; Sprafke and Obreht, 2016; Schulte and Lehmkuhl, 2018). Besides the factors influencing mobilization, transport, and sedimentation of the loess, e.g. distance to source areas or wind velocity (Újvári et al., 2016; Vandenberghe, 2013, Vandenberghe et al., 2018), the post-depositional alterations such as chemical weathering or colluviation also have a considerable influence on the grain size composition of loess deposits (Schulte and Lehmkuhl, 2018; Újvári et al., 2016). Grain-size distribution of loess can serve as an indicator to distinguish between loess and loess-like deposits (Vandenberghe et al., 2018), and may give insight into different processes that control loess formation. Coarser deposits formed e.g. under the influence of stronger wind activities or under the influence of non-aeolian processes, such as slope wash or soil creep. High contents of fine material (clay, fine and medium silt) are the result of large distances to the source region, weaker wind conditions, and/or post-depositional alterations such as pedogenesis (Újvári et al., 2016; Vandenberghe, 2013, Vandenberghe et al., 2018; Schulte and Lehmkuhl, 2018).

4.4. Conceptual model of loess distribution

Finally, based on our observation in Europe and comparison with other loess regions, we suggest a conceptual model of loess distribution, loess formation, and loess landscapes applicable to the entirety of Eurasia. In this model, a triangle of the three main ecozones (nival, humid, and arid environments, Fig. 21) is used to conceptualize the different modes of loess formation as factors of humidity and temperature, mainly controlling occurrence, abundance or absence of vegetation, the strength of periglacial processes, and glacier activity. The extreme nival regions with glaciers and the polar desert including the periglacial zone are at the top of the triangle. The more humid regions (densely vegetated and forested at the extreme end) are on the left side and the extreme arid regions (deserts) are on the right side of the triangle. Please note, that there are gradual transitions between the different environments, also

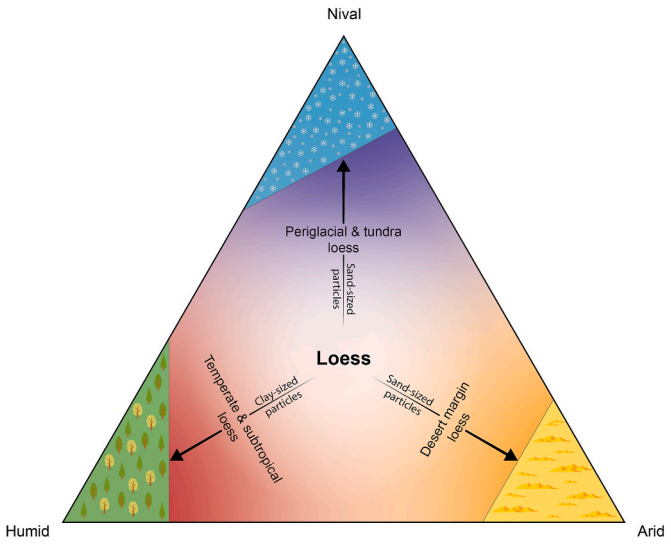

Fig. 21. Conceptual model of loess landscapes. Note that the corners represent the extreme end with no loess formation. Top: Nival zone and polar deserts with larger extent on the nival-humid axis. Left corner: Humid regions and forest with larger extent on the humid-nival axis. Right corner: Deserts.

towards the extreme regions at the corners. Loess, as a predominantly silt-sized aeolian sediment, can have different sources. As loess is found in different environments, a single genetic path cannot explain all loess occurrences (see Section 4.3). Here we introduce a model that tries to separate loess towards three genetic environments. Typical loess is situated in the center. We propose main loess formation in a balance between nival, humid, and arid ecozones and environments.

Permafrost and periglacial environmental conditions, such as found today in the northernmost regions and high mountains of Europe, are indicated towards the top of the triangle (nival regions = glaciers at the extreme end; they have larger extent on the nival-humid axis). These environments include deep freezing during the winter season and freezing-thawing cycles, which influences the geomorphological and pedogenic processes resulting in paleosols such as tundra gley soils (gelic Gleysols). Fluvial erosion and slope processes (slope wash, sheet flows, solifluction) are enhanced during glacial and periglacial climates. Desiccation due to low temperatures and frost enhanced the availability of small-sized particles (Smalley, 1995). Precipitation mainly occurred as snow during the cold season. This produced high meltwater discharge with its maximum during summer in glacial regions and/or during springtime in periglacial regions, respectively. This resulted in large braided river systems, which fell dry in late summer to autumn and during wintertime. During low water stands, floodplains act as important sand and silt source areas, especially in late winter to springtime (Sima et al., 2009; Smalley et al., 2009). Material from glacial grinding and frost weathering in particular lead to silt production and accumulation in the floodplains during high discharge seasons. Therefore, silt-sized particles are available but also sands can be found, especially close to rivers. In general, the dominance of coarse grain sizes (sand-sized particles) increases towards the polar and glacier region. The transport and relocation depend on the humidity, which enforced relocation by slope wash and solifluction. Li et al. (2020) proposed the continental glacier provenance-river transport and mountain provenance-river transport modes for such environments. Although loess-like sediments and loess derivates formed in these environments, the lack of a stabilization process as observed in more arid regions and prevalent geomorphic conditions have caused discordances and hiati. Such loess deposits are very characteristic for domains I – III and mostly formed during cold stadial conditions. Sometimes niveo-aeolian features formed under more humid conditions (depicted as diagonally shaped triangle edge). Other deposits outside of Europe also fall in this part of

the conceptual model. For example, the ultimate member on the nival-arid axis are arctic ice silts known as Yedoma deposits. They are found in the permafrost landscapes of Beringia (Central and Eastern Siberia, Alaska, and northern Canada) and contain ice-saturated or supersaturated silt and fine sand sediments (Murton et al., 2015; Strauss et al., 2017). They are characterized by a segregation ice content of 30–40% and syngenetic ice wedges (Strauss et al., 2017). Several hypotheses concerning their genesis have been proposed. Researchers working in the Yukon area and Alaska often characterize Yedoma silts as loess or re-transported loess (Péwé, 1955; Sanborn et al., 2006). According to Schirrmeister et al. (2013), a polygenetic hypothesis with a distinct aeolian input is the most popular in the recent scientific literature. Strauss et al. (2017) posed the opinion that the loess and polygenetic concepts could be merged, if the re-transportation of loess (also called secondary loess) is included in the loess concept. We suggest that parts of domain I and IIc-d were influenced by such nival-arid conditions during the Pleistocene. In the Carpathian Basin and eastern Europe there is a gradual transition from the periglacial loess landscapes towards the steppe loess regions (domains III to IV and IId to V, Chapter 4.2) more in the center and right side of the triangle.

The lower right side of the triangle depicts the loess deposits in arid and semi-arid regions, e.g. domains V and VIc. These deposits range from silty loess towards more sandy loess in the direction of increasing aridity. The nival-arid axis is distributed more towards the continental areas (domains Ib – IId – V), whereas the humid-arid axis is the transition from domain IV to V. Especially domain IV and the western part of domain V are situated more to the center of the triangle. Desert environments are located at the extreme end and are strictly speaking not found in Europe, but it is debatable if some deposits e.g. in Spain and southeastern Europe were formed under arid and desert margin conditions. In these landscape, dry riverbeds and exposed lacustrine deposits act as source areas for aeolian deflation also for mid- and long-distance transport of silt-sized particles. While in the center of the triangle, that depicts 'typical' loess, continuous and silt-sized dominated loess formation takes place (e.g. domain IV, most parts of V), a gradual increase in the contribution of sand-sized particles towards the arid corner is observed. Beside the proximity of source areas (e.g. large streams in Europe; e.g. Jipa, 2014) also a reduced vegetation cover leads to the formation of sandy loess deposits and sand formation especially at the desert margins of the world (e.g. Central Asian deserts, deserts in China). This transition towards the desert margin loess can be found e.g. in eastern and southeastern Europe towards Central Asia, e.g. at the Sea of Azov (Chen et al., 2020) and the Caspian Lowlands (Wei et al., 2020). Moreover, a general and continuous contribution of long range transported dust input stemming from desert margins in the Caspian Lowlands and western Central Asia is likely for southeastern European and western Central Asian Holocene and older interglacial soils (Constantin et al., 2019; Jordanova and Jordanova, 2020; Tecsa et al., 2020; Zhang et al., 2020). Please note that there was and still is also a long range transport of aeolian dust from desert regions (Goudie, 1983; Goudie, 1978; Schütz, 1980), which plays an important role in the global climate system (Lancaster, 2020). The significance of recent and Pleistocene coarse silt transport from the deserts of Central Asia towards the Carpathian area as already reported from the northern Black Sea by Jarke (1960) and also from the Saharan desert towards Europe (Costantini et al., 2018; Longman et al., 2017; Sabatier et al., 2020; Skonieczny et al., 2019; Stuut et al., 2009; Varga et al., 2016; Varga et al., 2013) was unrecognized for many years. However, during the last decade this dust contribution was accepted for being relevant for the entire Circum-Saharan realm and hence, also for the loess areas of southern and southeastern Europe (Muhs et al., 2010; von Suchodoletz et al., 2010). Nonetheless, the flux of Saharan dust is quantitively of minor importance if compared to local and regional sources and presumable constraint to interglacial times (Varga et al., 2016).

The left side of the triangle (humid = forested regions at the extreme end; they have a larger extent on the humid-nival axis) comprises humid temperate and subtropical (including Mediterranean) landscapes in the western and southern parts of Europe (domains IIIa, VIa, VIb) and at higher elevations in central-eastern Europe (domains IV, V). The climatic conditions, especially the availability of moisture and secondarily higher temperatures, lead to denser vegetation cover resulting in morphodynamic stability and increased chemical weathering and soil development. These processes enhanced the in-situ formation of clay-sized particles thereby reducing the amount of coarser (silt-sized) particles. Additionally, higher clay contents of more than 20% and cementation processes hampered deflation (Pye, 1995). This conceptual zone is limited towards its corner by the timberline since no loess deposits were formed under dense forest.

Our proposed temperate and subtropical loess and the paleosols formed within were mainly developed in regions with a distinct dry season (summer or winter, e.g. towards the Mediterranean regions with winter rainfall or in monsoonal regions with summer rainfall). Dust sources in these regions are and were mainly local and smaller in comparison to the other loess landscapes due to the higher vegetation cover and fewer dry riverbeds. Where humidity and temperature allowed, forest developed even during the LGM. Hence, in the mountains of southeastern Europe and in the Mediterranean realm not only an upper but also a lower altitudinally controlled timberline framed a zone of forest. As an example, at the Alpine-Dinaric piedmont Monegato et al. (2015) found evidence for a steep moisture gradient during the LGM, extending from the forested mountains to the semiarid alluvial plains which extended further south in the Paleo-Adriatic Plain, locally covered by loess (Peresani et al., 2020). Such humid loess deposits can be found at the foothills of the Carpathians in the Romanian Banat (Kels et al., 2014) and in Transcarpathia (Ukraine) between steppe and boreal forest at higher elevation (Nawrocki et al., 2016). Such settings with lateral shifts between more humid loess environments and more typical loess environments also occured at the upper reaches of the Dniester, between the southern margin of the Scandinavian ice sheets and the Carpathian Mountains, at the transition of the forest refugia in higher altitudes and the tundra environments towards the ice margin (Łanczont et al., 2019). Another example for subtropical loess and soil formation is the Stalać LPS in subdomain VIc (Bösken et al., 2017; Obreht et al., 2016). Here, last glacial and penultimate glacial paleosols are strongly weathered and the latter are expressed as reddish Cambisols highlighting the occurrence of humid Mediterranean paleoenvironmental conditions during their formation. A similar setting is found at the foothills of the southern Alps at the transition to the Po Plain (Zerboni et al., 2015). However, humid loess can be found in the subtropical regions of China (see below) and in South America (e.g. Campodonico et al., 2019). A potential example of humid loess could be also the loess from New Zealand, which is characterized by high contribution of clay and very low carbonate contents (Smalley, 1971), probably due to dissolution caused by high amounts of rainfall. Nevertheless, we highlight that the formation of such loess is scarce in Europe during the last glacial cycle, where an increase in humidity in temperate and subtropical areas was mostly related to pedogenesis and weathering resulting in accretionary soils. These soils contain only minor amounts of mineral dust and are therefore strictly speaking no proper loess deposits. In these cases, soil formation outpaced dust accumulation.

Finally, primary or typical loess is usually not formed in any of the extreme conditions depicted by the corners of the triangle in our conceptual model of loess landscape. We propose that this loess formation occurred mainly during the colder periods of the Pleistocene. However, in domain IV and partly in domain V these processes continued at least also during the Early Holocene (Chen et al., 2018; Tecsa et al., 2020; Zeeden et al., 2018). When conditions become fully nival, humid or arid, already formed loess is strongly altered, and the formation of thick and quasi-continuous silty deposits can be still ongoing. However, conditions indicated as extreme in the triangle have a potential to ultimately alter the loess in a way that its silt-sized origin is largely replaced by finer, strongly weathered material. In case of humid and nival

conditions, loess could be fully altered into soils due to pedogenesis and reduced dust flux or hampered preservation due to vegetation or snow cover. Under extreme arid conditions, the lack of vegetation and biogenically induced loessification can make loess vulnerable to aeolian deflation and other types of post-depositional erosion. This includes the preferential deflation of silty material, leaving only coarser components in the source areas.

The conceptual triangle also has relevance if used vertically. Towards higher elevation in more humid mountain regions of Europe, we reach a zone of periglacial and glacial dynamics, yet loess formation is quantitatively reduced by the lack of stable surfaces to support long-lasting dust accumulation (see the discussion in Chapter 4.2 of the distribution of loess in the European Alps; e.g. Gild et al., 2018). Additionally, in the rather high mountains and plateaus of arid Central Asia, e.g. the Tibetan Plateau and Qilian Shan, mountain loess deposits are found (Lehmkuhl et al., 2014; Lehmkuhl et al., 2000; Nottebaum et al., 2015; Nottebaum et al., 2014; Stauch et al., 2012; Yang et al., 2020). Here, the uppermost boundary of loess is periglacial loess, whereas the lowermost parts are desert margin loess (described in Nottebaum et al., 2015, Nottebaum et al., 2014). For these regions, there are still debates on the influence of glaciers and deserts in loess formation.

To further test if the conceptual model is applicable to regions outside Europe, we exemplify here the model for the Chinese Loess Plateau. In the Chinese Loess Plateau there is a gradual transition in grain-size from the more humid monsoonal areas in the southeast (left side of the triangle in Fig. 21) towards the semi-arid and arid regions with desert margin loess in the northwest (right side of the triangle, e.g. Bloemendal et al., 2008; Derbyshire et al., 1995; Yang and Ding, 2003). The thick beds of primary loess in western Manchuria (Obruchev, 1945) and in the mountain areas of western China could be placed in the upper half of our triangle towards the nival environments. These loess landscapes are also influenced by periglacial processes and slope wash (top of the triangle). Moreover, in southern China, e.g. in the Sichuan Basin, there is a debate on subtropical and strongly weathered aeolian (loess) deposits (Feng et al., 2014; Yang et al., 2010). This fits well to the subtropical loess landscapes on the humid-arid axis of our conceptual model. Feng et al. (2014) provides evidence that the Chengdu Clay contains aeolian material of possibly local origin. They assume alluvial sediments in the northwestern Sichuan Basin as the major source and transportation of the material by ancient katabatic winds over a short distance during glacial and stadial periods (subtropical). Even further north of the desert regions of Central Asia we reach another zone of desert margin loess (e.g. in Tajikistan Ding et al., 2002; or Kazakhstan Rao et al., 2013), whereas in northern Mongolia and Siberia periglacial or mountain loess appears (Andreeva et al., 2011; Lehmkuhl et al., 2012; Lehmkuhl et al., 2011; Muhs, 2014).

5. Conclusion

In this study, we present a new revised map of the distribution of aeolian sediments (mainly loess) and major potential source areas in Europe. We divided the European loess deposits into six major domains and 17 subdomains, based on their facies. Loess facies are differentiated by the silt production area (source), where especially rivers are important transport agents, and paleoenvironmental factors that influence loess formation, preservation, and transformation. By means of the new map and geomorphological cross-sections, we analyzed the various influences of geomorphology and paleoenvironment on loess deposits throughout Europe. The main loess domains in Europe are: (1) The northern European loess belt (domain II), (2) the loess adjacent to Central European high-altitude mountain ranges (domain III), (3) the Middle Danube Basin loess (domain IV), (4) the Pontic East European loess (domain V). Additional important loess regions with less extensive loess covers are the protogenetic zone north of the northern European loess belt (domain I) and areas in the Mediterranean (domain VI). In the Central European low mountain ranges loess occurs in smaller patches in areas above 600–800 m a.s.l., in thicknesses of less than two meters. In the periglacial zone of northern Europe silty material can also be incorporated in the periglacial cover beds.

The loess deposits in Europe show remarkable differences regarding their distribution and characteristics. These complex (post-)depositional milieus compared to other loess regions in the world are mainly due to: (1) the fluctuations of the British and Fennoscandian ice sheets volume and extent; (2) the permafrost and vegetation boundaries and their fluctuation; (3) the geographical position of Europe bordering the Atlantic Ocean that allows the moist air masses of the westerlies to travel throughout the continent creating a west-east gradient in precipitation, seasonality, and continentality; (4) variation in the topography, such as the (low) mountain ranges and the occurrence of extensive lowland basins; and (5) the position of different potential dust sources like the ice sheet margins, mountain glacier forelands, dry shelves and associated braided river systems, larger river systems, and alluvial fans in the more continental areas.

Based on our findings, we suggest a new conceptual model of loess distribution, loess formation, and loess landscapes visualized in the form of a humid – arid – nival triangle. This model presents three modes of loess formation controlled by climatic factors, namely water availability and temperature, which in turn constrain the prevailing vegetation biomes. The top of the triangle represents periglacial environments. Although loess-like sediments and loess derivates also formed in these environments, the prevalent environmental conditions have caused discordances and hiati. Such loess deposits are very characteristic for domains I-III and mostly formed during cold stadial conditions. The right side of the triangle presents loess in arid and semi-arid regions (e.g. domains V, VIc). These deposits range from silty loess towards more sandy loess in the direction of increasing aridity. The left side of the triangle describes humid temperate and subtropical landscapes as found in western and southern Europe (domains IIIa, VIa, VIb) and at higher elevations in central-eastern Europe (domains IV, V). The climatic conditions led to a denser vegetation cover resulting in morphodynamic stability, increased chemical weathering and soil development. These processes enhanced the formation of clay-sized particles and reduced the amount of coarser (silt-sized) particles. Finally, typical loess is not formed in any of the extreme conditions and we propose that typical loess formation occurred mainly in domain IV and partly in domain V during colder periods of the Pleistocene.

Even though our map focuses on loess landscapes formed and shaped during the LGM, this study can be related to older loess deposits dating to the Middle Pleistocene when ice sheets extended further south compared to their maximum extent during the last glacial-interglacial cycle. These shifts not only pushed the known paleoclimatic and paleoenvironmental boundaries, such as the permafrost boundary or the timberline, further south but they also had crucial ramifications on the size, nature, and location of silt production and deposition areas. Additionally, paleogeographic factors such as a vast pro-glacial lake, reduced the extent of potential source areas for dust deflation. These factors as well as the periglacial overprinting of loess deposits in subsequent glacial periods, led to the poor preservation of Middle Pleistocene loess deposits, especially in northern and western Europe.

Data availability

Our work highlights the value of the compiled geodata, which can be accessed freely at the CRC806 database (https://crc806db.uni-koeln.de/start/) at https://doi.org/10.5880/SFB806.56, https://doi.org/10.5880/SFB806.57, https://doi.org/10.5880/SFB806.58, https://doi.org/10.5880/SFB806.59, https://doi.org/10.5880/SFB806.60, https://doi.org/10.5880/SFB806.61 (Lehmkuhl et al., 2020a, 2020b, 2020c, 2020d, 2020e, 2020f).

CRediT authorship contribution statement

F. Lehmkuhl: Conceptualization, Supervision, Visualization, Writing - original draft, Funding acquisition. **J.J. Nett:** Project administration, Supervision, Methodology, Validation, Writing - original draft. **S. Pötter:** Methodology, Validation, Data curation, Writing - original draft. **P. Schulte:** Validation, Writing - original draft, Visualization. **T. Sprafke:** Resources, Writing - review & editing. **Z. Jary:** Resources, Writing - review & editing. **P. Antoine:** Resources, Writing - review & editing. **L. Wacha:** Resources, Data curation, Writing - review & editing. **D. Wolf:** Resources, Data curation, Validation. **A. Zerboni:** Resources, Data curation, Writing - review & editing. **J. Hošek:** Validation. **S.B. Marković:** Validation. **I. Obreht:** Validation. **P. Sümegi:** Validation. **D. Veres:** Validation. **C. Zeeden:** Validation. **B. Boemke:** Investigation, Data curation, Methodology. **V. Schaubert:** Visualization, Data curation, Formal analysis. **J. Viehweger:** Investigation, Data curation, Software. **U. Hambach:** Validation, Writing - review & editing.

Declaration of Competing Interest

The authors declare that the research was conducted in the absence of any commercial or financial relationships that could be construed as a potential conflict of interest.

Acknowledgements

The investigations were carried out in the frame of the CRC 806 “Our way to Europe”, subproject B1 “The Eastern Trajectory”: “Last Glacial Paleogeography and Archaeology of the Eastern Mediterranean and of the Balkan Peninsula”, funded by the Deutsche Forschungsgemeinschaft (DFG, German Research Foundation) – Projektnummer57444011 – SFB 806). We thank D. Haase for sharing shapefiles of the loess distribution map, P. Bertran for providing the shapefiles of the distribution of aeolian sediments modeled by his team, P. Ludwig for providing the data of the LGM regional dust model, and A. Weber for help with compiling the supplementary material. We thank G. Újvári and two anonymous reviewers for their suggestions that helped to improve the manuscript.

Appendix A. Supplementary data

Supplementary data to this article can be found online at https://doi.org/10.1016/j.earscirev.2020.103496.

References

Adebiyi, A.A., Kok, J.F., 2020. Climate models miss most of the coarse dust in the atmosphere. Sci. Adv. 6 https://doi.org/10.1126/sciadv.aaz9507 eaaz9507.

Amit, R., Zerboni, A., 2013. Report on the INQUA-AEOMED field trip workshop “Reconsidering Loess in Northern Italy” (Po Plain, 1-3 July 2013). Alpine Mediterr. Quat. 26, xi–xv.

Andreeva, D.B., Leiber, K., Glaser, B., Hambach, U., Erbajeva, M., Chimitdorgieva, G.D., Tashak, V., Zech, W., 2011. Genesis and properties of black soils in Buryatia, southeastern Siberia, Russia. Quat. Int. 243, 313–326. https://doi.org/10.1016/j.quaint.2010.12.017.

Andrieux, E., Bertran, P., Saito, K., 2016. Spatial analysis of the French Pleistocene permafrost by a GIS database: French Pleistocene permafrost database. Permafr. Periglac. Process. 27, 17–30. https://doi.org/10.1002/ppp.1856.

Anechitei-Deacu, V., Timar-Gabor, A., Fitzsimmons, K., Veres, D., Hambach, U., 2014. Multi-method luminescence investigations on quartz grains of different sizes extracted from a loess section in Southeast Romania interbedding the Campanian Ignimbrite ash layer. Geochronometria 41, 1–14. https://doi.org/10.2478/s13386-013-0143-4.

Antoine, P., Bonifay, E., Conchon, O., Lautridou, J.P., Macaire, J.J., Mandier, P., Monnier, J.L., Morzadec, M.T., Revel, J.C., Sommé, J., Tastet, J.-P., Legigan, P., 1999a. Extension des Loess et Sables Éoliens à 18±2 ka en France. La France Pendant les Deux Derniers Extrêmes Climatiques, Variabilité Naturelle des Environnements.

Antoine, P., Rousseau, D.-D., Lautridou, J.-P., Hatté, C., 1999b. Last interglacial-glacial climatic cycle in loess-palaeosol successions of North-Western France. Boreas 28, 551–563. https://doi.org/10.1111/j.1502-3885.1999.tb00241.x.

Antoine, P., Rousseau, D.-D., Zöller, L., Lang, A., Munaut, A.-V., Hatté, C., Fontugne, M., 2001. High-resolution record of the last interglacial–glacial cycle in the Nussloch loess–palaeosol sequences, Upper Rhine Area, Germany. Quat. Int. 76, 211–229.

Antoine, P., Catt, J., Lautridou, J.-P., Sommé, J., 2003. The loess and coversands of northern France and southern England. J. Quat. Sci. 18, 309–318. https://doi.org/10.1002/jqs.750.

Antoine, P., Rousseau, D.-D., Fuchs, M., Hatté, C., Gauthier, C., Marković, S.B., Jovanović, M., Gaudenyi, T., Moine, O., Rossignol, J., 2009a. High-resolution record of the last climatic cycle in the southern Carpathian Basin (Surduk, Vojvodina, Serbia). Quat. Int. 198, 19–36. https://doi.org/10.1016/j.quaint.2008.12.008.

Antoine, P., Rousseau, D.-D., Moine, O., Kunesch, S., Hatté, C., Lang, A., Tissoux, H., Zöller, L., 2009b. Rapid and cyclic aeolian deposition during the Last Glacial in European loess: a high-resolution record from Nussloch, Germany. Quat. Sci. Rev. 28, 2955–2973. https://doi.org/10.1016/j.quascirev.2009.08.001.

Antoine, P., Rousseau, D.-D., Degeai, J.-P., Moine, O., Lagroix, F., Kreutzer, S., Fuchs, M., Hatté, C., Gauthier, C., Svoboda, J., Lisá, L., 2013. High-resolution record of the environmental response to climatic variations during the last Interglacial–Glacial cycle in Central Europe: the loess-palaeosol sequence of Dolní Věstonice (Czech Republic). Quat. Sci. Rev. 67, 17–38. https://doi.org/10.1016/j.quascirev.2013.01.014.

Antoine, P., Goval, E., Jamet, G., Coutard, S., Moine, O., Hérisson, D., Auguste, P., Guérin, G., Lagroix, F., Schmidt, E., Robert, V., Debenham, N., Meszner, S., Bahain, J.-J., 2014. Les séquences loessiques pléistocène supérieur d’Havrincourt (Pas-de-Calais, France) : stratigraphie, paléoenvironnements, géochronologie et occupations paléolithiques. Quaternaire 321–368. https://doi.org/10.4000/quaternaire.7278.

Antoine, P., Coutard, S., Guerin, G., Deschodt, L., Goval, E., Locht, J.-L., Paris, C., 2016. Upper Pleistocene loess-palaeosol records from Northern France in the European context: Environmental background and dating of the Middle Palaeolithic. Quat. Int. 411, 4–24. https://doi.org/10.1016/j.quaint.2015.11.036.

Antoine, P., Lagroix, F., Jordanova, D., Jordanova, N., Lomax, J., Fuchs, M., Debret, M., Rousseau, D.-D., Hatté, C., Gauthier, C., Moine, O., Taylor, S.N., Till, J.L., Coutard, S., 2019. A remarkable late Saalian (MIS 6) loess (dust) accumulation in the lower Danube at Harletz (Bulgaria). Quat. Sci. Rev. 207, 80–100. https://doi.org/10.1016/j.quascirev.2019.01.005.

Antonioli, F., Vai, G.B., 2004. Litho-Paleoenvironmental Maps of Italy During the Last Two Climatic Extremes (ENEA).

Assadi-Langroudi, A., 2019. A conceptual model for loess in England: Principles and applications. Proc. Geol. Assoc. 130, 115–125. https://doi.org/10.1016/j.pgeola.2018.12.003.

Avramov, V.I., Jordanova, D., Hoffmann, V., Roesler, W., 2006. The role of dust source area and pedogenesis in three loess-palaeosol sections from North Bulgaria: a mineral magnetic study. Stud. Geophys. Geod. 50, 259–282. https://doi.org/10.1007/s11200-006-0015-y.

Badino, F., Pini, R., Ravazzi, C., Margaritora, D., Arrighi, S., Bortolini, E., Figus, C., Giaccio, B., Lugli, F., Marciani, G., Monegato, G., Moroni, A., Negrino, F., Oxilia, G., Peresani, M., Romandini, M., Ronchitelli, A., Spinapolice, E.E., Zerboni, A., Benazzi, S., 2019. An overview of Alpine and Mediterranean palaeogeography, terrestrial ecosystems and climate history during MIS 3 with focus on the Middle to Upper Palaeolithic transition. Quat. Int. https://doi.org/10.1016/j.quaint.2019.09.024. S1040618219307608.

Badura, J., Jary, Z., Smalley, I., 2013. Sources of loess material for deposits in Poland and parts of Central Europe: the lost big River. Quat. Int. 296, 15–22. https://doi.org/10.1016/j.quaint.2012.06.019.

Balasch, J.C., Poch, R.M., Rodríguez, R., Plata, J.M., Jiménez, D., Castelltort, X., Aran, M., Ascaso, E., Boixadera, J., 2019. Els sòls del loess -Unes notes en el front de batalla Itinerari edàfic per la Terra Alta i la Ribera d’Ebre. Departament de Medi Ambient i Ciències del Sòl, pp. 1–51.

Banak, A., Mandic, O., Sprovieri, M., Lirer, F., Pavelić, D., 2016. Stable isotope data from loess malacofauna: evidence for climate changes in the Pannonian Basin during the late Pleistocene. Quat. Int. 415, 15–24. https://doi.org/10.1016/j.quaint.2015.10.102.

Barta, G., 2014. Paleoenvironmental reconstruction based on the morphology and distribution of secondary carbonates of the loess-paleosol sequence at Süttő, Hungary. Quat. Int. 319, 64–75. https://doi.org/10.1016/j.quaint.2013.08.019.

Basarin, B., Vandenberghe, D.A.G., Marković, S.B., Catto, N., Hambach, U., Vasiliniuc, S., Derese, C., RonČević, S., Vasiljević, Dj.A., Rajić, Lj, 2011. The Belotinac section (Southern Serbia) at the southern limit of the European loess belt: initial results. Quat. Int. 240, 128–138. https://doi.org/10.1016/j.quaint.2011.02.022.

Basarin, B., Buggle, B., Hambach, U., Marković, S.B., Dhand, K.O., Kovačević, A., Stevens, T., Guo, Z., Lukić, T., 2014. Time-scale and astronomical forcing of Serbian loess–paleosol sequences. Glob. Planet. Chang. 122, 89–106. https://doi.org/10.1016/j.gloplacha.2014.08.007.

Bellwood, P.S., 2005. First Farmers: The Origins of Agricultural Societies. Blackwell Pub, Malden, MA.

Berg, L.S., 1916. The origin of loess. Commuications Russian Geographical Foundations 52, 579–646.

Bertran, P., Liard, M., Sitzia, L., Tissoux, H., 2016. A map of Pleistocene aeolian deposits in Western Europe, with special emphasis on France: Pleistocene aeolian deposits in western Europe. J. Quat. Sci. 31, 844–856. https://doi.org/10.1002/jqs.2909.

BGR [Bundesanstalt für Geowissenschaften und Rohstoffe], 2005. Soil Regions of the European Union and Adjacent Countries 1 : 5 000 000 (EUSR5000) Version 2.0. Special Publication, Ispra. EU catalogue number S.P.I.05.134.

Bibus, E., 2002. Zum Quartär Im Mittleren Neckarraum: Reliefentwicklung, Löß/Paläobodensequenzen, Paläoklima. Tübinger geowissenschaftliche Arbeiten. Geographisches Institut der Universität.

Bibus, E., Rähle, W., Wedel, J., 2002. Profilaufbau, Molluskenführung und Parallelisierungsmöglichkeiten des Altwürmabschnitts im Lössprofil Mainz-Weisenau. https://doi.org/10.23689/FIDGEO-1147.

Bloemendal, J., Liu, X., Sun, Y., Li, N., 2008. An assessment of magnetic and geochemical indicators of weathering and pedogenesis at two contrasting sites on the Chinese Loess plateau. Palaeogeogr. Palaeoclimatol. Palaeoecol. 257, 152–168. https://doi.org/10.1016/j.palaeo.2007.09.017.

Boixadera, J., Poch, R.M., Lowick, S.E., Balasch, J.C., 2015. Loess and soils in the eastern Ebro Basin. Quat. Int. 376, 114–133. https://doi.org/10.1016/j.quaint.2014.07.046.

Bokhorst, M.P., Beets, C.J., Marković, S.B., Gerasimenko, N.P., Matviishina, Z.N., Frechen, M., 2009. Pedo-chemical climate proxies in late Pleistocene Serbian–Ukranian loess sequences. Quat. Int. 198, 113–123. https://doi.org/10.1016/j.quaint.2008.09.003.

Bokhorst, M.P., Vandenberghe, J., Sümegi, P., Łanczont, M., Gerasimenko, N.P., Matviishina, Z.N., Marković, S.B., Frechen, M., 2011. Atmospheric circulation patterns in central and eastern Europe during the Weichselian Pleniglacial inferred from loess grain-size records. Quat. Int. 234, 62–74. https://doi.org/10.1016/j.quaint.2010.07.018.

Boretto, G., Zanchetta, G., Ciulli, L., Bini, M., Fallick, A.E., Lezzerini, M., Colonese, A.C., Zembo, I., Trombino, L., Regattieri, E., Sarti, G., 2017. The loess deposits of Buca Dei Corvi section (Central Italy): Revisited. Catena 151, 225–237. https://doi.org/10.1016/j.catena.2017.01.001.

Borsy, Z., Felszerfalvi, J., Szabo, P.P., 1979. Thermoluminescence dating of several layers of the loess sequences at Paks and Mende (Hungary). Acta Geol. Acad. Sci. Hung. 29, 451–459.

Bösken, J., Klasen, N., Zeeden, C., Obreht, I., Marković, S.B., Hambach, U., Lehmkuhl, F., 2017. New luminescence-based geochronology framing the last two glacial cycles at the southern limit of European Pleistocene loess in Stalać (Serbia). Geochronometria 44, 150–161. https://doi.org/10.1515/geochr-2015-0062.

Bösken, J., Obreht, I., Zeeden, C., Klasen, N., Hambach, U., Sümegi, P., Lehmkuhl, F., 2019. High-resolution paleoclimatic proxy data from the MIS3/2 transition recorded in northeastern Hungarian loess. Quat. Int. 502, 95–107. https://doi.org/10.1016/j.quaint.2017.12.008.

Bosq, M., Bertran, P., Degeai, J.-P., Kreutzer, S., Queffelec, A., Moine, O., Morin, E., 2018. Last Glacial aeolian landforms and deposits in the Rhône Valley (SE France): Spatial distribution and grain-size characterization. Geomorphology 318, 250–269. https://doi.org/10.1016/j.geomorph.2018.06.010.

Bosq, M., Bertran, P., Degeai, J.-P., Queffelec, A., Moine, O., 2020a. Geochemical signature of sources, recycling and weathering in the last Glacial loess from the Rhône Valley (Southeast France) and comparison with other European regions. Aeolian Res. 42, 100561. https://doi.org/10.1016/j.aeolia.2019.100561.

Bosq, M., Kreutzer, S., Bertran, P., Degeai, J.-P., Dugas, P., Kadereit, A., Lanos, P., Moine, O., Pfaffner, N., Queffelec, A., Sauer, D., 2020b. Chronostratigraphy of two late Pleistocene loess-palaeosol sequences in the Rhône Valley (Southeast France). Quat. Sci. Rev. 245, 106473. https://doi.org/10.1016/j.quascirev.2020.106473.

Botti, D., 2018. A phytoclimatic map of Europe. Cybergeo. https://doi.org/10.4000/cybergeo.29495.

British Geological Survey, 2013. Onshore Digital Geological Map of Great Britain, BGS Geology 625k/ DiGMapGB-625.

Bronger, A., 2003. Correlation of loess–paleosol sequences in East and Central Asia with SE Central Europe: towards a continental Quaternary pedostratigraphy and paleoclimatic history. Quat. Int. 106, 11–31.

Bruno, L., Marchi, M., Bertolini, I., Gottardi, G., Amorosi, A., 2020. Climate control on stacked paleosols in the Pleistocene of the Po Basin (northern Italy). J. Quat. Sci. 35, 559–571. https://doi.org/10.1002/jqs.3199.

Buggle, B., Hambach, U., Glaser, B., Gerasimenko, N., Marković, S.B., Glaser, I., Zöller, L., 2009. Stratigraphy, and spatial and temporal paleoclimatic trends in Southeastern/Eastern European loess–paleosol sequences. Quat. Int. https://doi.org/10.1016/j.quaint.2008.07.013.

Buggle, B., Glaser, B., Zöller, L., Hambach, U., Marković, S., Glaser, I., Gerasimenko, N., 2008. Geochemical characterization and origin of Southeastern and Eastern European loesses (Serbia, Romania, Ukraine). Quat. Sci. Rev. 27, 1058–1075. https://doi.org/10.1016/j.quascirev.2008.01.018.

Buggle, B., Hambach, U., Kehl, M., Marković, S.B., Zöller, L., Glaser, B., 2013. The progressive evolution of a continental climate in southeast-central European lowlands during the Middle Pleistocene recorded in loess paleosol sequences. Geology 41, 771–774. https://doi.org/10.1130/G34198.1.

Buggle, B., Hambach, U., Müller, K., Zöller, L., Marković, S.B., Glaser, B., 2014. Iron mineralogical proxies and Quaternary climate change in SE-European loess–paleosol sequences. Catena 117, 4–22. https://doi.org/10.1016/j.catena.2013.06.012.

Campodonico, V.A., Rouzaut, S., Pasquini, A.I., 2019. Campodonico, V.A., Rouzaut, S., Pasquini, A.I., 2019. Geochemistry of a Late Quaternary loess-paleosol sequence in central Argentina: Implications for weathering, sedimentary recycling and provenance. Geoderma 351, 235–249. https://doi.org/10.1016/j.geoderma.2019.04.024.

Catt, J.A., 1977. Loess and coversand. In: Shotton, F.W. (Ed.), British Quaternary Studies - Recent Advances. Clarendon Press, Oxford, pp. 221–229.

Catt, J.A., 1985. Soil particle size distribution and mineralogy as indicators of pedogenic and geomorphic history: Examples from the loessial soils of England and Wales. In: Richard, K.S., Arnet, R.R., Ellis, S. (Eds.), Geomorphology and Soils. G. Allen & Unwin, London, pp. 202–218.

Cegła, J., 1972. Sedymentacja lessów Polski (Loess Sedimentation in Poland). Acta Universitatis Wratislaviensis.

Chen, J., Yang, T., Matishov, G.G., Velichko, A.A., Zeng, B., He, Y., Shi, P., 2018. Luminescence chronology and age model application for the upper part of the Chumbur-Kosa loess sequence in the Sea of Azov, Russia. J. Mt. Sci. 15, 504–518. https://doi.org/10.1007/s11629-017-4689-0.

Chen, J., Yang, T., Qiang, M., Matishov, G.G., Velichko, A.A., Zeng, B., Xu, M., Shi, P., 2020. Interpretation of sedimentary subpopulations extracted from grain size distributions in loess deposits at the Sea of Azov, Russia. Aeolian Res. 45, 100597. https://doi.org/10.1016/j.aeolia.2020.100597.

Cheshitev, G., Kânčev, I., Vâlkov, V., Marinova, R., Shilyafova, J., Russeva, M., Iliev, K., 1989. Geological Map of P.R. Bulgaria.

Christ, P., 1942. Geologische Gerneralkarte der Schweiz - Blatt 2 Basel-Bern. Erläuterungen von A. Buxtorf 1951.

Christ, P., 1944. Geologische Generalkarte der Schweiz - Blatt 1 Neuchâtel. Notice explicative par D. Aubert & H. Badoux, 1956.

Christ, P., Nabholz, W., 1950. Geologische Generalkarte der Schweiz - Blatt 3 Zürich-Glarus. Erläuterungen von A. Buxtorf, mit Beiträgen von W. Nabholz, 1957.

Chu, W., 2018. The Danube Corridor Hypothesis and the Carpathian Basin: Geological, Environmental and Archaeological Approaches to Characterizing Aurignacian Dynamics. J. World Prehist. 31, 117–178. https://doi.org/10.1007/s10963-018-9115-1.

Constantin, D., Timar-Gabor, A., Veres, D., Begy, R., Cosma, C., 2012. SAR-OSL dating of different grain-sized quartz from a sedimentary section in southern Romania interbedding the Campanian Ignimbrite/Y5 ash layer. Quat. Geochronol. 10, 81–86. https://doi.org/10.1016/j.quageo.2012.01.012.

Constantin, D., Begy, R., Vasiliniuc, S., Panaiotu, C., Necula, C., Codrea, V., Timar-Gabor, A., 2014. High-resolution OSL dating of the Costineşti section (Dobrogea, SE Romania) using fine and coarse quartz. Quat. Int. 334–335, 20–29. https://doi.org/10.1016/j.quaint.2013.06.016.

Constantin, D., Veres, D., Panaiotu, C., Anechitei-Deacu, V., Groza, S.M., Begy, R., Kelemen, S., Buylaert, J.-P., Hambach, U., Marković, S.B., Gerasimenko, N., Timar-Gabor, A., 2019. Luminescence age constraints on the Pleistocene-Holocene transition recorded in loess sequences across SE Europe. Quat. Geochronol. 49, 71–77. https://doi.org/10.1016/j.quageo.2018.07.011.

Costantini, E.A.C., L'Abate, G., Barbetti, R., Fantappié, M., Lorenzetti, R., Magini, S., 2012. Mappa Dei Suoli d'Italia – Soil Map of Italy 1:1,000,000. In: Consiglio per la Ricerca e la Sperimentazione in Agricoltura. Ministero delle Politiche Agricole Alimentari e Forestali.

Costantini, E.A.C., Carnicelli, S., Sauer, D., Priori, S., Andreetta, A., Kadereit, A., Lorenzetti, R., 2018. Loess in Italy: Genesis, characteristics and occurrence. Catena 168, 14–33. https://doi.org/10.1016/j.catena.2018.02.002.

Cremaschi, M., 1987. Loess deposits of the Plain of the Po and of the adjoining Adriatic basin (Northern Italy). In: Pecsi, M., French, H.M. (Eds.), Loess and Periglacial Phenomena. Akademiai Kiado, Budapest, pp. 125–140.

Cremaschi, M. (Ed.), 1990a. The Loess in Northern and Central Italy: a Loess basin between the Alps and the Mediterranean region ; (guide-book to the excursion in Northern and Central Italy, September–October 1988), 1st ed. Quaderni di Geodinamica Alpina e Quaternaria. Centro di Studio per la Stratigrafia e Petrografia delle Alpi Centrale, Milano, Italy.

Cremaschi, M., 1990b. Stratigraphy and palaeoenvironmental significance of the loess deposits on Susak Island (Dalmatian archipelago). Quat. Int. 5, 97–106. https://doi.org/10.1016/1040-6182(90)90029-4.

Cremaschi, M., 2004. Late Pleistocene loess. In: Antonioli, F., Vai, G.B. (Eds.), Litho-Palaeoenvironmental Maps of Italy During the Last Two Climatic Extremes. Climex Maps Italy. Museo Geologico Giovanni Cappellini, Bologna, Italy.

Cremaschi, M., Ferraro, F., 2007. The upper Pleistocene in the Paglicci Cave (Gargano, southern Italy): loess and tephra in the anthropogenic sequence. In: Attie della Societa Toscana di Scienze Naturalie Memorie Serie A, pp. 153–163.

Cremaschi, M., Lanzinger, M., 1984. La successione stratigrafica e le fasi pedogenetiche del sito epigravettiano di Andalo, i loess tardiglaciali della Val d'Adige. Preistoria Alpina 19, 179–188.

Cremaschi, M., Lanzinger, M., 1987. Studio pedostratigrafico e geomorfologico dell'area circostante il sito tardo Paleolitico-Mesolitico di Terlago (Trento). In: Studi Trentini Scienze Naturali. Acta Geol, 64, pp. 99–120.

Cremaschi, M., Van Vliet-Lanoë, B., 1990. Traces of frost activity and ice segregation in Pleistocene loess deposits and till of northern Italy: deep seasonal freezing or permafrost? Quat. Int. 5, 39–48. https://doi.org/10.1016/1040-6182(90)90023-W.

Cremaschi, M., Fedoroff, N., Guerreschi, A., Huxtable, J., Colombi, N., Castelletti, L., Maspero, A., 1990. Sedimentary and pedological processes in the Upper Pleistocene loess of northern Italy. The Bagaggera sequence. Quat. Int. 5, 23–38. https://doi.org/10.1016/1040-6182(90)90022-V.

Cremaschi, M., Zerboni, A., Nicosia, C., Negrino, F., Rodnight, H., Spötl, C., 2015. Age, soil-forming processes, and archaeology of the loess deposits at the Apennine margin of the Po plain (northern Italy): New insights from the Ghiardo area. Quat. Int. 376, 173–188. https://doi.org/10.1016/j.quaint.2014.07.044.

Croatian Geological Survey, 2009. Geological Map of the Republic of Croatia, Scale 1, 300, p. 000.

Crouvi, O., Amit, R., Enzel, Y., Gillespie, A.R., 2010. Active sand seas and the formation of desert loess. Quat. Sci. Rev. 29, 2087–2098. https://doi.org/10.1016/j.quascirev.2010.04.026.

Danin, A., Ganor, E., 1991. Trapping of airborne dust by mosses in the Negev Desert, Israel. Earth Surf. Process. Landf. 16, 153–162. https://doi.org/10.1002/esp.3290160206.

de San José Mancha, M.A., 1973. Mapa Geológico de España nº 606 (Chinchón), 1 : 50,000.

Delpiano, D., Peresani, M., Bertola, S., Cremaschi, M., Zerboni, A., 2019. Lashed by the wind: short-term Middle Palaeolithic occupations within the loess-palaeosoil sequence at Monte Netto (Northern Italy). Quat. Int. 502, 137–147. https://doi.org/10.1016/j.quaint.2019.01.026.

Derbyshire, E., Kemp, R., Meng, X., 1995. Variations in loess and palaeosol properties as indicators of palaeoclimatic gradients across the Loess Plateau of North China. Quat. Sci. Rev. 14, 681–697. https://doi.org/10.1016/0277-3791(95)00077-1.

Ding, Z.L., Ranov, V., Yang, S.L., Finaev, A., Han, J.M., Wang, G.A., 2002. The loess record in southern Tajikistan and correlation with Chinese loess. Earth Planet. Sci. Lett. 200, 387–400. https://doi.org/10.1016/S0012-821X(02)00637-4.
Dobrzański, B., Kowaliński, S., Kuznicki, F., Witek, T., Zawadzki, S., 1974. Soil Map of Poland, 1 : 1,000,000.
Durn, G., Rubinić, V., Wacha, L., Patekar, M., Frechen, M., Tsukamoto, S., Tadej, N., Husnjak, S., 2018. Polygenetic soil formation on late Glacial Loess on the Susak Island reflects paleo-environmental changes in the Northern Adriatic area. Quat. Int. 494, 236–247. https://doi.org/10.1016/j.quaint.2017.06.072.
Ehlers, J., Gibbard, P.L., Hughes, P.D., 2011. Quaternary Glaciations - Extent and Chronology. Elsevier, Amsterdam.
Einwögerer, T., Friesinger, H., Händel, M., Neugebauer-Maresch, C., Simon, U., Teschler-Nicola, M., 2006. Upper Palaeolithic infant burials. Nature 444. https://doi.org/10.1038/444285a, 285–285.
EMODnet - Bathymetry, 2019. Understanding the Topography of the European Seas. https://portal.emodnet-bathymetry.eu/.
European Soils Bureau Network, 2005. Soil Atlas of Europe. In: European Commission. Office for Official Publications of the European Communities, Luxembourg.
Federal Geological Institute, 1970. Geological Map of SFR Yugoslavia, 1:500,000. Prepared by Institute for Geological and Mining Exploration and Investigation of Nuclear and Other Raw Materials, Belgrade.
Feng, J.-L., Hu, Z.-G., Ju, J.-T., Lin, Y.-C., 2014. The dust provenance and transport mechanism for the Chengdu Clay in the Sichuan Basin, China. CATENA 121, 68–80. https://doi.org/10.1016/j.catena.2014.04.018.
Fenn, K., Durcan, J.A., Thomas, D.S.G., Banak, A., 2020. A 180 ka record of environmental change at Erdut (Croatia): a new chronology for the loess–palaeosol sequence and its implications for environmental interpretation. J. Quat. Sci. 35, 582–593. https://doi.org/10.1002/jqs.3201.
Ferraro, F., 2009. Age, sedimentation, and soil formation in the Val Sorda loess sequence, Northern Italy. Quat. Int. 204, 54–64. https://doi.org/10.1016/j.quaint.2008.12.002.
Feurdean, A., Tămaş, T., Tanţău, I., Fărcaş, S., 2012. Elevational variation in regional vegetation responses to late-glacial climate changes in the Carpathians: Rapid vegetation responses to late-glacial climate. J. Biogeogr. 39, 258–271. https://doi.org/10.1111/j.1365-2699.2011.02605.x.
Fink, J., 1965. The pleistocene in eastern Austria. Geol. Soc. Am. Spec. Pap. 84, 179–200.
Fink, J., Kukla, G.J., 1977. Pleistocene climates in Central Europe: at least 17 interglacials after the Olduvai event. Quat. Res. 7, 363–371. https://doi.org/10.1016/0033-5894(77)90027-8.
Fink, J., Nagl, H., 1979. Quartäre Sedimente und Formen (Quaternary sediments and forms), 1:1,000,000. In: Österreichische Akademie der Wissenschaften (ÖAW). Kommission für Raumforschung, Atlas der Republik Österreich 1:1,000,000, Nr. II/6.
Fink, J., Haase, G., Ruske, R., 1977. Bemerkung zur Lößkarte von Europa 1:2,5 Mio. Petermanns Geogr. Mitt. 2, 81–97.
Fischer, P., Hambach, U., Klasen, N., Schulte, P., Zeeden, C., Steininger, F., Lehmkuhl, F., Gerlach, R., Radtke, U., 2019. Landscape instability at the end of MIS 3 in western Central Europe: evidence from a multi proxy study on a Loess-Palaeosol-Sequence from the eastern Lower Rhine Embayment, Germany. Quat. Int. https://doi.org/10.1016/j.quaint.2017.09.008.
Fischer, P., Jöris, O., Fitzsimmons, K.E., Vinnepand, M., Prud'homme, C., Schulte, P., Hatté, C., Hambach, U., Lindauer, S., Zeeden, C., Peric, Z., Lehmkuhl, F., Wunderlich, T., Wilken, D., Schirmer, W., Vött, A., 2021. Millennial-scale terrestrial ecosystem responses to Upper Pleistocene climatic changes: 4D-reconstruction of the Schwalbenberg Loess-Palaeosol-Sequence (Middle Rhine Valley, Germany). CATENA 196, 104913. https://doi.org/10.1016/j.catena.2020.104913.
Fitzsimmons, K.E., Marković, S.B., Hambach, U., 2012. Pleistocene environmental dynamics recorded in the loess of the middle and lower Danube basin. Quat. Sci. Rev. 41, 104–118. https://doi.org/10.1016/j.quascirev.2012.03.002.
Flint, R.F., 1971. Glacial and Quaternary Geology. Wiley, New York.
Florea, N., 2010. Loess was formed, but not sedimented. Rev. Roum. Géogr. 54, 159–169.
Forno, M.G., 1990. Aeolian and reworked loess in the Turin Hills (northwestern Italy). Quat. Int. 5, 81–87. https://doi.org/10.1016/1040-6182(90)90027-2.
Franc, O., Moine, O., Fülling, A., Auguste, P., Pasty, J., Gadiolet, P., Gaertner, V., Robert, V., 2017. Les séquences alluvio-lœssiques du Würm moyen/supérieur de Quincieux et de Lyon (Rhône-Alpes, France) : premières interprétations paléoenvironnementales et corrélations. Quaternaire 28, 423–453. https://doi.org/10.4000/quaternaire.8453.
Frechen, M., Schirmer, W., 2011. Luminescence chronology of the Schwalbenberg II loess in the Middle Rhine Valley. E&G Quat. Sci. J. 60, 78–89. https://doi.org/10.3285/eg.60.1.05.
Frechen, M., Horváth, E., Gábris, G., 1997. Geochronology of middle and upper pleistocene loess sections in Hungary. Quat. Res. 48, 291–312. https://doi.org/10.1006/qres.1997.1929.
Fuček, L., Matičec, D., Vlahović, I., Oštrić, N., Prtoljan, B., Kobar, T., Husinec, A., Palenik, D., 2014. Basic Geological Map of the Republic of Croatia Scale 1: 50.000 Sheet Cres 4. Croatian Geological Survey (Department of Geology).
Fuchs, M., Rousseau, D.-D., Antoine, P., Hatté, C., Gauthier, C., Marković, S., Zoeller, L., 2008. Chronology of the last climatic cycle (Upper Pleistocene) of the Surduk loess sequence, Vojvodina, Serbia. Boreas 37, 66–73. https://doi.org/10.1111/j.1502-3885.2007.00012.x.
Fuchs, M., Kreutzer, S., Rousseau, D.-D., Antoine, P., Hatté, C., Lagroix, F., Moine, O., Gauthier, C., Svoboda, J., Lisá, L., 2013. The loess sequence of Dolní Věstonice, Czech Republic: a new OSL-based chronology of the last Climatic Cycle: Loess sequence of Dolní Věstonice, Czech Republic: OSL chronology. Boreas 42, 664–677. https://doi.org/10.1111/j.1502-3885.2012.00299.x.
Gaar, D., Preusser, F., 2017. Age of the most extensive Glaciation of Northern Switzerland: evidence from the scientific drilling at Möhliner Feld. E&G Quat. Sci. J. 66, 1–5. https://doi.org/10.3285/eg.66.1.er1.
Gallet, S., Jahn, B., Torii, M., 1996. Geochemical characterization of the Luochuan loess-paleosol sequence, China, and paleoclimatic implications. Chem. Geol. 133, 67–88. https://doi.org/10.1016/S0009-2541(96)00070-8.
Galović, L., 2016. Sedimentological and mineralogical characteristics of the Pleistocene loess/paleosol sections in the Eastern Croatia. Aeolian Res. 20, 7–23. https://doi.org/10.1016/j.aeolia.2015.10.007.
Galović, L., Frechen, M., Halamić, J., Durn, G., Romić, M., 2009. Loess chronostratigraphy in Eastern Croatia—a luminescence dating approach. Quat. Int. 198, 85–97. https://doi.org/10.1016/j.quaint.2008.02.004.
Galović, L., Frechen, M., Peh, Z., Durn, G., Halamić, J., 2011. Loess/palaeosol section in Šarengrad, Croatia – a qualitative discussion on the correlation of the geochemical and magnetic susceptibility data. Quat. Int. 240, 22–34. https://doi.org/10.1016/j.quaint.2011.02.003, 2009.
Gehrt, E., 1994. Die äolischen Sedimente Im Bereich der nördlichen Lößgrenze Zwischen Leine Und Oker Und Deren Einflüsse Auf Die Bodenentwicklung, Diss. Univ. Göttingen, Göttingen.
Gehrt, E., Hagedorn, J., 1996. Zur Entstehung der nördlichen Lößgrenze in Mitteleuropa. – in: Böden als Zeugen der Landschaftsentwicklung., in: Festschrift Zum 80. Geburtstag von Prof. Dr. H. E. Stremme. Landesamt Für Natur Und Umwelt Des Landes Schleswig-Holstein, Abt. Geologie/Boden. Kiel, pp. 59–66.
Gild, C., Geitner, C., Sanders, D., 2018. Discovery of a landscape-wide drape of late-glacial aeolian silt in the western Northern Calcareous Alps (Austria): first results and implications. Geomorphology 301, 39–52. https://doi.org/10.1016/j.geomorph.2017.10.025.
Gouda, G., 1962. Untersuchungen an Lössen der Nordschweiz. Geographica Helvetica 17, 137–221.
Goudie, A.S., 1978. Dust storms and their geomorphological implications. J. Arid Environ. 1, 291–311. https://doi.org/10.1016/S0140-1963(18)31712-9.
Goudie, A.S., 1983. Dust storms in space and time. In: Progress in Physical Geography: Earth and Environment, 7, pp. 502–530. https://doi.org/10.1177/030913338300700402.
Gozhik, P., Komar, M., Łanczont, M., Fedorowicz, S., Bogucki, A., Mroczek, P., Prylypko, S., Kusiak, J., 2014. Paleoenvironmental history of the Middle Dnieper Area from the Dnieper to Weichselian Glaciation: a case study of the Maksymivka loess profile. Quat. Int. 334–335, 94–111. https://doi.org/10.1016/j.quaint.2013.11.037.
Grahmann, R., 1932. Der Löss in Europa, Mitteilungen Gesellschaft für Erdkunde. Duncker & Humblot, Leipzig.
Grichuk, V.P., 1992. Main types of vegetation (ecosystems) for the maximum cooling of the last glaciation. In: Frenzel, B., Pecsi, B., Velichko, A.A. (Eds.), Atlas of Palaeoclimates and Palaeoenvironments of the Northern Hemisphere. NQUA/Hungarian Academy of Sciences, Budapest, pp. 123–124.
Guenther, E.W., 1987. Zur Gliederung der Lösse des südlichen Oberrheintals. E&G Quat. Sci. J. 37, 67–77. https://doi.org/10.23689/fidgeo-1291.
Haase, G., Lieberoth, I., Ruske, R., 1970. Sedimente und Paläoböden im Lößgebiet. In: Richter, H., Haase, G., Lieberoth, I., Ruske, R. (Eds.), Periglazial – Löß – Paläolithikum Im Jungpleistozän Der Deutschen Demokratischen Republik. Ergänzungsheft Zu Petermanns Geographischen Mitteilungen. VEB Hermann Haack, pp. 99–212.
Haase, D., Fink, J., Haase, G., Ruske, R., Pécsi, M., Richter, H., Altermann, M., Jäger, K.-D., 2007. Loess in Europe—its spatial distribution based on a European Loess Map, scale 1:2,500,000. Quat. Sci. Rev. 26, 1301–1312. https://doi.org/10.1016/j.quascirev.2007.02.003.
Haesaerts, P., Juvigne, E., Kuyl, 0., Mucher, H., Roebroeks, W., 1981. An account of the excursion of June, 13, 1981 in the Hesbaye area and to Dutch Limbourg, devoted to the chronostratigraphy of Upper Pleistocene loess. Annales - Societe Geologique de Belgique 104, 223–240.
Haesaerts, P., Mestdagh, H., 2000. Pedosedimentary evolution of the last interglacial and early glacial sequence in the European loess belt from Belgium to Central Russia. Neth. J. Geosci. 79, 313–324. https://doi.org/10.1017/S001677460002179X.
Haesaerts, P., Borziak, I., Chirica, V., Damblon, F., Koulakovska, L., Van der Plicht, J., 2003. The east Carpathian loess record : a reference for the middle and late pleniglacial stratigraphy in Central Europe [La séquence loessique du domaine Est-carpatique : Une référence pour le Pléniglaciaire moyen et supérieur d'Europe Centrale.]. Quaternaire 14, 163–188. https://doi.org/10.3406/quate.2003.1740.
Haesaerts, P., Damblon, F., Sinitsyn, A., van der Plicht, J., 2004. Kostienki 14 (Voronezh, Central Russia): new data on stratigraphy and radiocarbon chronology. BAR Int. Ser. 1240, 169–180.
Haesaerts, P., Pirson, S., Meijs, E.P.M., 2011. New Proposal for the Quaternary Lithostratigraphic Units (Belgium). National Commission for Stratigraphy, Subcommission Quaternary.
Haesaerts, P., Damblon, F., Gerasimenko, N., Spagna, P., Pirson, S., 2016. The late Pleistocene loess-palaeosol sequence of Middle Belgium. Quat. Int. 411, 25–43. https://doi.org/10.1016/j.quaint.2016.02.012.
Hastings, D.A., Dunbar, P.K., Elphingstone, G.M., Bootz, M., Murakami, H., Maruyama, H., Masaharu, H., Holland, P., Payne, J., Bryant, N.A., Logan, T.L., Muller, J.-P., Schreier, G., MacDonald, J.S., 1999. The Global Land Onekilometer Base Elevation (GLOBE) Digital Elevation Model, Version 1.0.
Hatté, C., Gauthier, C., Rousseau, D.-D., Antoine, P., Fuchs, M., Lagroix, F., Markovic, S. B., Moine, O., Sima, A., 2013. Excursions to C_4 vegetation recorded in the Upper Pleistocene loess of Surduk (Northern Serbia): an organic isotope geochemistry study. Clim. Past 9, 1001–1014. https://doi.org/10.5194/cp-9-1001-2013.

Hauck, T.C., Lehmkuhl, F., Zeeden, C., Bösken, J., Thiemann, A., Richter, J., 2018. The Aurignacian way of life: Contextualizing early modern human adaptation in the Carpathian Basin. Quat. Int. 485, 150–166. https://doi.org/10.1016/j.quaint.2017.10.020.

Henze, N., Geologisches Institut, Geologisches Institut, 1998. Kennzeichnung Des Oberwürmlösses der Niederrheinischen Bucht, Kölner Forum für Geologie Und Paläontologie. Geologisches Institut der Universität zu Köln, Dissertation, Köln.

Hilgers, A., Gehrt, E., Janotta, A., Radtke, U., 2001a. A contribution to the dating of the northern boundary of the Weichselian Loess Belt in Northern Germany by luminescence dating and pedological analysis. Quat. Int. 76–77, 191–200. https://doi.org/10.1016/S1040-6182(00)00102-6.

Hilgers, A., Murray, A.S., Schlaak, N., Radtke, U., 2001b. Comparison of quartz OSL protocols using Lateglacial and Holocene dune sands from Brandenburg, Germany. Quat. Sci. Rev. 20, 731–736. https://doi.org/10.1016/S0277-3791(00)00050-0.

Hirniak, J.N., Smith, E.I., Johnsen, R., Ren, M., Hodgkins, J., Orr, C., Negrino, F., Riel-Salvatore, J., Fitch, S., Miller, C.E., Zerboni, A., Mariani, G.S., Harris, J.A., Gravel-Miguel, C., Strait, D., Peresani, M., Benazzi, S., Marean, C.W., 2020. Discovery of cryptotephra at Middle–Upper Paleolithic sites Arma Veirana and Riparo Bombrini, Italy: a new link for broader geographic correlations. J. Quat. Sci. 35, 199–212. https://doi.org/10.1002/jqs.3158.

Hošek, J., Hambach, U., Lisá, L., Grygar, T.M., Horáček, I., Meszner, S., Knésl, I., 2015. An integrated rock-magnetic and geochemical approach to loess/paleosol sequences from Bohemia and Moravia (Czech Republic): Implications for the Upper Pleistocene paleoenvironment in Central Europe. Palaeogeogr. Palaeoclimatol. Palaeoecol. 418, 344–358. https://doi.org/10.1016/j.palaeo.2014.11.024.

Hošek, J., Lisá, L., Hambach, U., Petr, L., Vejrostová, L., Bajer, A., Grygar, T.M., Moska, P., Gottvald, Z., Horsák, M., 2017. Middle Pleniglacial pedogenesis on the northwestern edge of the Carpathian basin: a multidisciplinary investigation of the Bíňa pedo-sedimentary section, SW Slovakia. Palaeogeogr. Palaeoclimatol. Palaeoecol. 487, 321–339. https://doi.org/10.1016/j.palaeo.2017.09.017.

Hughes, M.W., Almond, P.C., Roering, J.J., Tonkin, P.J., 2010. Late Quaternary loess landscape evolution on an active tectonic margin, Charwell Basin, South Island, New Zealand. Geomorphology 122, 294–308. https://doi.org/10.1016/j.geomorph.2009.09.034.

Hughes, P.D., Woodward, J.C., van Calsteren, P.C., Thomas, L.E., 2011. The glacial history of the Dinaric Alps, Montenegro. Quat. Sci. Rev. 30, 3393–3412. https://doi.org/10.1016/j.quascirev.2011.08.016.

Iovita, R., Fitzsimmons, K.E., Dobos, A., Hambach, U., Hilgers, A., Zander, A., 2012. Dealul Guran: evidence for lower Palaeolithic (MIS 11) occupation of the lower Danube loess steppe. Antiquity 86, 973–989.

Jahn, A., 1950. Less, jego pochodzenie i związek z klimatem epoki lodowej (Loess, its origin and connection with the climate of the glacial epoch). Acta Geol. Polonica I 257–310.

Jakab, S., 2007. Chrono-toposequences of soils on the river terraces in Transylvania (Romania). Catena 71, 406–410. https://doi.org/10.1016/j.catena.2007.03.016.

Jarke, J., 1960. Staubfall auf dem Schwarzen Meer. Deutsche Hydrographische Zeitschrift 13, 225–229. https://doi.org/10.1007/BF02224720.

Jary, Z., 1996. Chronostratigraphy and the course of loess sedimentation in SW Poland on the example of the Glubczyce Upland and Trzebnica Hills. In: Acta Universitatis Wratislaviensis 1766, Studia Geograficzne 63 (103 pp. in Polish with English summary).

Jary, Z., 2007. Record of Climate Changes in Upper Pleistocene loess-soil sequences in Poland and western part of Ukraine. In: Treatise of the Institute of Geography and Regional Development of the University of Wrocław 1 (in Polish with English summary).

Jary, Z., 2009. Periglacial markers within the late Pleistocene loess–palaeosol sequences in Poland and Western Ukraine. Quat. Int. 198, 124–135. https://doi.org/10.1016/j.quaint.2008.01.008.

Jary, Z., 2010. Loess-soil sequences as a source of climatic proxies: an example from SW Poland. Geologija 52, 40–45. https://doi.org/10.2478/v10056-010-0004-2.

Jary, Z., Ciszek, D., 2013. Late Pleistocene loess–palaeosol sequences in Poland and western Ukraine. Quat. Int. 296, 37–50. https://doi.org/10.1016/j.quaint.2012.07.009.

Jary, Z., Kida, J., 2000. Loess particles sources, transport and deposition on the example of SW Poland. Acta Universitatis Wratislaviensis 2269, 71–77.

Jary, Z., Kida, J., Snihur, M., 2002. Loess and loess-derived sediments in SW Poland. In: Loess in Lower Silesia, Czasopismo Geograficzne, pp. 63–100 (in Polish with English summary).

Jary, Z., Krawczyk, M., Raczyk, J., Ryzner, K., 2016. Loess in lower Silesia., in: Berlin, Geozon Science Media, 57–73. In: Faust, Dominik, Heller, Katja (Eds.), Erkundungen in Sachsen Und Schlesien: Quartäre Sedimente Im Landschaftsgenetischen Kontext. Geozon Science Media, Berlin, pp. 57–73.

JAXA EORC, 2016. ALOS Global Digital Surface Model "ALOS World 3D - 30m" (AW3D30). URL. http://www.eorc.jaxa.jp/ALOS/en/aw3d30/index.htm (accessed 2.15.18).

Jersak, J., 1973. Litologia I Stratygrafia Lessu wyżyn południowej Polski (Lithology and Stratigraphy of the Loess on the Southern Polish Uplands), Acta Geographica Lodziensia. Państwowe Wydawn, Lódź.

Jipa, D.C., 2014. The conceptual sedimentary model of the lower Danube loess basin: Sedimentogenetic implications. In: Quat. Int., 351, pp. 14–24. https://doi.org/10.1016/j.quaint.2013.06.008.

Jordanova, D., Jordanova, N., 2020. Diversity and peculiarities of soil formation in eolian landscapes – Insights from the mineral magnetic records. Earth Planet. Sci. Lett. 531, 115956. https://doi.org/10.1016/j.epsl.2019.115956.

Jordanova, D., Hus, J., Geeraerts, R., 2007. Palaeoclimatic implications of the magnetic record from loess/palaeosol sequence Viatovo (NE Bulgaria): Palaeoclimatic implications of the magnetic record. Geophys. J. Int. 171, 1036–1047. https://doi.org/10.1111/j.1365-246X.2007.03576.x.

Juvigné, E., Tallier, E., Haesaerts, P., Pirson, S., 2008. Un nouveau stratotype du téphra de Rocourt dans la carrière de Romont (Eben/ Bassenge, Belgique). Quaternaire. Revue de l'Association française pour l'étude du Quaternaire 19 (2), 133–139. https://doi.org/10.4000/quaternaire.2742.

Kadereit, A., Kind, C.-J., Wagner, G.A., 2013. The chronological position of the Lohne Soil in the Nussloch loess section – re-evaluation for a European loess-marker horizon. Quat. Sci. Rev. 59, 67–86. https://doi.org/10.1016/j.quascirev.2012.10.026.

Karger, D.N., Conrad, O., Böhner, J., Kawohl, T., Kreft, H., Soria-Auza, R.W., Zimmermann, N.E., Linder, H.P., Kessler, M., 2017. Climatologies at high resolution for the earth's land surface areas. Sci. Data 4, 170122. https://doi.org/10.1038/sdata.2017.122.

Kels, H., 2007. Bau Und Bilanzierung der Lössdecke Am Westlichen Niederrhein. Heinrich-Heine-Universität Düsseldorf, Düsseldorf.

Kels, H., Protze, J., Sitlivy, V., Hilgers, A., Zander, A., Anghelinu, M., Bertrams, M., Lehmkuhl, F., 2014. Genesis of loess-like sediments and soils at the foothills of the Banat Mountains, Romania – examples from the Paleolithic sites Românești and Coșava. Quat. Int. 351, 213–230. https://doi.org/10.1016/j.quaint.2014.04.063.

Koeniger, P., Barta, G., Thiel, C., Bajnóczi, B., Novothny, Á., Horváth, E., Techmer, A., Frechen, M., 2014. Stable isotope composition of bulk and secondary carbonates from the Quaternary loess-paleosol sequence in Süttő, Hungary. Quat. Int. 319, 38–49. https://doi.org/10.1016/j.quaint.2012.06.038.

Koloszar, L., 2010. The thickest and the most complete loess sequence in the Carpathian basin: the borehole Udvari-2A. Open Geosci. 2, 165–174. https://doi.org/10.2478/v10085-010-0004-9.

Košťálik, J., 1989. Spraše a fosílne pôdy Východného Slovenska, ich genéza, charakteristika, chronostratigrafia a využitie v Národnom Hospodárstve (the Loess and Fossils of Eastern Slovakia, their Genesis, Characteristics, Chronostratigraphy and Use in the National Economy). PhD thesis. VŠP Nitra.

Koster, E.A., 2005. Recent advances in luminescence dating of late Pleistocene (cold-climate) aeolian sand and loess deposits in western Europe. Permafr. Periglac. Process. 16, 131–143. https://doi.org/10.1002/ppp.512.

Kostić, N., Protić, N., 2000. Pedology and mineralogy of loess profiles at Kapela-Batajnica and Stalać, Serbia. Catena 41, 217–227. https://doi.org/10.1016/S0341-8162(00)00102-8.

Kozarski, S., Nowaczyk, B., 1991. Lithofacies Variation and Chronostratigraphy of Late Vistulian and Holocene Aeolian Phenomena in Northwestern Poland. Z. Geomorph. N.F., Suppl.-Bd 90, pp. 107–122.

Krauß, L., Zens, J., Zeeden, C., Schulte, P., Eckmeier, E., Lehmkuhl, F., 2016. A multi-proxy analysis of two loess-paleosol sequences in the northern Harz foreland, Germany. Palaeogeogr. Palaeoclimatol. Palaeoecol. 461, 401–417. https://doi.org/10.1016/j.palaeo.2016.09.001.

Krauß, L., Kappenberg, A., Zens, J., Kehl, M., Schulte, P., Zeeden, C., Eckmeier, E., Lehmkuhl, F., 2017. Reconstruction of late Pleistocene paleoenvironments in southern Germany using two high-resolution loess-paleosol records. Palaeogeogr. Palaeoclimatol. Palaeoecol. 509, 58–76. https://doi.org/10.1016/j.palaeo.2017.11.043.

Krolopp, E., Sümegi, P., 2002. A ságvári lösz-rétegsor csigafaunája (the mollusc fauna of the Ságvár loess profile). Malakológiai Tájékoztató 20, 7–14.

Krupenikov, I.A., Novak, T.S., Rodina, A.K., Ursu, A.F., 1969a. Soil Map of the Soviet Socialist Republic Moldavia.

Krupenikov, I.A., Novak, T.S., Rodina, A.K., Ursu, A.F., 1969b. Soil Map of the Soviet Socialist Republic Moldavia.

Kukla, G.J., 1975. Loess stratigraphy of Central Europe. In: Butzer, K.W., Isaac, G.L.I. (Eds.), After the Australopithecines. Mouton, The Hague, pp. 99–188.

Kukla, G.J., 1977. Pleistocene land—sea correlations I. Europe. Earth Sci. Rev. 13, 307–374. https://doi.org/10.1016/0012-8252(77)90125-8.

Kukla, G., 1978. The classical European glacial stages: correlation with deep-sea sediments. In: Transactions of the Nebraska Academy of Science and Affiliated Societies VI, pp. 57–93.

Kukla, G., Cílek, V., 1996. Plio-Pleistocene megacycles: record of climate and tectonics. Palaeogeogr. Palaeoclimatol. Palaeoecol. 120, 171–194. https://doi.org/10.1016/0031-0182(95)00040-2.

Küster, M., Preusser, F., 2010. Late Glacial and Holocene aeolian sands and soil formation from the Pomeranian outwash plain (Mecklenburg, NE-Germany). E&G Quat. Sci. J. 58, 156–163. https://doi.org/10.23689/fidgeo-1050.

Kwiecien, O., Arz, H.W., Lamy, F., Plessen, B., Bahr, A., Haug, G.H., 2009. North Atlantic control on precipitation pattern in the eastern Mediterranean/Black Sea region during the last glacial. Quat. Res. 71, 375–384. https://doi.org/10.1016/j.yqres.2008.12.004.

Lambeck, K., Rouby, H., Purcell, A., Sun, Y., Sambridge, M., 2014. Sea level and global ice volumes from the last Glacial Maximum to the Holocene. Proc. Natl. Acad. Sci. 111, 15296–15303. https://doi.org/10.1073/pnas.1411762111.

Lancaster, N., 2020. On the formation of desert loess. Quat. Res. 96, 105–122. https://doi.org/10.1017/qua.2020.33.

Łanczont, M., Wojtanowicz, J., 2009. Typologia przestrzenna lessów Europy (Spatial typology of European loess). In: Kostrzewski, A., Paluszkiewicz, R. (Eds.), Geneza, litologia i stratygrafia utworów czwartorzędowych, t. V, Seria Geografia nr 88, pp. 301–314.

Łanczont, M., Bogucki, A., Yatsyshyn, A., Terpiłowski, S., Mroczek, P., Orłowska, A., Hołub, B., Zieliński, P., Komar, M., Woronko, B., Kulesza, P., Dmytruk, R., Tomeniuk, O., 2019. Stratigraphy and chronology of the periphery of the Scandinavian ice sheet at the foot of the Ukrainian Carpathians. Palaeogeogr.

Palaeoclimatol. Palaeoecol. 530, 59–77. https://doi.org/10.1016/j.palaeo.2019.05.024.
Leger, M., 1990. Loess landforms. Quat. Int. 7–8, 53–61. https://doi.org/10.1016/1040-6182(90)90038-6.
Lehmkuhl, F., Klinge, M., Rees-Jones, J., Rhodes, E.J., 2000. Late quaternary aeolian sedimentation in central and South-Eastern Tibet. Quat. Int. Nat. Rutter Honorarium 68–71, 117–132. https://doi.org/10.1016/S1040-6182(00)00038-0.
Lehmkuhl, F., Hilgers, A., Fries, S., Hülle, D., Schlütz, F., Shumilovskikh, L., Felauer, T., Protze, J., 2011. Holocene geomorphological processes and soil development as indicator for environmental change around Karakorum, Upper Orkhon Valley (Central Mongolia). Catena 87, 31–44. https://doi.org/10.1016/j.catena.2011.05.005.
Lehmkuhl, F., Hülle, D., Knippertz, M., 2012. Holocene geomorphic processes and landscape evolution in the lower reaches of the Orkhon River (northern Mongolia). Catena 98, 17–28. https://doi.org/10.1016/j.catena.2012.06.003.
Lehmkuhl, F., Schulte, P., Zhao, H., Hülle, D., Protze, J., Stauch, G., 2014. Timing and spatial distribution of loess and loess-like sediments in the mountain areas of the northeastern Tibetan Plateau. CATENA 117, 23–33. https://doi.org/10.1016/j.catena.2013.06.008.
Lehmkuhl, F., Zens, J., Krauß, L., Schulte, P., Kels, H., 2016. Loess-paleosol sequences at the northern European loess belt in Germany: distribution, geomorphology and stratigraphy. Quat. Sci. Rev. 153, 11–30. https://doi.org/10.1016/j.quascirev.2016.10.008.
Lehmkuhl, F., Bösken, J., Hošek, J., Sprafke, T., Marković, S.B., Obreht, I., Hambach, U., Sümegi, P., Thiemann, A., Steffens, S., Lindner, H., Veres, D., Zeeden, C., 2018a. Loess distribution and related Quaternary sediments in the Carpathian Basin. J. Maps 14, 661–670. https://doi.org/10.1080/17445647.2018.1526720.
Lehmkuhl, F., Pötter, S., Pauligk, A., Bösken, J., 2018b. Loess and other quaternary sediments in Germany. J. Maps 14, 330–340. https://doi.org/10.1080/17445647.2018.1473817.
Lehmkuhl, F., Nett, J.J., Pötter, S., Schulte, P., Sprafke, T., Jary, Z., Antoine, P., Wacha, L., Wolf, D., Zerboni, A., Hošek, J., Marković, S.B., Obreht, I., Sümegi, P., Veres, D., Zeeden, C., Boemke, B.J., Schaubert, V., Viehweger, J., Hambach, U., 2020a. Geodata of European loess, sandy loess and aeolian sand. In: CRC806-Database. https://doi.org/10.5880/SFB806.56 [Dataset].
Lehmkuhl, F., Nett, J.J., Pötter, S., Schulte, P., Sprafke, T., Jary, Z., Antoine, P., Wacha, L., Wolf, D., Zerboni, A., Hošek, J., Marković, S.B., Obreht, I., Sümegi, P., Veres, D., Zeeden, C., Boemke, B.J., Schaubert, V., Viehweger, J., Hambach, U., 2020b. Geodata of alluvial fill and fluvial deposits in Europe during the last glacial maximum. In: CRC806-Database. https://doi.org/10.5880/SFB806.57 (Dataset).
Lehmkuhl, F., Nett, J.J., Pötter, S., Schulte, P., Sprafke, T., Jary, Z., Antoine, P., Wacha, L., Wolf, D., Zerboni, A., Hošek, J., Marković, S.B., Obreht, I., Sümegi, P., Veres, D., Zeeden, C., Boemke, B.J., Schaubert, V., Viehweger, J., Hambach, U., 2020c. Geodata of European loess domains. In: CRC806-Database. https://doi.org/10.5880/SFB806.58 (Dataset).
Lehmkuhl, F., Nett, J.J., Pötter, S., Schulte, P., Sprafke, T., Jary, Z., Antoine, P., Wacha, L., Wolf, D., Zerboni, A., Hošek, J., Marković, S.B., Obreht, I., Sümegi, P., Veres, D., Zeeden, C., Boemke, B.J., Schaubert, V., Viehweger, J., Hambach, U., 2020d. Geodata of northern timberline in Europe during the last glacial maximum. In: CRC806-Database. https://doi.org/10.5880/SFB806.59 (Dataset).
Lehmkuhl, F., Nett, J.J., Pötter, S., Schulte, P., Sprafke, T., Jary, Z., Antoine, P., Wacha, L., Wolf, D., Zerboni, A., Hošek, J., Marković, S.B., Obreht, I., Sümegi, P., Veres, D., Zeeden, C., Boemke, B.J., Schaubert, V., Viehweger, J., Hambach, U., 2020e. Geodata of paleochannels on dry continental shelves in Europe during the last glacial maximum. In: CRC806-Database. https://doi.org/10.5880/SFB806.60 (Dataset).
Lehmkuhl, F., Nett, J.J., Pötter, S., Schulte, P., Sprafke, T., Jary, Z., Antoine, P., Wacha, L., Wolf, D., Zerboni, A., Hošek, J., Marković, S.B., Obreht, I., Sümegi, P., Veres, D., Zeeden, C., Boemke, B.J., Schaubert, V., Viehweger, J., Hambach, U., 2020f. Geodata of continuous and discontinuous permafrost during the last glacial maximum in Europe. In: CRC806-Database. https://doi.org/10.5880/SFB806.61 (Dataset).
Leonova, N., Nesmeyanov, S., Vinogradova, E., Voeykova, O., 2015. Upper Paleolithic subsistence practices in the southern Russian Plain: paleolandscapes and settlement system of Kamennaya Balka sites. Quat. Int. 355, 175–187. https://doi.org/10.1016/j.quaint.2014.10.004.
Li, Y., Shi, W., Aydin, A., Beroya-Eitner, M.A., Gao, G., 2020. Loess genesis and worldwide distribution. Earth Sci. Rev. 201, 102947. https://doi.org/10.1016/j.earscirev.2019.102947.
Liang, Y., Yang, T., Velichko, A.A., Zeng, B., Shi, P., Wang, L., He, Y., Chen, J., Chen, Y., 2016. Paleoclimatic record from Chumbur-Kosa section in Sea of Azov region since Marine Isotope Stage 11. J. Mt. Sci. 13, 985–999. https://doi.org/10.1007/s11629-015-3738-9.
Lindner, L., Bogutsky, A., Gozhik, P., Marciniak, B., Marks, L., Lanczont, M., Wojtanowicz, J., 2002. Correlation of main climatic glacial-interglacial and loess-palaeosol cycles in the Pleistocene of Poland and Ukraine. Acta Geol. Pol. 52, 459–469.
Lindner, H., Lehmkuhl, F., Zeeden, C., 2017. Spatial loess distribution in the eastern Carpathian Basin: a novel approach based on geoscientific maps and data. J. Maps 13, 173–181. https://doi.org/10.1080/17445647.2017.1279083.
Lisá, L., 2004. Exoscopy of Moravian eolian sediments. Bull. Geosci. 79, 177–182.
Lisá, L., Uhler, P., 2006. Provenance of Würmian loess and loess-like sediments ofMoravia and Silesia (Czech Republic): a study of zircontypology and cathodoluminiscence. Geol. Carpath. 57, 397–403.
Little, E.C., Lian, O.B., Velichko, A.A., Morozova, T.D., Nechaev, V.P., Dlussky, K.G., Rutter, N.W., 2002. Quaternary stratigraphy and optical dating of loess from the east European Plain (Russia). Quat. Sci. Rev. 21, 1745–1762. https://doi.org/10.1016/S0277-3791(01)00151-2.
Liu, J., Liu, W., 2017. Soil nitrogen isotopic composition of the Xifeng loess-paleosol sequence and its potential for use as a paleoenvironmental proxy. Quat. Int. 440, 35–41. https://doi.org/10.1016/j.quaint.2016.04.018.
Lomax, J., Fuchs, M., Antoine, P., Rousseau, D.-D., Lagroix, F., Hatté, C., Taylor, S.N., Till, J.L., Debret, M., Moine, O., Jordanova, D., 2019. A luminescence-based chronology for the Harletz loess sequence, Bulgaria. Boreas 48, 179–194. https://doi.org/10.1111/bor.12348.
Longman, J., Veres, D., Ersek, V., Salzmann, U., Hubay, K., Bormann, M., Wennrich, V., Schäbitz, F., 2017. Periodic input of dust over the Eastern Carpathians during the Holocene linked with Saharan desertification and human impact. Clim. Past 13, 897–917. https://doi.org/10.5194/cp-13-897-2017.
Ludwig, P., Gavrilov, M.B., Markovic, S.B., Ujvari, G., Lehmkuhl, F., 2020. Simulated regional dust cycle in the Carpathian Basin and the Adriatic Sea region during the last Glacial Maximum. Quat. Int. https://doi.org/10.1016/j.quaint.2020.09.048. S1040618220306121.
Macoun, J., Šibrava, V., Tyráček, J., Kneblová-Vodičková, V., 1965. Kvartér Ostravska a Moravské brány. ÚÚG, Prague.
Magyari, E.K., Veres, D., Wennrich, V., Wagner, B., Braun, M., Jakab, G., Karátson, D., Pál, Z., Ferenczy, G., St-Onge, G., Rethemeyer, J., Francois, J.-P., von Reumont, F., Schäbitz, F., 2014. Vegetation and environmental responses to climate forcing during the last Glacial Maximum and deglaciation in the East Carpathians: attenuated response to maximum cooling and increased biomass burning. In: Quaternary Science Reviews, Dating, Synthesis, and Interpretation of Palaeoclimatic Records and Model-data Integration: Advances of the INTIMATE project(INTegration of Ice core, Marine and TErrestrial records, COST Action ES0907), 106, pp. 278–298. https://doi.org/10.1016/j.quascirev.2014.09.015.
Maher, B.A., MengYu, H., Roberts, H.M., Wintle, A.G., 2003. Holocene loess accumulation and soil development at the western edge of the Chinese Loess Plateau: implications for magnetic proxies of palaeorainfall. Quat. Sci. Rev. 22, 445–451. https://doi.org/10.1016/S0277-3791(02)00188-9.
Makeev, A.O., 2009. Pedogenic alteration of aeolian sediments in the upper loess mantles of the Russian Plain. Quat. Int. 209, 79–94. https://doi.org/10.1016/j.quaint.2009.03.007.
Malicki, A., 1950. Geneza i rozmieszczenie lessów w środkowej i wschodniej Polsce (The origin and distribution of loess in Central and Eastern Poland). Annales UMCS, sec. B, 4, 8, 4, 8, pp. 195–228.
Marechal, R., Tavernier, R., 1970. Associations de sols – pédologie, 1:500.000, Atlas de Belguique, Planche 11B. L'Institut Géographique Militaire.
Marković, S.B., Oches, E., Sümegi, P., Jovanović, M., Gaudenyi, T., 2006. An introduction to the Middle and Upper Pleistocene loess–paleosol sequence at Ruma brickyard, Vojvodina, Serbia. Quat. Int. 149, 80–86. https://doi.org/10.1016/j.quaint.2005.11.020.
Marković, S.B., Oches, E.A., McCoy, W.D., Frechen, M., Gaudenyi, T., 2007. Malacological and sedimentological evidence for "warm" glacial climate from the Irig loess sequence, Vojvodina, Serbia. Geochem. Geophys. Geosyst. 8, Q09008 https://doi.org/10.1029/2006GC001565.
Marković, S.B., Hambach, U., Catto, N., Jovanović, M., Buggle, B., Machalett, B., Zöller, L., Glaser, B., Frechen, M., 2009. Middle and Late Pleistocene loess sequences at Batajnica, Vojvodina, Serbia. Quat. Int. https://doi.org/10.1016/j.quaint.2008.12.004.
Marković, S.B., Bokhorst, M.P., Vandenberghe, J., McCoy, W.D., Oches, E.A., Hambach, U., Gaudenyi, T., Jovanović, M., Zöller, L., Stevens, T., Machalett, B., 2008. Late Pleistocene loess-palaeosol sequences in the Vojvodina region, North Serbia. J. Quat. Sci. 23, 73–84. https://doi.org/10.1002/jqs.1124.
Marković, S.B., Hambach, U., Stevens, T., Kukla, G.J., Heller, F., McCoy, W.D., Oches, E. A., Buggle, B., Zöller, L., 2011. The last million years recorded at the Stari Slankamen (Northern Serbia) loess-palaeosol sequence: revised chronostratigraphy and long-term environmental trends. Quat. Sci. Rev. 30, 1142–1154. https://doi.org/10.1016/j.quascirev.2011.02.004.
Marković, S.B., Korač, M., Mrđić, N., Buylaert, J.-P., Thiel, C., McLaren, S.J., Stevens, T., Tomič, N., Petič, N., Jovanovič, M., Vasiljević, D.A., Sümegi, P., Gavrilov, M.B., Obreht, I., 2014. Palaeoenvironment and geoconservation of mammoths from the Nosak loess–palaeosol sequence (Drmno, northeastern Serbia): initial results and perspectives. Quat. Int. 334–335, 30–39. https://doi.org/10.1016/j.quaint.2013.05.047.
Marković, S.B., Stevens, T., Kukla, G.J., Hambach, U., Fitzsimmons, K.E., Gibbard, P., Buggle, B., Zech, M., Guo, Z., Hao, Q., Wu, H., O'Hara Dhand, K., Smalley, I.J., Újvári, G., Sümegi, P., Timar-Gabor, A., Veres, D., Sirocko, F., Vasiljević, D.A., Jary, Z., Svensson, A., Jović, V., Lehmkuhl, F., Kovács, J., Svirčev, Z., 2015. Danube loess stratigraphy — Towards a pan-European loess stratigraphic model. Earth Sci. Rev. 148, 228–258. https://doi.org/10.1016/j.earscirev.2015.06.005.
Marković, S.B., Fitzsimmons, K.E., Sprafke, T., Gavrilović, D., Smalley, I.J., Jović, V., Svirčev, Z., Gavrilov, M.B., Beślin, M., 2016. The history of Danube loess research. Quat. Int. 399, 86–99.
Marković, S.B., Stevens, T., Mason, J., Vandenberghe, J., Yang, S., Veres, D., Újvári, G., Timar-Gabor, A., Zeeden, C., Guo, Z., Hao, Q., Obreht, I., Hambach, U., Wu, H., Gavrilov, M.B., Rolf, C., Tomić, N., Lehmkuhl, F., 2018a. Loess correlations – between myth and reality. Palaeogeogr. Palaeoclimatol. Palaeoecol. 509, 4–23. https://doi.org/10.1016/j.palaeo.2018.04.018.
Marković, S.B., Sümegi, P., Stevens, T., Schaetzl, R.J., Obreht, I., Chu, W., Buggle, B., Zech, M., Zech, R., Zeeden, C., Gavrilov, M.B., Perić, Z., Svirčev, Z., Lehmkuhl, F., 2018b. The Crvenka loess-paleosol sequence: a record of continuous grassland domination in the southern Carpathian Basin during the late Pleistocene.

Palaeogeogr. Palaeoclimatol. Palaeoecol. 509, 33–46. https://doi.org/10.1016/j.palaeo.2018.03.019.
Marton, P., 1979. Paleomagnetism of the Mende brickyard exposure. Unknown J. 55–61.
Maruszczak, H., 1969. Une analyse paléogéographique de la répartition du loess polonaise et de ses caractéres lithologiques directifs (a paleogeographic analysis of the distribution of the polish loess and its directive lithological characters). Biul. Peryglac. 20, 133–152.
Maruszczak, H., 1985. Main genetic features and relief of loess covers in southern Poland. In: Maruszczak, H. (Ed.), Problems of the Stratigraphy and Paleogeography of Loesses, Guide-Book of the International Symposium. UMCS Lublin, pp. 9–37.
Maruszczak, H., 1991. Ogólna charakterystyka lessów w Polsce (General features of the loesses in Poland). In: Maruszczak, H. (Ed.), Podstawowe Profile Lessów W Polsce (Main Section of Loesses in Poland). Wyd. UMCS, Lublin, pp. 1–12.
Maruszczak, H., 2000. Definition and classification of loesses and loess-like deposits (in polish with Englisch summary). Prz. Geol. 48, 580–586.
Matenco, L., Munteanu, I., ter Borgh, M., Stanica, A., Tilita, M., Lericolais, G., Dinu, C., Oaie, G., 2016. The interplay between tectonics, sediment dynamics and gateways evolution in the Danube system from the Pannonian Basin to the western Black Sea. Sci. Total Environ. 543, 807–827. https://doi.org/10.1016/j.scitotenv.2015.10.081.
Mayr, C., Matzke-Karasz, R., Stojakowits, P., Lowick, S.E., Zolitschka, B., Heigl, T., Mollath, R., Theuerkauf, M., Weckend, M.-O., Bäumler, R., Gregor, H.-J., 2017. Palaeoenvironments during MIS 3 and MIS 2 inferred from lacustrine intercalations in the loess–palaeosol sequence at Bobingen (southern Germany). E&G Quat. Sci. J. 66, 73–89. https://doi.org/10.5194/egqsj-66-73-2017.
Meijs, E.P.M., 2002. Loess stratigraphy in Dutch and Belgian Limburg. E&G Quat. Sci. J. 51, 114–130. https://doi.org/10.23689/fidgeo-1322.
Meijs, E.P.M., van Peer, P., de Warrimont, J.P.L.M.N., 2013. Geomorphologic context and proposed chronostratigraphic position of lower Palaeolithic artefacts from the Op de Schans pit near Kesselt (Belgium) to the west of Maastricht. Neth. J. Geosci. 91, 137–157. https://doi.org/10.1017/S0016774600001554.
Meszner, S., Kreutzer, S., Fuchs, M., Faust, D., 2013. Late Pleistocene landscape dynamics in Saxony, Germany: Paleoenvironmental reconstruction using loess-paleosol sequences. Quat. Int. 296, 94–107. https://doi.org/10.1016/j.quaint.2012.12.040.
Meszner, S., Kreutzer, S., Fuchs, M., Faust, D., 2014. Identifying depositional and pedogenetic controls of late Pleistocene loess-paleosol sequences (Saxony, Germany) by combined grain size and microscopic analyses. ZfG Suppl. 58, 63–90. https://doi.org/10.1127/0372-8854/2014/S-00169.
Moine, O., Antoine, P., Hatté, C., Landais, A., Mathieu, J., Prud'homme, C., Rousseau, D.-D., 2017. The impact of last Glacial climate variability in west-European loess revealed by radiocarbon dating of fossil earthworm granules. Proc. Natl. Acad. Sci. U. S. A. 114, 6209–6214. https://doi.org/10.1073/pnas.1614751114.
Monegato, G., Ravazzi, C., Culiberg, M., Pini, R., Bavec, M., Calderoni, G., Jež, J., Perego, R., 2015. Sedimentary evolution and persistence of open forests between the south-eastern Alpine fringe and the Northern Dinarides during the last Glacial Maximum. Palaeogeogr. Palaeoclimatol. Palaeoecol. 436, 23–40. https://doi.org/10.1016/j.palaeo.2015.06.025.
Morozova, T.D., Nechaev, V.P., 1997. The valdai periglacial zone as an area of cryogenic soil formation. Quat. Int. 41–42, 53–58. https://doi.org/10.1016/S1040-6182(96)00036-5.
Moska, P., Adamiec, G., Jary, Z., 2011. OSL dating and lithological characteristics of loess deposits from Biały Kościół. Geochronometria 38, 162–171. https://doi.org/10.2478/s13386-011-0013-x.
Moska, P., Adamiec, G., Jary, Z., 2012. High resolution dating of loess profile from Biały Kościół, south–West Poland. Quat. Geochronol. 10, 87–93. https://doi.org/10.1016/j.quageo.2012.04.003.
Moska, P., Jary, Z., Adamiec, G., Bluszcz, A., 2019. Chronostratigraphy of a loess-palaeosol sequence in Biały Kościół, Poland using OSL and radiocarbon dating. Quat. Int. 502, 4–17. https://doi.org/10.1016/j.quaint.2018.05.024.
Muhs, D.R., 2013. The geologic records of dust in the Quaternary. Aeolian Res. 9, 3–48. https://doi.org/10.1016/j.aeolia.2012.08.001.
Muhs, D.R., 2014. Origins and properties of quaternary loess deposits. In: Reference Module in Earth Systems and Environmental Sciences. Elsevier. https://doi.org/10.1016/B978-0-12-409548-9.09431-8.
Muhs, D.R., Bettis, E.A., 2003. Quaternary loess-Paleosol sequences as examples of climate-driven sedimentary extremes. In: Special Paper 370: Extreme Depositional Environments: Mega End Members in Geologic Time. Geological Society of America, pp. 53–74. https://doi.org/10.1130/0-8137-2370-1.53.
Muhs, D.R., Budahn, J., Avila, A., Skipp, G., Freeman, J., Patterson, D., 2010. The role of African dust in the formation of Quaternary soils on Mallorca, Spain and implications for the genesis of Red Mediterranean soils. Quat. Sci. Rev. 29, 2518–2543. https://doi.org/10.1016/j.quascirev.2010.04.013.
Murton, J.B., Goslar, T., Edwards, M.E., Bateman, M.D., Danilov, P.P., Savvinov, G.N., Gubin, S.V., Ghaleb, B., Haile, J., Kanevskiy, M., Lozhkin, A.V., Lupachev, A.V., Murton, D.K., Shur, Y., Tikhonov, A., Vasil'chuk, A.C., Vasil'chuk, Y.K., Wolfe, S.A., 2015. Palaeoenvironmental Interpretation of Yedoma Silt (Ice complex) Deposition as Cold-climate Loess, Duvanny Yar, Northeast Siberia: Palaeoenvironmental Interpretation of Yedoma Silt, Duvanny Yar. Permafr. Periglac. Process. 26, 208–288. https://doi.org/10.1002/ppp.1843.
Nawrocki, J., Łanczont, M., Rosowiecka, O., Bogucki, A.B., 2016. Magnetostratigraphy of the loess-palaeosol key Palaeolithic section at Korolevo (Transcarpathia, W Ukraine). Quat. Int. 399, 72–85. https://doi.org/10.1016/j.quaint.2014.12.063.
Nawrocki, J., Gozhik, P., Łanczont, M., Pańczyk, M., Komar, M., Bogucki, A., Williams, I. S., Czupyt, Z., 2018. Palaeowind directions and sources of detrital material archived in the Roxolany loess section (southern Ukraine). Palaeogeogr. Palaeoclimatol. Palaeoecol. 496, 121–135. https://doi.org/10.1016/j.palaeo.2018.01.028.
Nawrocki, J., Bogucki, A.B., Gozhik, P., Łanczont, M., Pańczyk, M., Standzikowski, K., Komar, M., Rosowiecka, O., Tomeniuk, O., 2019. Fluctuations of the Fennoscandian Ice Sheet recorded in the anisotropy of magnetic susceptibility of periglacial loess from Ukraine. Boreas 48, 940–952. https://doi.org/10.1111/bor.12400.
Necula, C., Dimofte, D., Panaiotu, C., 2015a. Rock magnetism of a loess-palaeosol sequence from the western Black Sea shore (Romania). Geophys. J. Int. 202, 1733–1748. https://doi.org/10.1093/gji/ggv250.
Necula, C., Panaiotu, C., Schinteie, G., Palade, P., Kuncser, V., 2015b. Reconstruction of superparamagnetic particle grain size distribution from Romanian loess using frequency dependent magnetic susceptibility and temperature dependent Mössbauer spectroscopy. Glob. Planet. Chang. 131, 89–103. https://doi.org/10.1016/j.gloplacha.2015.05.009.
Neugebauer-Maresch, C., 1993. Zur altsteinzeitlichen Besiedlungsgeschichte des Galgenberges von Stratzing/Krems-Rehberg. Archäologie Österreichs 4, 10–19.
Neugebauer-Maresch, C., 2008. Krems-Hundssteig – Mammutjägerlager der Eiszeit. Ein Nutzungsareal paläolithischer Jäger- und Sammler(innen) vor 41.000–27.000 Jahren, Mitteilungen der Prähistorischen Kommission. ÖAW, Wien.
Neugebauer-Maresch, C., Hambach, U., Anghelinu, M., 2014. Loess and the record of Upper Palaeolithic cultures in the Danube Basin. Quat. Int. 351, 1–4. https://doi.org/10.1016/j.quaint.2014.10.041.
Nigst, P.R., Haesaerts, P., Damblon, F., Frank-Fellner, C., Mallol, C., Viola, B., Götzinger, M., Niven, L., Trnka, G., Hublin, J.-J., 2014. Early modern human settlement of Europe north of the Alps occurred 43,500 years ago in a cold steppe-type environment. PNAS. https://doi.org/10.1073/pnas.1412201111, 201412201.
Nottebaum, V., Lehmkuhl, F., Stauch, G., Hartmann, K., Wünnemann, B., Schimpf, S., Lu, H., 2014. Regional grain size variations in aeolian sediments along the transition between Tibetan highlands and north-western Chinese deserts – the influence of geomorphological settings on aeolian transport pathways. Earth Surf. Process. Landf. 39, 1960–1978. https://doi.org/10.1002/esp.3590.
Nottebaum, V., Stauch, G., Hartmann, K., Zhang, J., Lehmkuhl, F., 2015. Unmixed loess grain size populations along the northern Qilian Shan (China): Relationships between geomorphologic, sedimentologic and climatic controls. Quat. Int. 372, 151–166. https://doi.org/10.1016/j.quaint.2014.12.071.
Novothny, Á., Horváth, E., Frechen, M., 2002. The loess profile at Albertirsa, Hungary—improvements in loess stratigraphy by luminescence dating. Quat. Int. 95–96, 155–163. https://doi.org/10.1016/S1040-6182(02)00036-8.
Novothny, Á., Frechen, M., Horváth, E., Bradák, B., Oches, E.A., McCoy, W.D., Stevens, T., 2009. Luminescence and amino acid racemization chronology of the loess–paleosol sequence at Süttő, Hungary. Quat. Int. 198, 62–76. https://doi.org/10.1016/j.quaint.2008.01.009.
Novothny, Á., Frechen, M., Horváth, E., Wacha, L., Rolf, C., 2011. Investigating the penultimate and last glacial cycles of the Süttő loess section (Hungary) using luminescence dating, high-resolution grain size, and magnetic susceptibility data. Quat. Int. 234, 75–85. https://doi.org/10.1016/j.quaint.2010.08.002.
Obreht, I., Buggle, B., Catto, N., Marković, S.B., Bösel, S., Vandenberghe, D.A.G., Hambach, U., Svirčev, Z., Lehmkuhl, F., Basarin, B., Gavrilov, M.B., Jović, G., 2014. The late Pleistocene Belotinac section (southern Serbia) at the southern limit of the European loess belt: Environmental and climate reconstruction using grain size and stable C and N isotopes. Quat. Int. 334–335, 10–19. https://doi.org/10.1016/j.quaint.2013.05.037.
Obreht, I., Zeeden, C., Hambach, U., Veres, D., Marković, S.B., Bösken, J., Svirčev, Z., Bačević, N., Gavrilov, M.B., Lehmkuhl, F., 2016. Tracing the influence of Mediterranean climate on Southeastern Europe during the past 350,000 years. Sci. Rep. 6, 36334. https://doi.org/10.1038/srep36334.
Obreht, I., Hambach, U., Veres, D., Zeeden, C., Bösken, J., Stevens, T., Marković, S.B., Klasen, N., Brill, D., Burow, C., Lehmkuhl, F., 2017. Shift of large-scale atmospheric systems over Europe during late MIS 3 and implications for Modern Human dispersal. Sci. Rep. 7, 5848. https://doi.org/10.1038/s41598-017-06285-x.
Obreht, I., Zeeden, C., Hambach, U., Veres, D., Marković, S.B., Lehmkuhl, F., 2019. A critical reevaluation of palaeoclimate proxy records from loess in the Carpathian Basin. Earth Sci. Rev. 190, 498–520. https://doi.org/10.1016/j.earscirev.2019.01.020.
Obruchev, V.A., 1945. Loess types and their origin. Am. J. Sci. 243, 256–262. https://doi.org/10.2475/ajs.243.5.256.
Oliva, M., Palacios, D., Fernández-Fernández, J.M., Rodríguez-Rodríguez, L., García-Ruiz, J.M., Andrés, N., Carrasco, R.M., Pedraza, J., Pérez-Alberti, A., Valcárcel, M., Hughes, P.D., 2019. Late Quaternary glacial phases in the Iberian Peninsula. Earth Sci. Rev. 192, 564–600. https://doi.org/10.1016/j.earscirev.2019.03.015.
Orgiazzi, A., Ballabio, C., Panagos, P., Jones, A., Fernández-Ugalde, O., 2018. LUCAS Soil, the largest expandable soil dataset for Europe: a review: LUCAS Soil, pan-European open-access soil dataset. Eur. J. Soil Sci. 69, 140–153. https://doi.org/10.1111/ejss.12499.
Orth, A., 1872. Geognostische Durchforschung Des Schlesischen Schwemmlandes Zwischen Dem Zobtener Und Trebnitzer Gebirge. Wiegandt u, Hempel, Berlin, LVIII.
Pavlaković, S. Mikulčić, Crnjaković, M., Tibljaš, D., Šoufek, M., Wacha, L., Frechen, M., Lacković, D., 2011. Mineralogical and geochemical characteristics of Quaternary sediments from the Island of Susak (Northern Adriatic, Croatia). Quat. Int. 234, 32–49. https://doi.org/10.1016/j.quaint.2010.02.005.
Ovejanu, I., Candrea, B., Crăciunescu, V., 1968. Harta Geologica a Reppublicii Socialiste Romania (Geological Map of the Socialist Republic of Romania) 1:200.000. Bukarest: Comittul de stat al geologiei Institutul geologic (State Geological Survey).
Pécsi, M., 1987. The loess-paleosol and related subaereal sequence in Hungary. GeoJournal 15, 151–162. https://doi.org/10.1007/BF00157941.
Pécsi, M., 1990. Loess is not just the accumulation of dust. Quat. Int. 7, 1–21.
Pécsi, M., Richter, G., 1996. Löss - Herkunft - Gliederung - Landschaften. Zeitschrift für Geomorphologie, Supplementary Issues 98.

Pendea, I.F., Tantau, I., Gray, J., Ghaleb, B., Beldean, C., Badarau, A.S., Miclea, A., Balc, R., Toth, A., 2008. Middle Weichselian paleoenvironments in North-Western Transylvania: Sedimentology, palynology and malacofauna analysis. Acta Palaeontologica Romaniae 6, 349–358.

Pendea, I.F., Gray, J.T., Ghaleb, B., Tantau, I., Badarau, A.S., Nicorici, C., 2009. Episodic build-up of alluvial fan deposits during the Weichselian Pleniglacial in the western Transylvanian Basin, Romania and their paleoenvironmental significance. Quat. Int. 198, 98–112. https://doi.org/10.1016/j.quaint.2008.05.002.

Peresani, M., Cremaschi, M., Ferraro, F., Falguères, C., Bahain, J.-J., Gruppioni, G., Sibilia, E., Quarta, G., Calcagnile, L., Dolo, J.-M., 2008. Age of the final Middle Palaeolithic and Uluzzian levels at Fumane Cave, Northern Italy, using 14C, ESR, 234U/230Th and thermoluminescence methods. J. Archaeol. Sci. 35, 2986–2996. https://doi.org/10.1016/j.jas.2008.06.013.

Peresani, M., Monegato, G., Ravazzi, C., Bertola, S., Margaritora, D., Breda, M., Fontana, A., Fontana, F., Janković, I., Karavanić, I., Komšo, D., Mozzi, P., Pini, R., Furlanetto, G., Maria De Amicis, M.G., Perhoč, Z., Posth, C., Ronchi, L., Rossato, S., Vukosavljević, N., Zerboni, A., 2020. Hunter-gatherers across the great Adriatic-Po region during the Last Glacial Maximum: Environmental and cultural dynamics. Quat. Int. https://doi.org/10.1016/j.quaint.2020.10.007. S1040618220306285.

Péwé, T.L., 1955. Origin of the upland silt near Fairbanks, Alaska. Geol. Soc. Am. Bull. 66, 699. https://doi.org/10.1130/0016-7606(1955)66[699:OOTUSN]2.0.CO;2.

Pötter, S., Schmitz, A., Lücke, A., Schulte, P., Obreht, I., Zech, M., Wissel, H., Marković, S. B., Lehmkuhl, F., 2020. Middle to late Pleistocene environments based on stable organic carbon and nitrogen isotopes of loess-palaeosol sequences from the Carpathian Basin. Boreas. https://doi.org/10.1111/bor.12470. In Press.

Pouclet, A., Juvigne, E., 2009. The Eltville tephra, a late Pleistocene widespread tephra layer in Germany, Belgium and the Netherlands; symptomatic compositions of the minerals. Geol. Belg. 12, 93–103.

Profe, J., Neumann, L., Novothny, Á., Barta, G., Rolf, C., Frechen, M., Ohlendorf, C., Zolitschka, B., 2018a. Paleoenvironmental conditions and sedimentation dynamics in Central Europe inferred from geochemical data of the loess-paleosol sequence at Süttő (Hungary). Quat. Sci. Rev. 196, 21–37. https://doi.org/10.1016/j.quascirev.2018.07.034.

Profe, J., Wacha, L., Frechen, M., Ohlendorf, C., Zolitschka, B., 2018b. XRF scanning of discrete samples – a chemostratigraphic approach exemplified for loess-paleosol sequences from the Island of Susak, Croatia. Quat. Int. 494, 34–51. https://doi.org/10.1016/j.quaint.2018.05.006.

Prud'homme, C., Lécuyer, C., Antoine, P., Moine, O., Hatté, C., Fourel, F., Martineau, F., Rousseau, D.-D., 2016. Palaeotemperature reconstruction during the last Glacial from δ 18 O of earthworm calcite granules from Nussloch loess sequence, Germany. Earth Planet. Sci. Lett. 442, 13–20. https://doi.org/10.1016/j.epsl.2016.02.045.

Pye, K., 1995. The nature, origin and accumulation of loess. Quat. Sci. Rev. 14, 653–667. https://doi.org/10.1016/0277-3791(95)00047-X.

Rao, Z., Xu, Y., Xia, D., Xie, L., Chen, F., 2013. Variation and paleoclimatic significance of organic carbon isotopes of Ili loess in arid Central Asia. Org. Geochem. 63, 56–63. https://doi.org/10.1016/j.orggeochem.2013.08.007.

Roesner, U., 1990. Die Mainfränkische Lößprovinz. Sedimentologische, pedologische und morphodynamische Prozesse der Lößbildung während des Pleistozäns in Mainfranken. Mitteilungen der Fränkischen Geographischen Gesellschaft 37, 1–290.

Rolf, C., Hambach, U., Novothny, Á., Horváth, E., Schnepp, E., 2014. Dating of a last Glacial loess sequence by relative geomagnetic palaeointensity: a case study from the Middle Danube Basin (Süttő, Hungary). Quat. Int. 319, 99–108. https://doi.org/10.1016/j.quaint.2013.08.050.

Römer, W., Lehmkuhl, F., Sirocko, F., 2016. Late Pleistocene aeolian dust provenances and wind direction changes reconstructed by heavy mineral analysis of the sediments of the Dehner dry maar (Eifel, Germany). Glob. Planet. Chang. 147, 25–39. https://doi.org/10.1016/j.gloplacha.2016.10.012.

Ronchi, B., Barão, L., Clymans, W., Vandevenne, F., Batelaan, O., Govers, G., Struyf, E., Dassargues, A., 2015. Factors controlling Si export from soils: a soil column approach. CATENA 133, 85–96. https://doi.org/10.1016/j.catena.2015.05.007.

Rousseau, D., 1987. Paleoclimatology of the Achenheim series (middle and upper pleistocene, Alsace, France) A. malacological analysis. Palaeogeogr. Palaeoclimatol. Palaeoecol. https://doi.org/10.1016/0031-0182(87)90087-3.

Rousseau, D.-D., 2001. Loess biostratigraphy: new advances and approaches in mollusk studies. In: Earth-Science Reviews, Recent Research on Loess and Palaeosols, Pure and Applied, 54, pp. 157–171. https://doi.org/10.1016/S0012-8252(01)00046-0.

Rousseau, D.-D., Puisségur, J.-J., 1990. A 350,000-year climatic record from the loess sequence of Achenheim, Alsace, France. Boreas 19, 203–216. https://doi.org/10.1111/j.1502-3885.1990.tb00446.x.

Rousseau, D.-D., Zöller, L., Valet, J.-P., 1998. Late Pleistocene climatic variations at Achenheim, France, based on a magnetic susceptibility and TL chronology of loess. Quat. Res. 49, 255–263. https://doi.org/10.1006/qres.1998.1972.

Rousseau, D.-D., Gerasimenko, N., Matviischina, Z., Kukla, G., 2001. Late Pleistocene environments of the Central Ukraine. Quat. Res. 56, 349–356. https://doi.org/10.1006/qres.2001.2270.

Rousseau, D.-D., Sima, A., Antoine, P., Hatté, C., Lang, A., Zöller, L., 2007. Link between European and North Atlantic abrupt climate changes over the last glaciation. Geophys. Res. Lett. 34, L22713 https://doi.org/10.1029/2007GL031716.

Rousseau, D.-D., Antoine, P., Gerasimenko, N., Sima, A., Fuchs, M., Hatté, C., Moine, O., Zoeller, L., 2011. North Atlantic abrupt climatic events of the last glacial period recorded in Ukrainian loess deposits. Clim. Past 7, 221–234. https://doi.org/10.5194/cp-7-221-2011.

Rousseau, D.-D., Derbyshire, E., Antoine, P., Hatté, C., 2013. LOESS RECORDS | Europe. In: Mock, S.A.E.J. (Ed.), Encyclopedia of Quaternary Science, Second edition. Elsevier, Amsterdam, pp. 606–619.

Rousseau, D.-D., Chauvel, C., Sima, A., Hatté, C., Lagroix, F., Antoine, P., Balkanski, Y., Fuchs, M., Mellett, C., Kageyama, M., Ramstein, G., Lang, A., 2014. European glacial dust deposits: Geochemical constraints on atmospheric dust cycle modeling: European Glacial Dust Deposits. Geophys. Res. Lett. 41, 7666–7674. https://doi.org/10.1002/2014GL061382.

Rousseau, D.-D., Svensson, A., Bigler, M., Sima, A., Steffensen, J.P., Boers, N., 2017. Eurasian contribution to the last glacial dust cycle: how are loess sequences built? Clim. Past. https://doi.org/10.5194/cp-13-1181-2017.

Rousseau, D.-D., Antoine, P., Boers, N., Lagroix, F., Ghil, M., Lomax, J., Fuchs, M., Debret, M., Hatté, C., Moine, O., Gauthier, C., Jordanova, D., Jordanova, N., 2020. Dansgaard-Oeschger-like events of the penultimate climate cycle: the loess point of view. Clim. Past 16, 713–727. https://doi.org/10.5194/cp-16-713-2020.

Rubinić, V., Galović, L., Lazarević, B., Husnjak, S., Durn, G., 2018. Pseudogleyed loess derivates – the most common soil parent materials in the Pannonian region of Croatia. Quat. Int. 494, 248–262. https://doi.org/10.1016/j.quaint.2017.06.044.

Ruszkiczay-Rüdiger, Z., Kern, Z., 2016. Permafrost or seasonal frost? A review of paleoclimate proxies of the last glacial cycle in the east central European lowlands. Quat. Int. 415, 241–252. https://doi.org/10.1016/j.quaint.2015.07.027.

Rutter, N.W., Rokosh, D., Evans, M.E., Little, E.C., Chlachula, J., Velichko, A., 2003. Correlation and interpretation of paleosols and loess across European Russia and Asia over the last interglacial–glacial cycle. Quat. Res. 60, 101–109. https://doi.org/10.1016/S0033-5894(03)00069-3.

Sabatier, P., Nicolle, M., Piot, C., Colin, C., Debret, M., Swingedouw, D., Perrette, Y., Bellingery, M.-C., Chazeau, B., Develle, A.-L., Leblanc, M., Skonieczny, C., Copard, Y., Reyss, J.-L., Malet, E., Jouffroy-Bapicot, I., Kelner, M., Poulenard, J., Didier, J., Arnaud, F., Vannière, B., 2020. Past African dust inputs in the western Mediterranean area controlled by the complex interaction between the Intertropical Convergence Zone, the North Atlantic Oscillation, and total solar irradiance. Clim. Past 16, 283–298. https://doi.org/10.5194/cp-16-283-2020.

Šajgalík, J., Modlitba, I., 1983. Spraše Podunajskej nížiny a Ich Vlastnosti (the Loess of the Danube Lowlands and their Properties). VEDA, Bratislava.

Samlley, I.J., Marković, S.B., 2014. Loessification and hydroconsolidation: There is a connection. Catena 117, 94–99. https://doi.org/10.1016/j.catena.2013.07.006.

Sanborn, P.T., Smith, C.A.S., Froese, D.G., Zazula, G.D., Westgate, J.A., 2006. Full-glacial paleosols in perennially frozen loess sequences, Klondike goldfields, Yukon Territory, Canada. Quat. Res. 66, 147–157. https://doi.org/10.1016/j.yqres.2006.02.008.

Săndulescu, M., Kräutner, H., Borcoș, M., Năstăseanu, S., Patrulius, D., Ștefănescu, M., Ghenea, C., Lupu, M., Savu, H., Bercia, I., Marinescu, F., 1978. România - Atlas Geologic Foaia 1 (Geological Atlas of Romania), Scale 1:1,000,000.

Schaetzl, R.J., Bettis, E.A., Crouvi, O., Fitzsimmons, K.E., Grimley, D.A., Hambach, U., Lehmkuhl, F., Marković, S.B., Mason, J.A., Owczarek, P., Roberts, H.M., Rousseau, D.-D., Stevens, T., Vandenberghe, J., Zárate, M., Veres, D., Yang, S., Zech, M., Conroy, J.L., Dave, A.K., Faust, D., Hao, Q., Obreht, I., Prud'homme, C., Smalley, I., Tripaldi, A., Zeeden, C., Zech, R., 2018. Approaches and challenges to the study of loess—Introduction to the LoessFest special issue. Quat. Res. 89, 563–618. https://doi.org/10.1017/qua.2018.15.

Schaffernicht, E.J., Ludwig, P., Shao, Y., 2020. Linkage between dust cycle and loess of the last Glacial Maximum in Europe. Atmos. Chem. Phys. 20, 4969–4986. https://doi.org/10.5194/acp-20-4969-2020.

Schatz, A.-K., Zech, M., Buggle, B., Gulyás, S., Hambach, U., Marković, S.B., Sümegi, P., Scholten, T., 2011. The late Quaternary loess record of Tokaj, Hungary: Reconstructing palaeoenvironment, vegetation and climate using stable C and N isotopes and biomarkers. Quat. Int. 240, 52–61. https://doi.org/10.1016/j.quaint.2010.10.009.

Schatz, A.-K., Buylaert, J.-P., Murray, A., Stevens, T., Scholten, T., 2012. Establishing a luminescence chronology for a palaeosol-loess profile at Tokaj (Hungary): a comparison of quartz OSL and polymineral IRSL signals. Quat. Geochronol. 10, 68–74.

Schatz, A.-K., Qi, Y., Siebel, W., Wu, J., Zöller, L., 2015a. Tracking potential source areas of central European loess: examples from Tokaj (HU), Nussloch (D) and Grub (AT). Open Geosci. 7, 678–720. https://doi.org/10.1515/geo-2015-0048.

Schatz, A.-K., Scholten, T., Kühn, P., 2015b. Paleoclimate and weathering of the Tokaj (Hungary) loess–paleosol sequence. Palaeogeogr. Palaeoclimatol. Palaeoecol. 426, 170–182. https://doi.org/10.1016/j.palaeo.2015.03.016.

Schirmer, W., 2003. Die Eben-Zone im Oberwürmlöss zwischen Maas und Rhein. In: Schirmer, W. (Ed.), Landschaftsgeschichte Im Europäischen Rheinland. LIT Verlag, Münster, pp. 351–416.

Schirmer, W., 2016. Late Pleistocene loess of the lower Rhine. Quat. Int. 411, 44–61. https://doi.org/10.1016/j.quaint.2016.01.034.

Schirrmeister, L., Froese, D., Tumskoy, V., Grosse, G., Wetterich, S., 2013. Permafrost and periglacial features | Yedoma: late Pleistocene Ice-Rich Syngenetic Permafrost of Beringia. In: Encyclopedia of Quaternary Science. Elsevier, pp. 542–552. https://doi.org/10.1016/B978-0-444-53643-3.00106-0.

Schulte, P., Lehmkuhl, F., 2018. The difference of two laser diffraction patterns as an indicator for post-depositional grain size reduction in loess-paleosol sequences. Palaeogeogr. Palaeoclimatol. Palaeoecol. 509, 126–136. https://doi.org/10.1016/j.palaeo.2017.02.022.

Schütz, L., 1980. Long range transport of dester dust with special emphasis on the Sahara. Ann. N. Y. Acad. Sci. 338, 515–532. https://doi.org/10.1111/j.1749-6632.1980.tb17144.x.

Sebe, K., Csillag, G., Ruszkiczay-Rüdiger, Z., Fodor, L., Thamó-Bozsó, E., Müller, P., Braucher, R., 2011. Wind erosion under cold climate: a Pleistocene periglacial mega-yardang system in Central Europe (Western Pannonian Basin, Hungary). Geomorphology 134, 470–482. https://doi.org/10.1016/j.geomorph.2011.08.003.

Semmel, A., 1998. Zur paläopedologischen Grundgliederung des älteren Würmlösses in Mitteleuropa. Mitteilungen deutscher bodenkundlichen Gesellschaft 88, 449–452.
Semmel, A., Terhorst, B., 2010. The concept of the Pleistocene periglacial cover beds in Central Europe: a review. Quat. Int. 222, 120–128. https://doi.org/10.1016/j.quaint.2010.03.010.
Sima, A., Rousseau, D.-D., Kageyama, M., Ramstein, G., Schulz, M., Balkanski, Y., Antoine, P., Dulac, F., Hatté, C., 2009. Imprint of North-Atlantic abrupt climate changes on western European loess deposits as viewed in a dust emission model. Quat. Sci. Rev. 28, 2851–2866. https://doi.org/10.1016/j.quascirev.2009.07.016.
Skonieczny, C., McGee, D., Winckler, G., Bory, A., Bradtmiller, L.I., Kinsley, C.W., Polissar, P.J., De Pol-Holz, R., Rossignol, L., Malaizé, B., 2019. Monsoon-driven Saharan dust variability over the past 240,000 years. Sci. Adv. 5 https://doi.org/10.1126/sciadv.aav1887 eaav1887.
Skurzyński, J., Jary, Z., Kenis, P., Kubik, R., Moska, P., Raczyk, J., Seul, C., 2020. Geochemistry and mineralogy of the late Pleistocene loess-palaeosol sequence in Złota (near Sandomierz, Poland): Implications for weathering, sedimentary recycling and provenance. Geoderma 375, 114459. https://doi.org/10.1016/j.geoderma.2020.114459.
Smalley, I.J., 1971. "In-situ" theories of loess formation and the significance of the calcium-carbonate content of loess. Earth Sci. Rev. 7, 67–85. https://doi.org/10.1016/0012-8252(71)90082-1.
Smalley, I., 1995. Making the material: the formation of silt sized primary mineral particles for loess deposits. Quat. Sci. Rev. 14, 645–651. https://doi.org/10.1016/0277-3791(95)00046-1.
Smalley, I., Leach, J.A., 1978. The origin and distribution of the loess in the Danube basin and associated regions of East-Central Europe — a review. Sediment. Geol. 21, 1–26. https://doi.org/10.1016/0037-0738(78)90031-3.
Smalley, I., Obreht, I., 2018. The formation of loess ground by the process of loessification: a history of the concept. Geologos 24, 163–170. https://doi.org/10.2478/logos-2018-0015.
Smalley, I., O'Hara-Dhand, K., Wint, J., Machalett, B., Jary, Z., Jefferson, I., 2009. Rivers and loess: the significance of long river transportation in the complex event-sequence approach to loess deposit formation. Quat. Int. 198, 7–18. https://doi.org/10.1016/j.quaint.2008.06.009.
Smalley, I., Marković, S.B., Svirčev, Z., 2011. Loess is [almost totally formed by] the accumulation of dust. Quat. Int. 240, 4–11. https://doi.org/10.1016/j.quaint.2010.07.011.
Sokolovsky, A.N., Krupsky, N.K., Voronin, A.V., Bogdanovich, V.G., 1977a. Soil Map of Ukraine.
Sokolovsky, A.N., Krupsky, N.K., Voronin, A.V., Bogdanovich, V.G., 1977b. Soil Map of Ukraine.
Sommer, M., Kaczorek, D., Kuzyakov, Y., Breuer, J., 2006. Silicon pools and fluxes in soils and landscapes—a review. J. Plant Nutr. Soil Sci. 169, 310–329. https://doi.org/10.1002/jpln.200521981.
Sprafke, T., 2016. Löss in Niederösterreich – Archiv quartärer Klima- Und Landschaftsveränderungen (Loess in Lower Austria - Archive of Quaternary Climate and Landscape Development). Würzburg University Press, Würzburg.
Sprafke, T., Obreht, I., 2016. Loess: Rock, sediment or soil – what is missing for its definition? Quat. Int. 399, 198–207. https://doi.org/10.1016/j.quaint.2015.03.033.
Sprafke, T., Thiel, C., Terhorst, B., 2014. From micromorphology to palaeoenvironment: the MIS 10 to MIS 5 record in Paudorf (Lower Austria). Catena 117, 60–72. https://doi.org/10.1016/j.catena.2013.06.024.
Sprafke, T., Schulte, P., Meyer-Heintze, S., Händel, M., Einwögerer, T., Simon, U., Peticzka, R., Schäfer, C., Lehmkuhl, F., Terhorst, B., 2020. Paleoenvironments from robust loess stratigraphy using high-resolution color and grain-size data of the last glacial Krems-Wachtberg record (NE Austria). Quat. Sci. Rev. 248, 106602. https://doi.org/10.1016/j.quascirev.2020.106602.
Stauch, G., IJmker, J., Pötsch, S., Zhao, H., Hilgers, A., Diekmann, B., Dietze, E., Hartmann, K., Opitz, S., Wünnemann, B., Lehmkuhl, F., 2012. Aeolian sediments on the north-eastern Tibetan Plateau. Quat. Sci. Rev. 57, 71–84. https://doi.org/10.1016/j.quascirev.2012.10.001.
Steup, R., Fuchs, M., 2017. The loess sequence at Münzenberg (Wetterau/Germany): a reinterpretation based on new luminescence dating results. Z. Geomorphol. 61, 101–120. https://doi.org/10.1127/zfg_suppl/2016/0408. Supplementary Issues.
Stevens, T., Sechi, D., Bradák, B., Orbe, R., Baykal, Y., Cossu, G., Tziavaras, C., Andreucci, S., Pascucci, V., 2020. Abrupt last glacial dust fall over Southeast England associated with dynamics of the British-Irish ice sheet. Quat. Sci. Rev. 250, 106641. https://doi.org/10.1016/j.quascirev.2020.106641.
Stojak, J., McDevitt, A.D., Herman, J.S., Searle, J.B., Wójcik, J.M., 2015. Post-glacial colonization of eastern Europe from the Carpathian refugium: evidence from mitochondrial DNA of the common vole Microtus arvalis. Biol. J. Linn. Soc. 115, 927–939. https://doi.org/10.1111/bij.12535.
Strauss, J., Schirrmeister, L., Grosse, G., Fortier, D., Hugelius, G., Knoblauch, C., Romanovsky, V., Schädel, C., Schneider von Deimling, T., Schuur, E.A.G., Shmelev, D., Ulrich, M., Veremeeva, A., 2017. Deep Yedoma permafrost: a synthesis of depositional characteristics and carbon vulnerability. Earth Sci. Rev. 172, 75–86. https://doi.org/10.1016/j.earscirev.2017.07.007.
Strunk, H., 1990. Das Quartärprofil von Hagelstadt im Bayerischen Tertiärhügelland. Eiszeit. Gegenw. 40, 85–96.
Stuut, J.-B., Smalley, I., O'Hara-Dhand, K., 2009. Aeolian dust in Europe: African sources and European deposits. Quat. Int. 198, 234–245. https://doi.org/10.1016/j.quaint.2008.10.007.
Sümegi, P., Krolopp, E., 2002. Quatermalacological analyses for modeling of the Upper Weichselian palaeoenvironmental changes in the Carpathian Basin. Quat. Int. 91, 53–63. https://doi.org/10.1016/S1040-6182(01)00102-1.
Sümegi, P., Rudner, E., Beszeda, I., 2000. Stratigraphical and palaeoecological investigation of the fossil soil comprising Upper Palaeolithic tools at Bodrogkeresztúr – Henye. In: Dobosi, T.V. (Ed.), Bodrogkeresztúr – Henye (NE Hungary) Upper Palaeolithic Site. Magyar Nemzeti Múzeum Kiadványa, Budapest, pp. 217–220.
Sümegi, P., Gulyás, S., Persaits, G., GergelyPáll, D., Molnár, D., 2011. The loess-paleosol sequence of Basaharc (Hungary) revisited: Mollusc-based paleoecological results for the Middle and Upper Pleistocene. Quat. Int. 240, 181–192. https://doi.org/10.1016/j.quaint.2011.05.005.
Sümegi, P., Magyari, E., Dániel, P., Molnár, M., Törőcsik, T., 2013. Responses of terrestrial ecosystems to Dansgaard–Oeshger cycles and Heinrich-events: a 28,000-year record of environmental changes from SE Hungary. In: Quaternary International, Advancing Pleistocene and Holocene Climate Change Research in the Carpathian-Balkan Region, 293, pp. 34–50. https://doi.org/10.1016/j.quaint.2012.07.032.
Sümegi, P., Marković, S.B., Molnár, D., Sávai, S., Náfrádi, K., Szelepcsényi, Z., Novák, Z., 2016a. Črvenka loess-paleosol sequence revisited: local and regional Quaternary biogeographical inferences of the southern Carpathian Basin. Open Geosci. 8, 390–404. https://doi.org/10.1515/geo-2016-0031.
Sümegi, P., Törőcsik, T., Náfrádi, K., Sümegi, B., Majkut, P., Molnár, D., Tapody, R., 2016b. Radiocarbon dated complex paleoecological and geoarcheological analyses at the Bodrogkeresztúr-Henye Gravettian site (NE Hungary). Archeometriai Műhely 31–41, 2016/XIII./1.
Sümegi, P., Gulyás, S., Molnár, D., Náfrádi, K., Törőcsik, T., Sümegi, B.P., Müller, T., Szilágyi, G., Varga, Z., 2017. Ice Age Terrestrial and Freshwater Gastropod Refugia in the Carpathian Basin, Central Europe. Biol. Resour. Water. https://doi.org/10.5772/intechopen.71910.
Sümegi, P., Gulyás, S., Molnár, D., Sümegi, B.P., Almond, P.C., Vandenberghe, J., Zhou, L., Pál-Molnár, E., Törőcsik, T., Hao, Q., Smalley, I., Molnár, M., Marsi, I., 2018. New chronology of the best developed loess/paleosol sequence of Hungary capturing the past 1.1 ma: Implications for correlation and proposed pan-Eurasian stratigraphic schemes. Quat. Sci. Rev. 191, 144–166. https://doi.org/10.1016/j.quascirev.2018.04.012.
Svirčev, Z., Marković, S.B., Stevens, T., Codd, G.A., Smalley, I., Simeunović, J., Obreht, I., Dulić, T., Pantelić, D., Hambach, U., 2013. Importance of biological loess crusts for loess formation in semi-arid environments. Quat. Int. 296, 206–215. https://doi.org/10.1016/j.quaint.2012.10.048.
Svirčev, Z., Dulić, T., Obreht, I., Codd, G.A., Lehmkuhl, F., Marković, S.B., Hambach, U., Meriluoto, J., 2019. Cyanobacteria and loess—an underestimated interaction. Plant Soil 439, 293–308. https://doi.org/10.1007/s11104-019-04048-3.
Sycheva, S., Frechen, M., Terhorst, B., Sedov, S., Khokhlova, O., 2020. Pedostratigraphy and chronology of the late Pleistocene for the extra glacial area in the Central Russian Upland (reference section Aleksandrov quarry). Catena 194, 104689. https://doi.org/10.1016/j.catena.2020.104689.
Tecsa, V., Gerasimenko, N., Veres, D., Hambach, U., Lehmkuhl, F., Schulte, P., Timar-Gabor, A., 2020. Revisiting the chronostratigraphy of late Pleistocene loess-paleosol sequences in southwestern Ukraine: OSL dating of Kurortne section. Quat. Int. 542, 65–79. https://doi.org/10.1016/j.quaint.2020.03.001.
Terhorst, B., 2013. A stratigraphic concept for Middle Pleistocene Quaternary sequences in Upper Austria. E&G Quat. Sci. J. 62, 4–13. https://doi.org/10.3285/eg.62.1.01.
Terhorst, B., Sedov, S., Sprafke, T., Peticzka, R., Meyer-Heintze, S., Kühn, P., Solleiro Rebolledo, E., 2015. Austrian MIS 3/2 loess–palaeosol records—Key sites along a west–east transect. Palaeogeogr. Palaeoclimatol. Palaeoecol. 418, 43–56. https://doi.org/10.1016/j.palaeo.2014.10.020.
Thiel, C., Buylaert, J.-P., Murray, A., Terhorst, B., Hofer, I., Tsukamoto, S., Frechen, M., 2011a. Luminescence dating of the Stratzing loess profile (Austria) – Testing the potential of an elevated temperature post-IR IRSL protocol. Quat. Int. 234, 23–31. https://doi.org/10.1016/j.quaint.2010.05.018.
Thiel, C., Buylaert, J.-P., Murray, A.S., Terhorst, B., Tsukamoto, S., Frechen, M., Sprafke, T., 2011b. Investigating the chronostratigraphy of prominent palaeosols in Lower Austria using post-IR IRSL dating. E&G Quat. Sci. J. 60, 137–152. https://doi.org/10.3285/eg.60.1.10.
Torre, G., Gaiero, D.M., Cosentino, N.J., Coppo, R., 2020. The paleoclimatic message from the polymodal grain-size distribution of late Pleistocene-early Holocene Pampean loess (Argentina). Aeolian Res. 42, 100563. https://doi.org/10.1016/j.aeolia.2019.100563.
Tóth, G., Jones, A., Montanarella, L., European Commission, Joint Research Centre, Institute for Environment and Sustainability, 2013. LUCAS Topsoil Survey: Methodology, Data and Results. Publications Office, Luxembourg.
Tsatskin, A., Heller, F., Hailwood, E.A., Gendler, T.S., Hus, J., Montgomery, P., Sartori, M., Virina, E.I., 1998. Pedosedimentary division, rock magnetism and chronology of the loess/palaeosol sequence at Roxolany (Ukraine). Palaeogeogr. Palaeoclimatol. Palaeoecol. 143, 111–133. https://doi.org/10.1016/S0031-0182(98)00073-X.
Tsoar, H., Pye, K., 1987. Dust transport and the question of desert loess formation. Sedimentology 34, 139–153. https://doi.org/10.1111/j.1365-3091.1987.tb00566.x.
Tutkovsky, P.A., 1899. K woprosu o sposobje obrazovanija lossa (the question of the origin of loess). Zemlevedenie 1–2, 213–311.
Újvári, G., Klötzli, U., 2015. U–Pb ages and Hf isotopic composition of zircons in Austrian last glacial loess: constraints on heavy mineral sources and sediment transport pathways. Int. J. Earth Sci. (Geol Rundsch) 104, 1365–1385. https://doi.org/10.1007/s00531-014-1139-x.
Újvári, G., Varga, A., Balogh-Brunstad, Z., 2008. Origin, weathering, and geochemical composition of loess in southwestern Hungary. Quat. Res. 69, 421–437. https://doi.org/10.1016/j.yqres.2008.02.001.
Újvári, G., Kovács, J., Varga, G., Raucsik, B., Marković, S.B., 2010. Dust flux estimates for the last Glacial Period in East Central Europe based on terrestrial records of loess

deposits: a review. Quat. Sci. Rev. 29, 3157–3166. https://doi.org/10.1016/j.quascirev.2010.07.005.
Újvári, G., Varga, A., Ramos, F.C., Kovács, J., Németh, T., Stevens, T., 2012. Evaluating the use of clay mineralogy, Sr–Nd isotopes and zircon U–Pb ages in tracking dust provenance: an example from loess of the Carpathian Basin. Chem. Geol. 304–305, 83–96. https://doi.org/10.1016/j.chemgeo.2012.02.007.
Újvári, G., Klötzli, U., Kiraly, F., Ntaflos, T., 2013. Towards identifying the origin of metamorphic components in Austrian loess: insights from detrital rutile chemistry, thermometry and U–Pb geochronology. Quat. Sci. Rev. 75, 132–142. https://doi.org/10.1016/j.quascirev.2013.06.002.
Újvári, G., Kok, J.F., Varga, G., Kovács, J., 2016. The physics of wind-blown loess: Implications for grain size proxy interpretations in Quaternary paleoclimate studies. Earth Sci. Rev. 154, 247–278. https://doi.org/10.1016/j.earscirev.2016.01.006.
Újvári, G., Stevens, T., Molnár, M., Demény, A., Lambert, F., Varga, G., Jull, A.J.T., Páll-Gergely, B., Buylaert, J.-P., Kovács, J., 2017. Coupled European and Greenland last glacial dust activity driven by North Atlantic climate. PNAS 114, E10632–E10638. https://doi.org/10.1073/pnas.1712651114.
van Baelen, A., 2017. The Lower to Middle Palaeolithic Transition in Northwestern Europe: Evidence from Kesselt-Op de Schans, 01 ed. Leuven University Press, Leuven, Belgium.
van Kolfschoten, T., Roebroeks, W., Vandenberghe, J., 1993. The Middle and late Pleistocene sequence at Maastricht-Belvédère: the Type Locality of the Belvédère Interglacial. Med. Rijks Geol. Dienst. 47, 81–91.
Vancampenhout, K., Langohr, R., Slaets, J., Buurman, P., Swennen, R., Deckers, J., 2013. Paleo-pedological record of the Rocourt Pedosequence at Veldwezelt–Hezerwater (Belgian Pleistocene loess belt): part 1 — Evolution of the parent material. CATENA 107, 118–129. https://doi.org/10.1016/j.catena.2013.02.005.
Vandenberghe, J., Huijzer, B.S., Mücher, H., Laan, W., 1998. Short climatic oscillations in a western European loess sequence (Kesselt, Belgium). J. Quat. Sci. 13, 471–485. https://doi.org/10.1002/(SICI)1099-1417(1998090)13:5<471::AID-JQS401>3.0.CO;2-T.
Vandenberghe, J., Renssen, H., van Huissteden, K., Nugteren, G., Konert, M., Lu, H., Dodonov, A., Buylaert, J.-P., 2006. Penetration of Atlantic westerly winds into Central and East Asia. Quat. Sci. Rev. 25, 2380–2389. https://doi.org/10.1016/j.quascirev.2006.02.017.
Vandenberghe, J., 2013. Grain size of fine-grained windblown sediment: A powerful proxy for process identification. Earth-Science Reviews. https://doi.org/10.1016/j.earscirev.2013.03.001.
Vandenberghe, J., French, H.M., Gorbunov, A., Marchenko, S., Velichko, A.A., Jin, H., Cui, Z., Zhang, T., Wan, X., 2014a. The last Permafrost Maximum (LPM) map of the Northern Hemisphere: permafrost extent and mean annual air temperatures, 25-17 ka BP: the last Permafrost Maximum (LPM) map of the Northern Hemisphere. Boreas 43, 652–666. https://doi.org/10.1111/bor.12070.
Vandenberghe, J., Markovič, S.B., Jovanovič, M., Hambach, U., 2014b. Site-specific variability of loess and palaeosols (Ruma, Vojvodina, northern Serbia). Quat. Int. 334–335, 86–93. https://doi.org/10.1016/j.quaint.2013.10.036.
Vandenberghe, J., Sun, Y., Wang, X., Abels, H.A., Liu, X., 2018. Grain-size characterization of reworked fine-grained aeolian deposits. Earth Sci. Rev. 177, 43–52. https://doi.org/10.1016/j.earscirev.2017.11.005.
Varga, G., Kovács, J., Újvári, G., 2013. Analysis of Saharan dust intrusions into the Carpathian Basin (Central Europe) over the period of 1979–2011. Glob. Planet. Chang. 100, 333–342. https://doi.org/10.1016/j.gloplacha.2012.11.007.
Varga, G., Cserháti, C., Kovács, J., Szalai, Z., 2016. Saharan dust deposition in the Carpathian Basin and its possible effects on interglacial soil formation. Aeolian Res. 22, 1–12. https://doi.org/10.1016/j.aeolia.2016.05.004.
Varga, G., Újvári, G., Kovács, J., 2019. Interpretation of sedimentary (sub)populations extracted from grain size distributions of central European loess-paleosol series. Quat. Int. 502, 60–70. https://doi.org/10.1016/j.quaint.2017.09.021.
Vaškovský, I., 1977. Kvartér Slovenska. – Geologický ústav Dionýza Štúra. Bratislava (247 pp. in Slovak. Bratislava).
Velichko, A.A., 1990. Loess-paleosol formation on the Russian plain. Quat. Int. 7–8, 103–114. https://doi.org/10.1016/1040-6182(90)90044-5.
Velichko, A.A., Morozova, T.D., Nechaev, V.P., Rutter, N.W., Dlusskii, K.G., Little, E.C., Catto, N.R., Semenov, V.V., Evans, M.E., 2006. Loess/paleosol/cryogenic formation and structure near the northern limit of loess deposition, east European Plain, Russia. Quat. Int. 152–153, 14–30. https://doi.org/10.1016/j.quaint.2005.12.003.
Velichko, A.A., Catto, N.R., Yu Kononov, M., Morozova, T.D., Yu Novenko, E., Panin, P. G., Ya Ryskov, G., Semenov, V.V., Timireva, S.N., Titov, V.V., Tesakov, A.S., 2009. Progressively cooler, drier interglacials in southern Russia through the Quaternary: evidence from the Sea of Azov region. Quat. Int. 198, 204–219. https://doi.org/10.1016/j.quaint.2008.06.005.
Veres, D., Lane, C.S., Timar-Gabor, A., Hambach, U., Constantin, D., Szakács, A., Fülling, A., Onac, B.P., 2013. The Campanian Ignimbrite/Y5 tephra layer–a regional stratigraphic marker for Isotope Stage 3 deposits in the lower Danube region, Romania. Quat. Int. 293, 22–33.
Veres, D., Tecsa, V., Gerasimenko, N., Zeeden, C., Hambach, U., Timar-Gabor, A., 2018. Short-term soil formation events in last glacial east European loess, evidence from multi-method luminescence dating. Quat. Sci. Rev. 200, 34–51. https://doi.org/10.1016/j.quascirev.2018.09.037.
Vetters, H., 1933. Geologische Karte der Republik Österreich und der Nachbargebiete (Die Ostalpen, ihre Ausläufer und Vorlande nebst den angrenzenden Teilen der fränkischen Alb und des böhmischen Massivs). (Geological Map of the Austrian Republic and its neighbouring regions - the eastern alps, its foothills and forelands, the neighbouring parts of Franconian Jura and the Bohemian Massif). Geologische Karte 1 : 500,000.
Vinnepand, M., Fischer, P., Fitzsimmons, K., Thornton, B., Fiedler, S., Vött, A., 2020. Combining inorganic and organic carbon stable isotope signatures in the schwalbenberg loess-palaeosol-sequence near remagen (Middle Rhine valley, Germany). Frontiers in Earth Science 8, 276. https://doi.org/10.3389/feart.2020.00276.
von Suchodoletz, H., Oberhänsli, H., Hambach, U., Zöller, L., Fuchs, M., Faust, D., 2010. Soil moisture fluctuations recorded in Saharan dust deposits on Lanzarote (Canary Islands) over the last 180ka. Quat. Sci. Rev. 29, 2173–2184. https://doi.org/10.1016/j.quascirev.2010.05.014.
Wacha, L., Mikulčić Pavlaković, S., Frechen, M., Crnjaković, M., 2011a. The Loess Chronology of the Island of Susak, Croatia. Quat. Sci. J. EuG 60, 153–169. https://doi.org/10.3285/eg.60.1.11.
Wacha, L., Mikulčić Pavlaković, S., Novothny, Á., Crnjaković, M., Frechen, M., 2011b. Luminescence dating of Upper Pleistocene loess from the Island of Susak in Croatia. Quat. Int. 234, 50–61. https://doi.org/10.1016/j.quaint.2009.12.017.
Wacha, L., Frechen, M., 2011. The geochronology of the "Gorjanović loess section" in Vukovar, Croatia. Quat. Int. Second Loessfest 240, 87–99. https://doi.org/10.1016/j.quaint.2011.04.010.
Wacha, L., Galović, L., Koloszár, L., Magyari, Á., Chikán, G., Marsi, I., 2013. The chronology of the Šarengrad II loess-palaeosol section (Eastern Croatia). Geol. Cro 66, 191–203. https://doi.org/10.4154/GC.2013.18.
Wacha, L., Rolf, C., Hambach, U., Frechen, M., Galović, L., Duchoslav, M., 2018. The last Glacial aeolian record of the Island of Susak (Croatia) as seen from a high-resolution grain–size and rock magnetic analysis. Quat. Int. 494, 211–224. https://doi.org/10.1016/j.quaint.2017.08.016.
Wagner, M., 1979. Mollusc Fauna of the Mende Loess Profile.
Wagner, B., Vogel, H., Zanchetta, G., Sulpizio, R., 2010. Environmental change within the Balkan region during the past ca. 50 ka recorded in the sediments from lakes Prespa and Ohrid. Biogeosciences 7, 3187–3198. https://doi.org/10.5194/bg-7-3187-2010.
Walter, H., 1974. Die Vegetation Osteuropas, Nord- Und Zentralasiens, Vegetationsmonographien der Einzelnen Grossräume. G. Fischer, Stuttgart.
Wei, H., Wang, L., Azarmdel, H., Khormali, F., Frechen, M., Li, G., Chen, F., 2020. Quartz OSL dating of loess deposits since the late glacial in the Southeast of Caspian Sea. Quat. Int. https://doi.org/10.1016/j.quaint.2020.04.042. S1040618220302068.
Whittle, A.W.R., Whittle, A.W.R., 1996. Europe in the Neolithic: The creation of new worlds, Cambridge world archaeology. In: Cambridge University Press, Cambridge. York, New.
Willmes, C., 2015. LGM sealevel change (HiRes), CRC806 database. Collab. Res. Centre 806.
Wolf, D., Kolb, T., Alcaraz-Castaño, M., Heinrich, S., Baumgart, P., Calvo, R., Sánchez, J., Ryborz, K., Schäfer, I., Bliedtner, M., Zech, R., Zöller, L., Faust, D., 2018. Climate deteriorations and Neanderthal demise in interior Iberia. Sci. Rep. 8, 7048. https://doi.org/10.1038/s41598-018-25343-6.
Wolf, D., Ryborz, K., Kolb, T., Zapata, R.C., Vizcaino, J.S., Zöller, L., Faust, D., 2019. Origins and genesis of loess deposits in Central Spain, as indicated by heavy mineral compositions and grain-size variability. Sedimentology 66, 1139–1161. https://doi.org/10.1111/sed.12539.
Wright, J.S., 2001. "Desert" loess versus "glacial" loess: quartz silt formation, source areas and sediment pathways in the formation of loess deposits. Geomorphology 36, 231–256. https://doi.org/10.1016/S0169-555X(00)00060-X.
Yang, S.L., Ding, Z.L., 2003. Color reflectance of Chinese loess and its implications for climate gradient changes during the last two glacial-interglacial cycles: Color Reflectance of Chinese Loess. Geophys. Res. Lett. 30 https://doi.org/10.1029/2003GL018346.
Yang, S., Fang, X., Shi, Z., Lehmkuhl, F., Song, C., Han, Y., Han, W., 2010. Timing and provenance of loess in the Sichuan Basin, southwestern China. Palaeogeogr. Palaeoclimatol. Palaeoecol. 292, 144–154. https://doi.org/10.1016/j.palaeo.2010.03.039.
Yang, Fei, Zhang, G.-L., Sauer, D., Yang, Fan, Yang, R.-M., Liu, F., Song, X.-D., Zhao, Y.-G., Li, D.-C., Yang, J.-L., 2020. The geomorphology – sediment distribution – soil formation nexus on the northeastern Qinghai-Tibetan Plateau: Implications for landscape evolution. Geomorphology 354, 107040. https://doi.org/10.1016/j.geomorph.2020.107040.
Zagwijn, W.H., Van Staalduinen, C.J., 1975. Toelichtingen bij the Geologische Overzichtskarten Van Nederland.
Zech, R., Zech, M., Marković, S., Hambach, U., Huang, Y., 2013. Humid glacials, arid interglacials? Critical thoughts on pedogenesis and paleoclimate based on multi-proxy analyses of the loess–paleosol sequence Crvenka, Northern Serbia. Palaeogeogr. Palaeoclimatol. Palaeoecol. 387, 165–175. https://doi.org/10.1016/j.palaeo.2013.07.023.
Zeeberg, J., 1998. The European sand belt in eastern Europe - and comparison of late Glacial dune orientation with GCM simulation results. Boreas 27, 127–139. https://doi.org/10.1111/j.1502-3885.1998.tb00873.x.
Zeeden, C., Kels, H., Hambach, U., Schulte, P., Protze, J., Eckmeier, E., Marković, S.B., Klasen, N., Lehmkuhl, F., 2016. Three climatic cycles recorded in a loess-palaeosol sequence at Semlac (Romania) – Implications for dust accumulation in South-Eastern Europe. Quat. Sci. Rev. 154, 130–142. https://doi.org/10.1016/j.quascirev.2016.11.002.
Zeeden, C., Hambach, U., Veres, D., Fitzsimmons, K., Obreht, I., Bösken, J., Lehmkuhl, F., 2018. Millennial scale climate oscillations recorded in the lower Danube loess over the last glacial period. Palaeogeogr. Palaeoclimatol. Palaeoecol. 509, 164–181. https://doi.org/10.1016/j.palaeo.2016.12.029.
Zeeden, C., Obreht, I., Veres, D., Kaboth-Bahr, S., Hošek, J., Marković, S.B., Bösken, J., Lehmkuhl, F., Rolf, C., Hambach, U., 2020. Smoothed millennial-scale palaeoclimatic reference data as unconventional comparison targets: Application to

European loess records. Sci. Rep. 10, 5455. https://doi.org/10.1038/s41598-020-61528-8.
Zeman, A., Havlíček, P., Minaříková, D., Růžička, M., Fejfar, O., 1980. Kvartérní sedimenty střední Moravy (Quaternary sediments of Central Moravia). Anthropozoic 13, 3791.
Zeman, A., Bezvodová, B., Havlíček, P., Minaříková, D., Růžičková, E., Fejfar, O., Kovanda, J., 1986. Zpráva O přehledném výzkumu kvartéru a Geomorfologie V úseku Jih se zaměřením na morfostrukturní analýzu pro vyhledávání ložisek přírodních uhlovodíků (Report on Quaternary Geometrical and Geomorphological Research in the South Section with a Focus on Morphostructural Analysis for the Search of Natural Hydrocarbon Deposits). Czech Geological Survey, Praha.
Zens, J., Zeeden, C., Römer, W., Fuchs, M., Klasen, N., Lehmkuhl, F., 2017. The Eltville Tephra (Western Europe) age revised: Integrating stratigraphic and dating information from different last Glacial loess localities. Palaeogeogr. Palaeoclimatol. Palaeoecol. 466, 240–251. https://doi.org/10.1016/j.palaeo.2016.11.033.
Zens, J., Schulte, P., Klasen, N., Krauß, L., Pirson, S., Burow, C., Brill, D., Eckmeier, E., Kels, H., Zeeden, C., Spagna, P., Lehmkuhl, F., 2018. OSL chronologies of paleoenvironmental dynamics recorded by loess-paleosol sequences from Europe: Case studies from the Rhine-Meuse area and the Neckar Basin. Palaeogeogr. Palaeoclimatol. Palaeoecol. 509, 105–125. https://doi.org/10.1016/j.palaeo.2017.07.019.
Zerboni, A., Trombino, L., Frigerio, C., Livio, F., Berlusconi, A., Michetti, A.M., Rodnight, H., Spötl, C., 2015. The loess-paleosol sequence at Monte Netto: a record of climate change in the Upper Pleistocene of the Central Po Plain, northern Italy. J. Soils Sediments 15, 1329–1350. https://doi.org/10.1007/s11368-014-0932-2.
Zerboni, A., Amit, R., Baroni, C., Coltorti, M., Ferrario, M.F., Fioraso, G., Forno, M.G., Frigerio, C., Gianotti, F., Irace, A., Livio, F., Mariani, G.S., Michetti, A.M., Monegato, G., Mozzi, P., Orombelli, G., Perego, A., Porat, N., Rellini, I., Trombino, L., Cremaschi, M., 2018. Towards a map of the Upper Pleistocene loess of the Po Plain Loess Basin (Northern Italy). Alpine Mediterr. Quat. 31, 253–256.
Zeuner, F.E., 1937. The climate of the countries adjoining the ice-sheet of the Pleistocene. Proc. Geol. Assoc. 48, 379–395. https://doi.org/10.1016/S0016-7878(37)80049-8.
Zeuner, F.E., 1956. Loess and palaeolithic chronology. Proc. Prehist. Soc. 21, 51–64. https://doi.org/10.1017/S0079497X00017400.
Zhang, J., Rolf, C., Wacha, L., Tsukamoto, S., Durn, G., Frechen, M., 2018. Luminescence dating and palaeomagnetic age constraint of a last glacial loess-palaeosol sequence from Istria, Croatia. Quat. Int. 494, 19–33. https://doi.org/10.1016/j.quaint.2018.05.045.
Zhang, X.-X., Claiborn, C., Lei, J.-Q., Vaughan, J., Wu, S.-X., Li, S.-Y., Liu, L.-Y., Wang, Z.-F., Wang, Y.-D., Huang, S.-Y., Zhou, J., 2020. Aeolian dust in Central Asia: Spatial distribution and temporal variability. Atmos. Environ. 238, 117734. https://doi.org/10.1016/j.atmosenv.2020.117734.
Zöller, L., Semmel, A., 2001. 175 years of loess research in Germany—long records and "unconformities". In: Earth-Science Reviews, Recent Research on Loess and Palaeosols, Pure and Applied, 54, pp. 19–28. https://doi.org/10.1016/S0012-8252(01)00039-3.
Zollinger, G., 1991. Die Lößdeckschichten der Ziegelei in Allschwil (Kanton Basel - Landschaft/Schweiz) - Ein Beitrag zur Quartärstratigraphie am südlichen Oberrheingraben. Ber. Naturf. Ges. Freiburg i. Br. 79, 165–176.